

# MASTER OF SCIENCE IN ELECTRICAL AND ELECTRONIC ENGINEERING



## Performance Analysis of Model Predictive Controller in Non Linear Applications

**Abdur Raquib Ridwan**

Department of Electrical and Electronic Engineering  
Islamic University of Technology (IUT)  
Gazipur-1704, Bangladesh.

August, 2012.

## CERTIFICATE OF APPROVAL

---

The thesis titled “Performance Analysis of Model Predictive Controller in Nonlinear Applications” submitted by Abdur Raquib Ridwan bearing Student No. 092614 of Academic Year 2009-2010 has been found as satisfactory and accepted as partial fulfillment of the requirement for the degree of Master of Science in Electrical and Electronic Engineering on 26 August 2012.

### BOARD OF EXAMINERS

---

- |  |                                  |
|--|----------------------------------|
| <p>-----</p> <p>1. <b>Dr. Kazi Khairul Islam</b><br/>Professor<br/>Department of Electrical and Electronic Engineering<br/>Islamic University of Technology (IUT)<br/>Gazipur, Bangladesh.</p>         | <p>Chairman<br/>(Supervisor)</p> |
| <p>-----</p> <p>2. <b>Dr. Md. Shahid Ullah</b><br/>Professor and Head<br/>Department of Electrical and Electronic Engineering<br/>Islamic University of Technology (IUT)<br/>Gazipur, Bangladesh.</p>  | <p>Member<br/>(Ex-Officio)</p>   |
| <p>-----</p> <p>3. <b>Dr. Md. Ashraful Hoque</b><br/>Professor<br/>Department of Electrical and Electronic Engineering<br/>Islamic University of Technology (IUT)<br/>Gazipur, Bangladesh.</p>         | <p>Member</p>                    |
| <p>-----</p> <p>4. <b>Dr. Md. Aynal Haque</b><br/>Professor<br/>Department of Electrical and Electronic Engineering<br/>Bangladesh University of Engineering and Technology<br/>Dhaka, Bangladesh.</p> | <p>Member<br/>(External)</p>     |

## DECLARATION OF CANDIDATE

It is hereby declared that this Thesis or any part of it has not been submitted elsewhere for the award of any Degree or Diploma.

-----  
**Dr. Kazi Khairul Islam**

Professor and Supervisor

Department of Electrical and Electronic Engineering

Islamic University of Technology (IUT)

Gazipur-1704, Bangladesh.

-----  
**Abdur Raquib Ridwan**

Student No. 092614

Academic Year: 2009-2010

*Dedicated to*

**My Beloved Parents, My Colleague Md. Riyasat Azim  
&  
My Adorable Wife**

**TABLE OF CONTENTS**

<b>No.</b>	<b>Topic</b>		<b>Page</b>
	<b>Chapter 1</b>		
	<b>Introduction</b>		
1	1.1	Background	1
	1.2	Related Work	4
	1.3	Motivation	6
	1.4	Research Objectives	7
	1.5	Outline of the Thesis	7
	<b>Chapter 2</b>		
	<b>Model Predictive Controller (MPC) and its use in Nonlinear Applications</b>		
2	2.1	Introduction to MPC	9
	2.1.1	Basic Working Principle	9
	2.1.2	Optimization Process and Cost Function	11
	2.1.3	A Brief History of Industrial MPC	13
	2.2	The Receding Horizon Idea	13
	2.3	Applications of MPC	15
	2.4	Control of MPC	17
	2.5	Tuning Procedures of MPC	21
	<b>Chapter 3</b>		
	<b>Dynamic Modeling of Nonlinear Systems and Performance analysis using MPC and PID</b>		
3	3.1	Dynamic Modeling of the Robotic Leg	22
	3.1.1	Modeling of the DC Motor used to generate the Torque	23
	3.1.2	Summary of the Result	31
	3.2	Modeling of a Stirred Tank Heater	31
	3.2.1	Linearization of the STH System	42
	3.2.2	Tabulation of the Simulated Results	43
	3.2.3	Summary of the Simulated Results for the STH System	44
	3.3	Modeling of a single phase Speed Controller and a Current	45

Controller for a Linearized Small Signal model of a Switched  
Reluctance Motor (SRM)

3.3.2	Single Phase Current Control of the Linearized Small Signal SRM	50
3.3.3	Single Phase Speed Control of the Linearized Small Signal SRM	54
3.3.4	Tabulated results obtained from simulations	57
3.3.5	Stability analysis of the SRM system	58

## Chapter 4

### Ornithopter, its Dynamics and Flight Control Method

4	4.1	Introduction to Ornithopter	60
	4.2	Recent Applications of Ornithopter	62
	4.3	Flight Dynamics and modeling of the Ornithopter	63
	4.3.1	A General Two Dimensional Model of the Ornithopter	64
	4.4	Flight Control of the Ornithopter	68
	4.4.1	Flight Control of the Ornithopter using PID Controller	70
	4.4.2	SISO, MISO Model Predictive Controller in the Flight Control of the Ornithopter	72
	4.4.3	MIMO Model Predictive Controller in the Flight Control of the Ornithopter	76
	4.5	Linearized Model of the Ornithopter	79

## Chapter 5

### PERFORMANCE ANALYSIS OF MPC AND PID CONTROLLER ON THE FLIGHT CONTROL OF THE ORNITHOPTER

5	5.1	Simulation results using the Adaptive PID Controller	80
	5.2	Simulation Results using the SISO MPC Controller	83
	5.3	Simulation Results using the MISO MPC Controller	86
	5.4	Simulation Results using the MIMO	89
	5.5	Tuning Parameters for the MPC Controller	90

5.6	Tuning method employed for the PID Controller	91
5.7	Simulation results	91
5.8	Simulation Results shown in a tabulated format	92

## **Chapter 6**

### **Conclusion and Future Work**

6	6.1	Summary	94
	6.2	Contribution	95
	6.3	Conclusion	96
	6.4	Recommendations for Future Work	96

Reference	98
Appendix A	105
Appendix B	105
Appendix C	106
Appendix D	106

## LIST OF TABLES

No.	Title	Page
<b>Chapter 3</b>		
3.1	Control Parameters of the PID Controller for Robotic leg	26
3.2	Control Parameters of the MPC Controller for Robotic leg	28
3.3	Control Parameters of the MPC Controller for STH	42
3.4	Control Parameters of the PID Controller for STH	43
3.5	Summary of the simulated results of the STH system	45
3.6	Result Comparison using the Simulated results for the SRM system	58
<b>Chapter 5</b>		
5.1	Control Parameters of the MPC for the Ornithopter system	73
5.2	Simulated Results of the Ornithopter Tabulated	107
<b>Chapter 6</b>		
6.1	System Parameters of the STH System	105
6.2	Motor and system Parameters	106
6.3	System Parameters of the ornithopter system	106



## LIST OF FIGURES

No.	Title	Page
<b>Chapter 2</b>		
2.1	Basic structure of MPC	10
2.2	Process of MPC to trace the reference trajectory	11
2.3	Process of Constraint Input of MPC	11
2.4	Cost Minimization Curve	12
2.5	The receding horizon concept showing Optimization Problem	13
2.6	Use of MPC in Vehicle Path Planning and Control	16
2.7	Use of MPC in Spacecraft applications.	17
2.8	Plant with Input and Output Signals	17
2.9	MPC Controllers	19
2.10	Flow Chart for MPC Control	20
<b>Chapter 3</b>		
3.1	Cylindrical model of a Robotic Leg	22
3.2	DC Motor (a) Circuit Diagram (b) Block Diagram	23
3.3	DC Motor and the Nonlinear Robotic Human Leg Combined	24
3.4	Simulink Representation of the PID Controller	25
3.5	Simulink Model incorporating the PID controller	26
3.6	Simulink Model of the MPC Controller for the DC MOTOR OPERATED ROBOTIC LEG	27
3.7	Angular Response using Reference Voltage of 10V corresponding to an angle of 90 degree using PID Controller	28
3.8	Angular Response using MPC Controller	29
3.9	Angular response for an input voltage of 4 V using PID controller	29
3.10	Angular response for an input voltage of 4 V using MPC controller	30
3.11	Stirred Tank Heater	32

3.12	Total Simulink Representation of the Stirred Tank Heater	33
3.13	Input-Output Simulink Model of the Stirred Water Tank Heater	34
3.14	PID Control of the STH with $\dot{V}_j$ as the manipulated	35
3.15	PID control of the STH with $T_{ji}$ as the manipulated variable	36
3.16	Simulation results using the PID controller for STH	36
3.17	MPC Simulink block for controlling STH with $\dot{V}_j$ as the manipulated variable	37
3.18	MPC of the Stirred Water Tank Heater with $T_j$ as the manipulated variable	37
	Simulation Results for the SISO MPC control of STH	38
3.19	MISO MPC Representation of the Stirred Water Tank Heater	39
3.20	Simulation results using the MISO MPC control of STH.	40
3.22	Block Diagram of the linearized SRM	41
3.23	Reduced Block Diagram of the SRM	48
3.24	Block Diagram of the SRM Drive	48
3.25	Simulink Model of the PID Controller	49
3.26	Block Diagram of the Current Control Loop	50
3.27	Simulink Model of the Current Control Loop using PID	51
3.28	Step Response for a reference current of 1.5 pu.	51
3.29	Simulink Model of the Current Control Loop using MPC	52
3.30	Step Response for a reference current of 1.5 p.u	52
3.31	Ramp response for a reference ramp current of slope 1.5 using PID	53
3.32	Ramp response for a reference ramp current of slope 1.5 using MPC	53
3.33	Approximated speed loop diagram	54
3.34	Simulink model of the Speed Control Loop using PID	55
3.35	Step Response for a reference speed of 1.pu using PID	55
3.36	Simulink Model for the Speed Control loop using MPC	56
3.37	Step Response for a reference speed of 1.pu using MPC	57

## Chapter 4

4.1	Mr. Bill Ornithopter	61
4.2	Kestrel Ornithopter	63
4.3	Two Dimensional Model of the Ornithopter	64
4.4	Total Nonlinear Simulink Representation of the Ornithopter	67
4.5	Ornithopter Simulink Model	68
4.6	The internal Simulink Representation of the PID Controller	69
4.7	PID Controller using thrust as the only Manipulated Variable and Velocity as Output	70
4.8	Continuation of Figure 4.7 with Angular Position as the output	70
4.9	Continuation of Figure 4.8 with Altitude as the output	71
4.10	PID Controller with Lift as the Manipulated Variable and the output as the altitude	72
4.11	MPC Controller scheme for controlling the velocity with the manipulated variable as Thrust	72
4.12	MPC Controller with Manipulated Variable as the Lift	73
4.13	MPC Controller with Manipulated Variable as the Tail Command angle	74
4.14	MPC Controller with three Manipulated Variables and Angular Position as Output	75
4.15	MPC Controller with three Manipulated Variables and Velocity as Output	75
4.16	MPC Controller with three Manipulated Variables and Altitude as Output	76
4.17	MPC Controller with three Manipulated Variables and Velocity, Altitude and Angular Position as the Output	77
4.18	Model Predictive Controller featuring the Initial Acceleration Mode of Operation	78

## Chapter 5

5.1	Step response for reference velocity = 1.pu	80
5.2	Step response for a reference altitude of 1.pu	81
5.3	Step response for a reference Angular Position of 1.pu	82

5.4	Step response for reference velocity of 1.pu	83
5.5	Step response for a reference altitude of 1.pu	84
5.6	Step response for a reference angular Position of 1.pu	85
5.7	Step response for reference velocity of 1.pu.	86
5.8	Step response for a reference altitude of 1.pu	87
5.9	Step response for a reference angular Position of 1.pu	88
5.10	Step response for a reference velocity, altitude and angular position of 1.pu	89
5.11	Ramp response for a reference ramp velocity of slope 1 and step response reference angular position of 1.pu	92
5.12	Altitude response for the reference ramp velocity of slope 1 and reference angular position of 1 p.u	93

## LIST OF SYMBOLS AND ABBREVIATIONS

$P$	Prediction Horizon
$H$	Control Horizon
$N$	Control Interval
$T_m$	Motor Torque
$D$	Viscous Damping
$K_b$	Back EMF constant
$I_a$	Armature Current
$L_a$	Armature Inductance
$V_b$	Back EMF
$E_a$	Armature Voltage
$\rho_j$	Jacket Fluid Density
$K_t$	Current-Torque Coefficient
$HA$	Product of Heat transfer Coefficient and Area of Heat Transfer
$\rho_t$	Tank fluid Density
$V_t$	Volume of the fluid in the Tank
$V_j$	Volume of the fluid in the Jacket
$c_{pt}$	Heat capacity of Tank Fluid
$c_{pj}$	Heat Capacity of Jacket Fluid
$I$	Inertia of the Ornithopter
$m$	Mass of the Ornithopter
$\delta_E$	Tail Command Angle
MIMO	Multiple Input Multiple Output
MISO	Multiple Input Single Output
SISO	Single Input Single Output
MPC	Model Predictive Controller

## **ACKNOWLEDGEMENTS**

I would like to express my heartiest gratitude to my supervisor, Prof. Dr. Kazi Khairul Islam for his keen supervision, inspiration and motivation for doing this thesis. I would also like to pay my heartiest gratitude to Dr. Md. Ashraful Hoque, for giving me the confidence of undertaking this thesis. I would like to thank wholeheartedly Asstt. Prof. Mr. Ashik Ahmed who was instrumental in getting me started with the ornithopter control with MPC. I am also thankful to the Head of the Department Prof. Dr. Md. Shahid Ullah for his guideline and support for my thesis. Last but not the least I am thankful to my parents and my beloved wife who have always supported me in my work.

## ABSTRACT

This thesis is concerned with depicting the performance of MPC as a controller in nonlinear systems covering various fields of engineering. The Adaptive PID controller is used as the generic means of controller comparison. Main Emphasis and theme of this thesis is to visualize the performance of MPC as a controller for the flight control of the Micro Aviation Vehicle Ornithopter. The velocity, altitude and angular position are taken as the flight outputs to be controlled. A two dimensional model of the ornithopter is selected because it accommodates the inseparability of thrust and lift in its system which is instrumental for describing the flight operation of the ornithopter. Both the acceleration phase and steady state cruise motion control of the ornithopter is considered. The entire nonlinear mathematical model describing the equations of motion of the ornithopter is simulated in the Simulink Environment of the Matlab Software. The performance of the Model Predictive Controller for the flight control of MAV ornithopter is evaluated by comparing the responses with that of an Adaptive PID controller.

Although a very improved and significant flight control of the ornithopter is possible with the Model Predictive Controller, a disturbance prone scenario, changing wind direction and speed is needed to completely visualize the impact of Model Predictive Controller in the flight control of an ornithopter. Moreover a better system model comprising a three dimensional mathematical model is required to successfully proceed with further altitude and velocity control. Other directional outputs such as the angular velocity, acceleration can also be investigated.

Hence this thesis can be considered as the basis of properly understanding the control mechanism of the Model Predictive Controller and finally would serve as the platform from which the flight control of ornithopter can be investigated with Model Predictive Controller under more realistic and practical instances in which the ornithopter needs to be controlled.

# CHAPTER 1

## INTRODUCTION

### 1.1 Background

Almost all systems exhibit nonlinearity because the root of every possible mechanism existing in the nature is complex and is described by highly complicated mathematical modeling only derived from empirical and theoretical study of multifarious systems. To accommodate all the aspects working in harmony for the proper functioning of a nonlinear system is always a challenge and have haunted researchers over the history. When it involves imitating the sophisticated control mechanism of a natural being such as the bird or any other living objects, the difficulty escalates and makes it impossible to materialize the system in reality because of the limitations of science and its benefactor the engineering tool of “Technical Know How”. Human beings have responded to the task with a simplistic approach compatible with the available resources at hand. Most Nonlinear Systems are quite difficult to control and moreover requires the development of sophisticated controllers having the ability to anticipate and literally think like a human. Many intelligent controllers have evolved through generations with the expansion of artificial intelligence and every time human beings were fascinated by the state of the art performance of these smart controllers. Researchers were intrigued by knowing that human capability can conquer all horizons and this unquenching thirst of the scientific luminaries of modern days have been instrumental in the growing development of controllers of unbounding capabilities of which the ability of predicting the future stands out from all other highly tuned functions of the controllers of today. Amongst all the innovations of controllers till now, Model Predictive Controller (MPC) has entered into the era of intelligent controllers with a strong



statement. MPC have a unique controlling capability in that it can mimic the behavioral pattern of a human brain. It mainly imitates how the brain utilizes its sense of vision to anticipate its next movement. This has made the Model Predictive Controller (MPC) a very lucrative tool for controlling systems of diversified fields. On the other hand PID controllers have always been the platform and a benchmark for investigating the performance of other controllers. In many ways the PID controllers have been modified and computationally expanded with some innovative features to make it more adaptive in controlling multifarious systems of almost all field of engineering [53]. This thesis would investigate the performance of MPC and as a generic means of analysis would be compared with the benchmark adaptive PID controllers. Moreover the range of possibilities of MPC controlled systems would be scoured by observing its performance on a range of systems covering various disciplines of engineering. Initially a rudimentary analysis is done with a very simplistic nonlinear model comprising of the DC motor controller Robotic leg. After that the comprehensive features of the MPC is analyzed by launching it as a controller in some nonlinear plants such as the Stirred water Tank Heater (STH) which is extensively used in chemical processing plants and Switched Reluctance Motor (SRM) which quite recently has supplanted the induction motor in its use in various fields demanding variable speed drives and partly as a result of development of power electronic drives [37]. Finally the suitability and effectivity of the MPC controller is explored by thoroughly investigating the flight control of an ornithopter which is associated with a complex nonlinear dynamics and thereby demands highly sophisticated controllers for its flight control. In every control analysis of the systems considered in this thesis work, linearization of the nonlinear systems is carried out to make the process simpler and understand the crude aspects of its controllable features by making the system feasible for carrying out simulations in the Matlab environment.

Emphasis is hugely given in the implementation of a good performance controller for flight control of the ornithopter. Ornithopters are aerial systems mainly comprising of Micro Aviation Vehicles (MAVS) that mimic the flapping wing flight of birds [1]. Although many of the subtle controlling features of the birds involving the feather dynamics are eliminated in the design of the ornithopters, the swiftness and agility that the ornithopter promises to provide makes it very attractive in surveillance arenas of application where an unobtrusive flight is necessary and the aspect of swift motion is quite apparent [4] [5]. It differs from its contemporary fixed-wing aircraft from the fact that the dynamics of the ornithopter incorporates both the thrust and the lift mechanism inseparably thus making it very complicated to control. On the other hand the aircrafts have its wing's fixed which means that the lift mechanism and thrust mechanism is separated and considered as two different entities working together separately to provide the flight operation. Hence in a fixed- wing aircraft both the lateral and longitudinal motion are separated by decoupling the lateral and longitudinal equations of motion. However, the nonlinear equations of motion describing an ornithopter is quite complex because the wings of the ornithopters are not fixed [7] [11] [12]. Hence the decoupling of the lateral and longitudinal equations are generally avoided and in most cases of research on ornithopters the entire system dynamics is considered and this necessitates the use of a very sophisticated controller that has the ability to modulate all the complex directions and kinematics of motion. Generally a dimensional approach is taken for describing the dynamics of an ornithopter [4] [6] [7]. A one dimensional mathematical model is done which due to its simplicity fails to provide a complete description of the ornithopter. A three dimensional approach is also done, but the complex nature of the mathematics that involves the description of 3D dynamics of the ornithopter makes it very difficult [14] [17] to explore the flight control of the ornithopter using the existing controllers of

today. The possible mechanism of controlling the ornithopter model in the three dimensional approach would involve the innovation of a nonlinear adaptive control system. However the two dimensional mathematical representation of the ornithopter although not so complicated as the 3D model, it still contains all the necessary information depicting the kinematics of the ornithopter. Each and every direction of motion although incorporated in the system dynamics of the 2D model of the ornithopter, every equation of motion is simplistically represented [4]. The two dimensional approach remains as the ground in which research can be done for a realization of a sophisticated flight control of the ornithopter. In this thesis the two dimensional model is considered. Both the cruise motion and the initial acceleration phase of the ornithopter is elaborately encapsulated in the 2D dynamic model of the ornithopter and thus renders it possible to observe the flight control of the ornithopter in both of these phase of motion of the ornithopter using the MPC controller. The performance analysis is also evaluated by comparing the performance of MPC and PID controller in the two phase of motion of the ornithopter. The 2D mathematical model of the ornithopter was implemented using Simulink and finally the linearization of the Simulink model was carried out using the linearization toolbox present in the Simulink environment of Matlab. Finally simulations were done using Matlab providing a thorough performance analysis of Model Predictive Controller in the flight control of the Ornithopter.

## **1.2 Related Work**

Many researchers worked on ornithopter modeling and control. De Laurier *et al.* [2] have laid general foundation for the aerodynamic model of the flapping wing flight known as the ornithopter. Fowler *et al.* [3] has presented a feasible design of the ornithopter explaining the flight control of this flapping wing flight model. A study of the unsteady aerodynamics of a

flapping wing was done in [4] for a flapping wing MAV in hover. A flapping wing MAV was studied in [14] in order to understand the modeling of MAV. A wing's force and flow structures were studied in [12] for a simplified flapping motion similar to that of an insect. This is important in that it offers insight into the feasibility of control of the simplified ornithopter. Several authors [4] [7] have proposed schemes for controlling the velocity and altitude of the ornithopter. The simplified model of the (MAV) was studied in [12] and the control schemes involving feedback controllers and feed-forward control operations were investigated. PID controllers in the feedback loop and frequency limiting and saturated thrust and lift forces in ornithopters were studied in [6]. Cruise Motion and acceleration motion of the ornithopter was studied [6] [11] [13] to gain an insight of the desired responses of the ornithopter in such stages of motion.

Moreover study on the single phase linearized SRM model was done, Ray and Davis *et al.* [35] suggested a superior approach which depended on linearizing the inductance that allowed the voltage to be switched at any point in the cycle and enabled control strategies to be examined with sufficient accuracy inclusive of component ratings. Hybrid controllers and Genetic algorithm based controllers was studied from [24] where hybrid controller by Paramasivam *et al.* [37] has reduced the steady state error as compared with PI-type fuzzy logic control (FLC), while keeping the merits of PI-type FLC. Reay *et al.* [38] proposed neural network based SRM drive.

Brief study on the mathematical modeling of STH was done from a case study by Dr. Kevin Craig from Rennsselaer Polytechnique Institute and the use of MPC for a SISO control of the STH was studied in [40] where the control of the temperature of STH using single constraint manipulated variables was carried out.

Modeling Motion Control of Robotic arm was done in [35] which delineated the use of PID controllers in DC motors and also the simplistic representation of a robotic arm. This gave me the impetus to delve into the study of a simplistic approach to designing the robotic leg and use MPC for its control.

### **1.3 Motivation**

As an intelligent and sophisticated control technology, the Model Predictive controller can give robust adaptive response of a complex aviation system highly intertwined with nonlinearity, external wind disturbances and random variation in parameters. Moreover its ability to be tuned with features such as input constraints and output constraints to maintain the stability of the system under severe control scenarios of a plant can solve the complicated vehicular motion of complicated systems and fast electronic drives. From the above literature review, we saw that complex feedforward controllers, adaptive feedback PI controllers, nonlinear adaptive controllers have been used in the systems presented in my thesis. Smart GA algorithm based and fuzzy logic based controllers are also widely used in mitigating the problems involved in the flight control of the ornithopter [7] [13]. Particle Swarm Optimization technique embedded in PID controllers for controlled and predictive tuning has been carried out for managing nonlinear control mechanisms ranging from motion control of ornithopters to electric drive control of Switched Reluctance Motor. No research work has so far used MPC in the flight control of ornithopters and the current and speed control of switched reluctance motor. Although MPC has been widely used in the temperature control of STH, a comprehensive analysis of the STH taking into account the aspect of controlling it with multivariable inputs and MPC controller for that

purpose has not been carried out. Good result obtained from the simulation of this research can instigate further experimental work using the 2D model of the ornithopter and MPC as the basis of control for future research work. Moreover a satisfactory flight control of the 2D model of the ornithopter can also facilitate and inspire researchers to develop a MPC controller for the flight control of the 3D model of the ornithopter.

## **1.4 Research Objectives**

The objectives of the work can be listed as follows:

- ✓ MATLAB Simulink Modeling of a 2D Ornithopter, A Multiple Input Single Output (MISO) model of a Stirred Tank Heater, a small signal single phase Switched Reluctance Motor (SRM) and a DC motor operated Robotic Leg.
- ✓ Linearization of the systems making sure that the systems don't lose its integrity after linearization for its proper operation using MPC controllers.
- ✓ Evaluate the performance of the systems with conventional PID controller.
- ✓ Evaluate the performance of the systems with the proposed MPC controller.
- ✓ Compare the performance between the conventional PID and MPC controllers.
- ✓ Drawing the conclusion based on the comparison of the results

## **1.5 Outline of the Thesis**

Chapter 1 represents the background of the present work, motivation and objectives and related work with this project.

Chapter 2 describes briefly about MPC, its control strategies and its impact on nonlinear applications.

Chapter 3 discusses the modeling of nonlinear models comprising of systems involving various field of engineering such as a switched reluctance motor, a stirred tank heater and DC motor operated Robotic Leg. Simulation results to evaluate the performance analysis of the systems using both PID and MPC controllers are also manifested.

Chapter 4 elaborately discusses the concept of an ornithopter and the detailed dynamics and modeling of an ornithopter for its flight control. The linearization technique for the analysis of the nonlinear system is discussed. Representation of the models using Simulink block diagrams is also described in this chapter.

Chapter 5 presents the simulation results of the flight control of the ornithopter under different operating scenarios using both PID and MPC controllers.

Chapter 6 summarizes the research work presented in this thesis and discusses the scopes of future works possible.

## **Chapter 2**

# **Model Predictive Controller (MPC) and its use in Nonlinear Applications**

## **2.1 Introduction about MPC**

### **2.1.1 Basic Working Principle:**

Model predictive control (MPC) refers to a class of computer control algorithms that utilize an explicit process model to predict the future response of a plant [46] [51]. At each control interval an MPC algorithm attempts to optimize future plant behavior by computing a sequence of future manipulated variable adjustments. The first input in the optimal sequence is then sent into the plant, and the entire calculation is repeated at subsequent control intervals. Originally developed to meet the specialized control needs of power plants and petroleum refineries, MPC technology can now be found in a wide variety of application areas including chemicals, food processing, automotive, autonomous robots and aerospace applications,[41] [43].

The working process of MPC can be well described by the game of chess. A player, when plays chess, tries to predict the future moves of the opponent. So, to win the match, he predicts about some future moves depending upon his past experiences and memories. A good player has always got some plans about his next moves or actions.



Figure 2.1 shows the basic structure of MPC in block diagrams. Depending upon the past inputs and outputs, model predicts the future output. It is compared with reference value and the subtracted result or future error is sent to the optimizer. With the help of quadratic cost function and suitable constraints, it creates the future inputs of the optimizer which finally becomes the past memory of the model for the next event. Thus an iterative method is subsequently followed until it reaches close to the desired reference value [34].

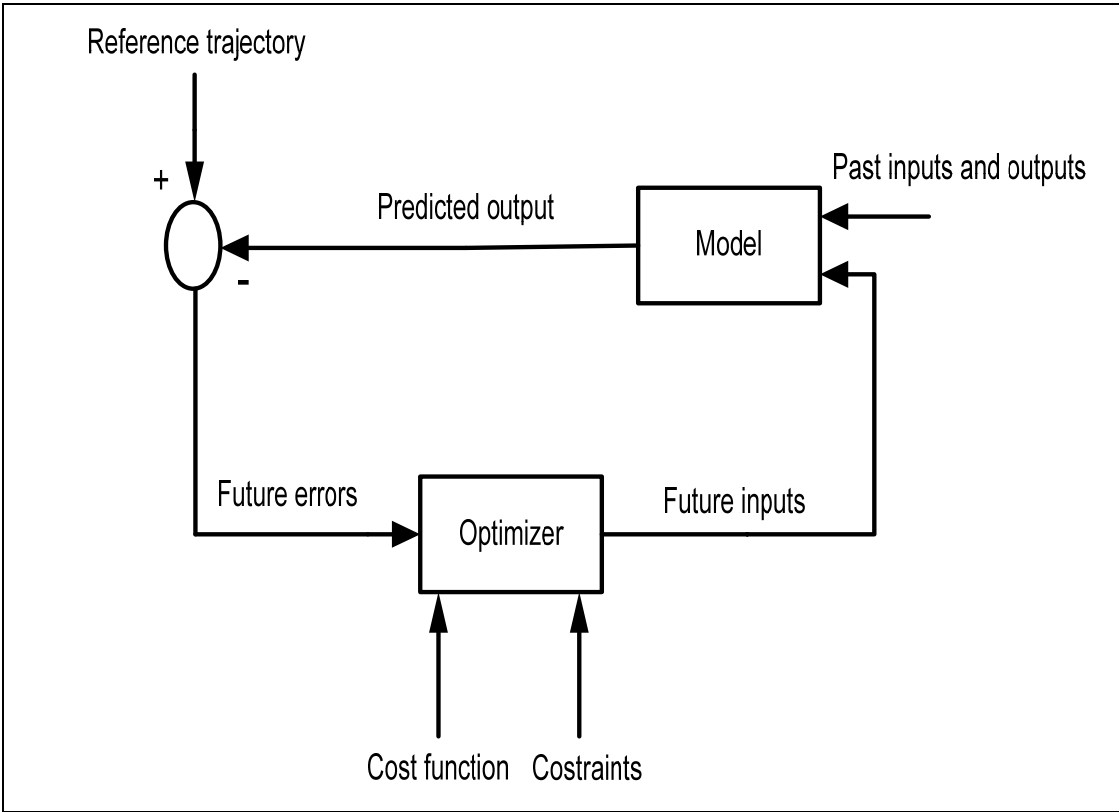


Figure 2.1: Basic structure of MPC

A model is used to predict the future plant outputs based on past and current values and the proposed optimal future control actions. These actions are calculated by the optimizer taking into account the cost function (where the future tracking error is considered) as well as the constraints [42].

### 2.1.2 Optimization Process and Cost Function

The set of future control signals is calculated by optimizing a determined criterion in order to keep the process as close as possible to the reference trajectory. This criterion usually takes the form of a quadratic function of the errors between the predicted output signal and the predicted reference trajectory. The control effort is included in the objective function in most cases.

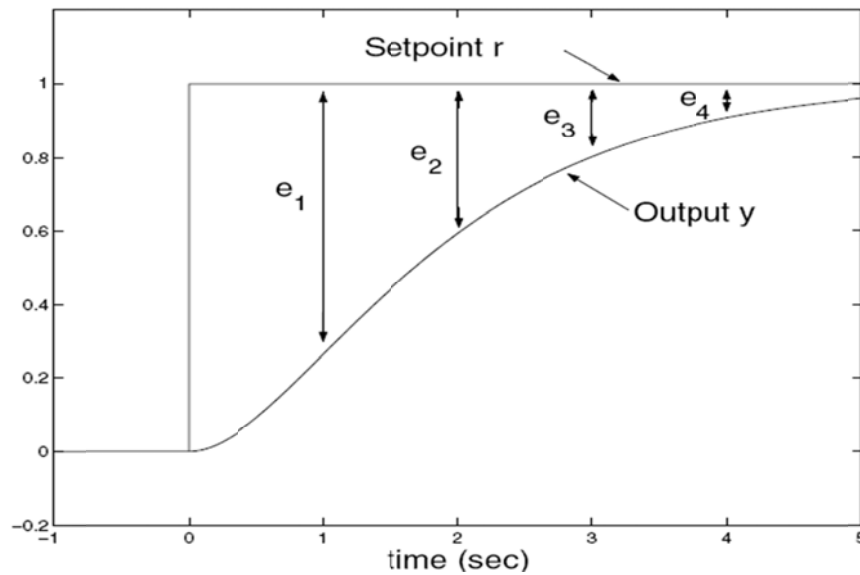


Figure 2.2 Process of MPC to trace reference trajectory

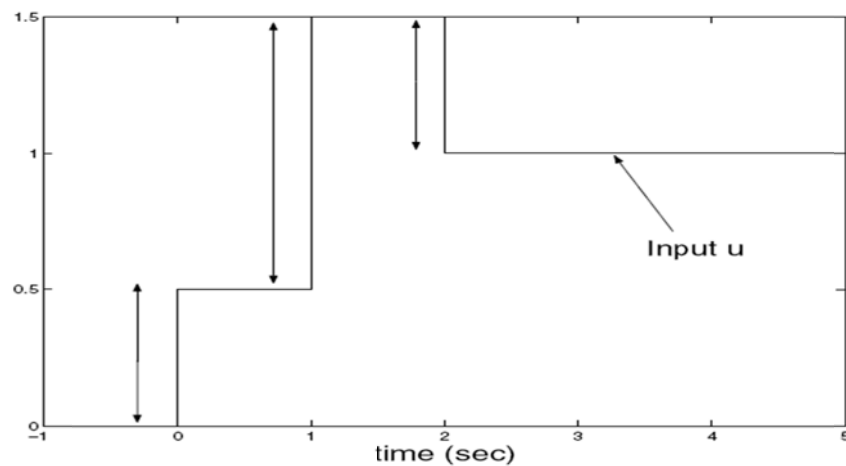


Figure 2.3 Process of Constraint Input of MPC

Figure 2.2 and Figure 2.3 shows that the Model Predictive controller utilizes the errors between the output and the reference trajectory and the difference in the input from one sampling interval to the next and incorporates it in a cost function [29].

$$J = \sum_{k=0}^{Np} q(\hat{y} - r)^2 + \sum_{k=0}^{Np} r\Delta u^2 \quad (2.1)$$

The main principle of optimization resides on solving J for a minimum cost function which is basically

$$\frac{\partial J}{\partial u} = 0 \quad (2.2)$$

By solving this we get the future optimal control value. It is a complex computation problem but it can be shown illustratively as follows:

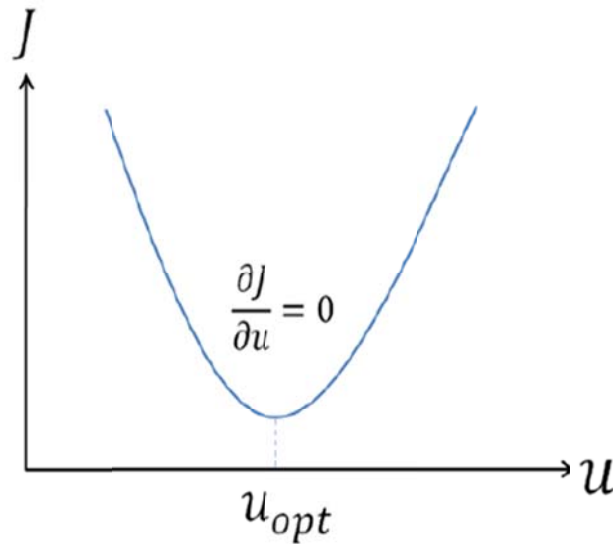


Figure 2.4 Cost function minimization Curve

where  $u_{opt}$  is the desired optimal future control move of the MPC controller.

### 2.1.3 A Brief History of Industrial MPC:

Rawlings[44] provides an excellent introductory tutorial aimed at control practitioners. Allgower, Badgwell, Qin, Rawlings, and Wright [47] present a more comprehensive overview of nonlinear MPC and moving horizon estimation, including a summary of recent theoretical developments and numerical solution techniques. Mayne, Rawlings, Rao, and Scokaert[48] provide a comprehensive review of theoretical results on the closed-loop behavior of MPC algorithms. The authors presented a survey of industrial MPC technology based on linear models at the 1996 Chemical Process Control V Conference (Qin & Badgwell [49]), summarizing applications through 1995. Young, Bartusiak, and Fontaine [50], Downs [51], and Hillestad and Andersen [52] report development of MPC technology within operating companies. A survey of MPC technology in Japan provides a wealth of information on application issues from the point of view of MPC users (Ohshima, Ohno, & Hashimoto [53]). The first description of MPC control applications was presented by Richalet et al. in 1976 Conference (Richalet et al. [54]) and later summarized at 1978 in Automatica paper (Richalet et al. [55]). They described their approach as model predictive heuristic control (MPHC).

### 2.2: The “Receding Horizon” Idea:

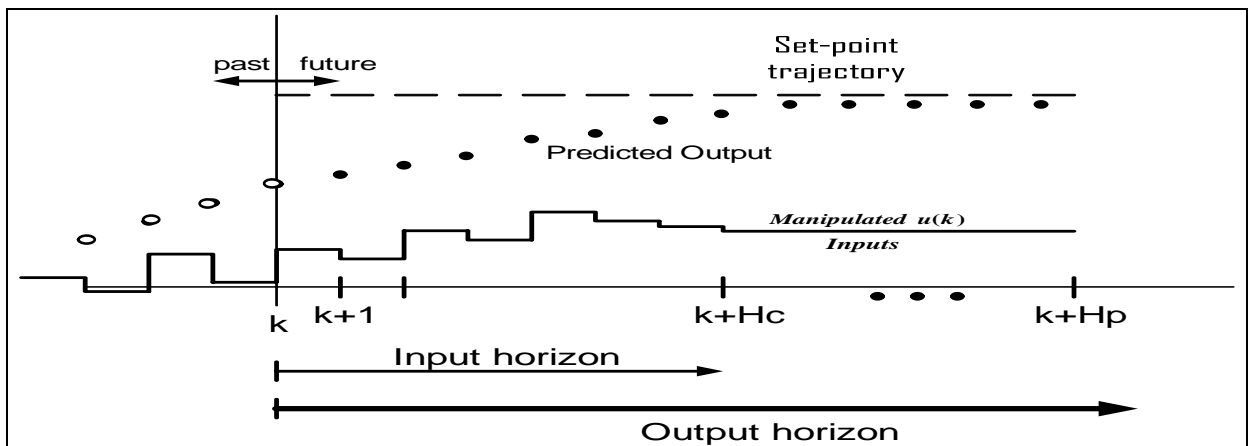


Figure 2.5: The receding horizon concept showing Optimization Problem

At a current instant  $k$ , the MPC solves an optimization problem over a finite prediction horizon  $[k, k + H_p]$  with respect to a predetermined objective function such that the predicted state variable  $\hat{x}$  or output  $\hat{y}$  can optimally stay close to a reference trajectory. The control is computed over a control horizon  $[k, k + H_c]$ , which is smaller than the prediction horizon ( $H_c \leq H_p$ ) [44]. If there were no disturbances, no model-plant mismatch and the prediction horizon is infinite, one could apply the control strategy found at current time  $k$  for all times. However, due to the disturbances, model-plant mismatch and finite prediction horizon, the true system behavior is different from the predicted behavior. In order to incorporate the feedback information about the true system state, the computed optimal control is implemented only until the next measurement instant  $(k, k + 1)$ , at which point the entire computation is repeated [46].

MPC approach can be expressed considering the following finite horizon cost function [56]

$$J^{rh}(x_t, [u_0(t), \dots, u_{H-1}(t)]) = \sum_{i=1}^{H-1} h(\bar{x}_{t+i\Delta T}(u), u_i(t)) + g(\bar{x}_{t+H\Delta T}(u)) \quad (2.3)$$

where  $t$  is the current time;  $H$  is the length of the optimization horizon;  $\Delta T$  is the sample period. If  $i > 0$ , then  $\bar{x}_{t+i\Delta T}(u)$  denotes the controlled trajectory at time  $t + i\Delta T$  from  $x_t$  under piecewise controls  $u = [u_0(t), \dots, u_{i-1}(t)] \in U^H$ ;  $h$  is the running cost; and  $g$  is the terminal cost. We assume that  $h$  is non-negative function and  $g$  satisfies  $g(x) \geq \alpha |x - x_{eq}|$  for all  $x$ , where  $x_{eq}$  is some desired equilibrium and  $\alpha > 0$  is some positive constant. That is,  $g$  is an ‘upward’ function whose lowest point is at the system equilibrium. This condition on  $g(x)$  ensures that the control design attempts to reach the system equilibrium. Moreover a weighted cost function is also implemented by the MPC controller to incorporate systematic design approach for handling interaction in a

multivariable system. This feature of MPC enables handling the input constraints and output constraints imposed on the multivariable system. The priorities of the input constraint and output constraint can be adjusted by tuning the weighted factor in the modified cost function equation. Moreover the process of solving this complex quadratic cost function equation ensures an unbiased offset free tracking which is a key objective for proper control.

The modified J equation [49] is as follows:

$$J = \sum_{i=n_w}^{n_y} \|W_y(\mathbf{r}_{k+i} - \mathbf{y}_{k+i})\|_2^2 + \lambda \sum_{i=0}^{n_u-1} \|W_u(\Delta \mathbf{u}_{k+i})\|_2^2 \quad (2.4)$$

where  $W_y$  and  $W_u$  are positive definite weight factors which can vary even with the change in the horizon  $i$ .

### 2.3 Use of Model Predictive Controller in Nonlinear Applications

Model Predictive Controller has been widely used in nonlinear applications because of its unique and sophisticated ability to handle multivariable constraint problem based plant operations. Generally the nonlinear industrial processes are MIMO systems and are very sensitive to input changes. An unexpected input change can totally render the whole industrial plant totally out of stability and would require very precise monitoring of the plant output. The integrated ability of MPC to predict future outcomes [24] taking into account of the input constraints makes it very suitable for such challenging nonlinear applications.

Its feasibility and a wide range of tuning ability has made it perform significantly better than many other existing intelligent controllers such as fuzzy logic, neural network and adaptive

controllers [54]. Its performance outweighs that of a PID controller and will be manifested in the next chapter where MPC will be utilized in many benchmark and highly demanding nonlinear models. An important aspect is the necessity to linearize the mathematical modeling of the nonlinear systems before using Model Predictive controllers. This not only reduces the computation burden but also ensures fast tracking and response of the systems [42].

Moreover on-line and off-line control becomes easier and hence in general Model Predictive Controller mainly capitalizes on the linear modeling of the nonlinear systems for an efficient control of the systems [34][42][43].

Its successful operation on nonlinear applications ranging from chemical processes, electrical drives, aerodynamics, autonomous robotic systems; has made it an attractive tool to solve future optimization control problems [29][47].

The emerging nonlinear applications of MPC involve:

- Vehicle path planning and control:



Figure 2.6 Use of MPC in Vehicle Path Planning and Control

- Hybrid plant control and nonlinear state estimation of complex network control systems

- Spacecraft rendezvous with space stations.

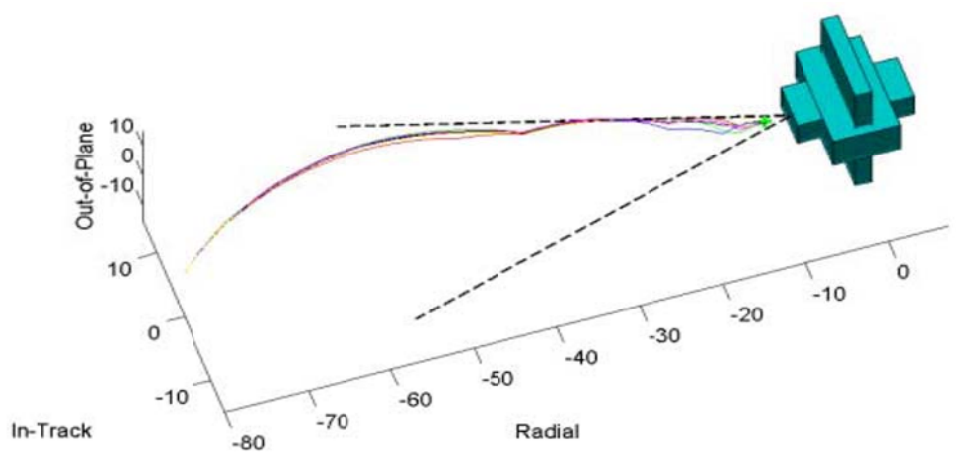


Figure 2.7 Use of MPC in Spacecraft applications

## 2.4 Control of MPC

The MPC design problem is handled by the MPC toolbox available in ‘Matlab’. A Model Predictive Control Toolbox design requires a plant model, which defines the mathematical relationship between the plant inputs and outputs as shown in Figure 2.8. The controller uses it to predict plant behavior. The toolbox software requires the model to be linear, time invariant (LTI).

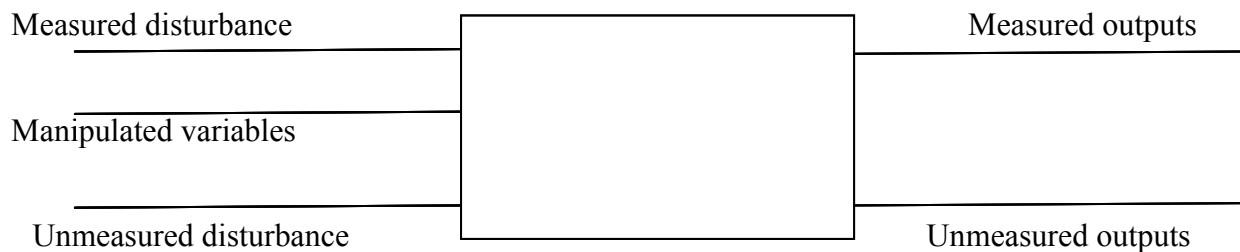


Figure 2.8: Plant with Input and Output Signals



The *plant inputs* are the independent variables affecting the plant. As shown in the previous figure, there are three types:

**Measured disturbances (MD):** The controller can't adjust them, but uses them for feedforward compensation.

**Manipulated variables (MV):** The controller adjusts these in order to achieve its goals.

**Unmeasured disturbances:** These are independent inputs of which the controller has no direct knowledge, and for which it must compensate.

The *plant outputs* are the dependent variables (outcomes) one wishes to control or monitor. As shown in figure 2.8, there are two types:

**Measured outputs:** The controller uses these to estimate unmeasured quantities and as feedback on the success of its adjustments.

**Unmeasured outputs:** The controller estimates these based on available measurements and the plant model. The controller can also hold unmeasured outputs at setpoints or within constraint boundaries.

The design and performance evaluation of the MPC is conducted based on changing the following parameters (Figure 2.9):

- Model and Horizons
- Constraint
- Weight Tuning
- Estimation

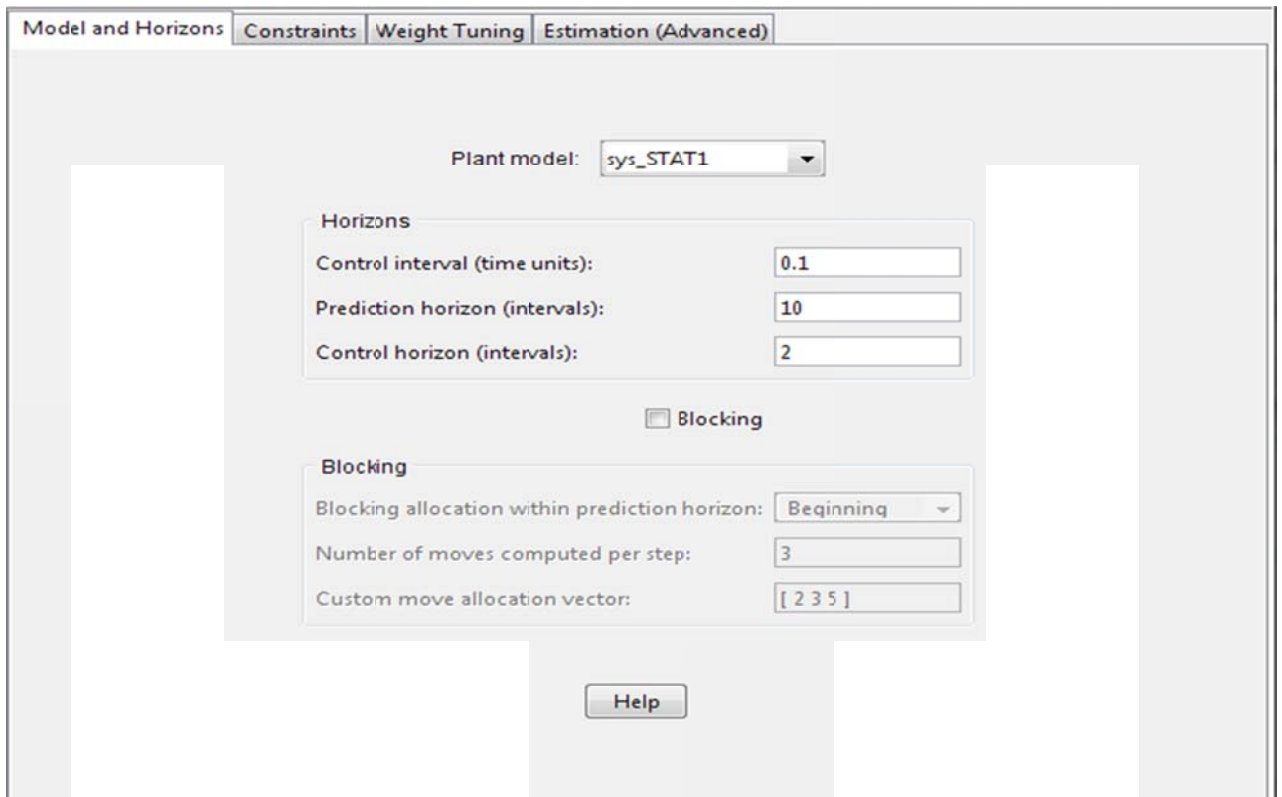


Figure 2.9: MPC controllers

From Fig.2.9 we can see that the model and horizons tab has parameters:

- Control interval (time units),
- Prediction horizon (intervals)
- Control horizon (intervals).

**Prediction horizon** ( $H_p$ ) is the number of steps for which the controller will estimate the output of the system say (5,10,20,30,40,50 intervals, etc) also known as output horizon. **Control horizon** ( $H_c$ ) is the number of steps (2, 4, 6, 8, etc) for which the controller will create future control action to fulfill all the requirements. **Control interval** (sampling period in sec) is the interval (0.1, 0.3, 0.7, 1, etc) separating successive sampling instants.

It is better to set the **constraints** for all manipulated variables, but it's unwise to enter constraints on outputs unless they are an essential aspect of the application. The “Max down rate” should be nonpositive (or blank). It limits the amount a manipulated variable can decrease in a single control interval. Similarly, the “Max up rate” should be nonnegative. It limits the increasing rate. Leave both unconstrained (i.e., blank). The **weights** specify trade-offs in the controller design. First consider the Output weights. The controller will try to minimize the deviation of each output from its setpoint or reference value. For each sampling instant in the prediction horizon, the controller multiplies predicted deviations for each output by the output's weight, squares the result, and sums over all sampling instants and all outputs. One of the controller's objectives is to minimize this sum, i.e., to provide good setpoint tracking. The **Estimation** tab allows to adjust the controller's response to unmeasured disturbances.

A summary of the control mechanism of Model Predictive Controller can be explained via a flow chart as follows:

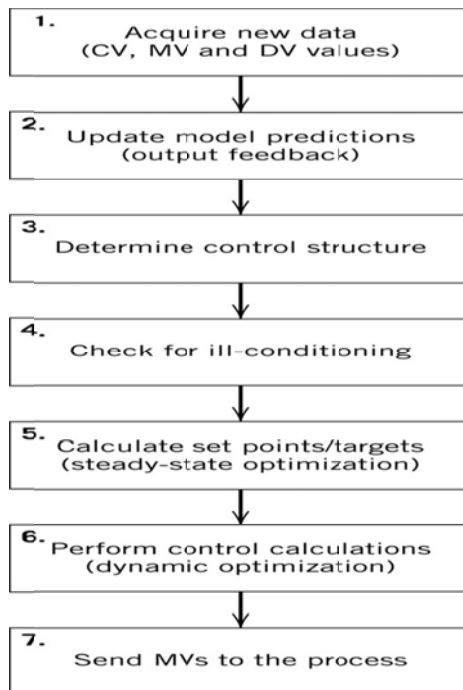


Figure 2.10: Flow Chart for MPC Control

## 2.5 Tuning Procedures of MPC

Tuning of MPC involves some important criterions without which systems cannot be operable and may lead to instability and unwanted oscillations. A systemic tuning approach will lead to an

efficient controllability of the system. The tuning procedure for satisfactory performance is summarized as follows [41] [46] [51]:

- Control Interval/Sampling time (T): Stability is not affected by T but larger T deteriorates system performance under frequent disturbances.
- Control Horizon (M): If Prediction horizon (P) is equal to control horizon (M) then the system becomes vulnerable to oscillations and hence M must be always less than P to get a desired response.
- Optimization horizon/Prediction horizon (P): Increasing P will lead to better responses only if the system modeling is very precise and accurate. In most cases it is necessary to keep the value of P larger than M but not very large, because the modeling of the plant is generally done with a simplistic approach.
- It is wise to select the parameters such that it doesn't affect the settling time of the plant.

Finally the parameters of the MPC controller should be adjusted depending on the system dynamics and the settling time of the plant.

## Chapter 3

# Dynamic Modeling of Nonlinear Systems and Performance analysis using MPC and PID

### 3.1 Dynamic Modeling of the Robotic leg.

A robotic leg can be modeled taking into account a simplistic model of a human leg that relates the output angular rotation about the hip joint to the input torque generated by the leg muscle. A simplified model for the robotic leg assumes an applied torque  $T_m$  supplied by the DC motor, viscous damping,  $D$ , at the hip joint, and inertia  $J$ , around the hip joint. Finally the component of the weight of the leg,  $Mg$ , where  $M$  is the mass of the leg and  $g$  is the acceleration due to gravity creates a nonlinear torque. Assuming the robotic leg to be of uniform density, the weight can be applied at  $L/2$ , where  $L$  is the length of the leg [56]. A pictorial representation of the cylindrical model of a robotic human leg is shown below.

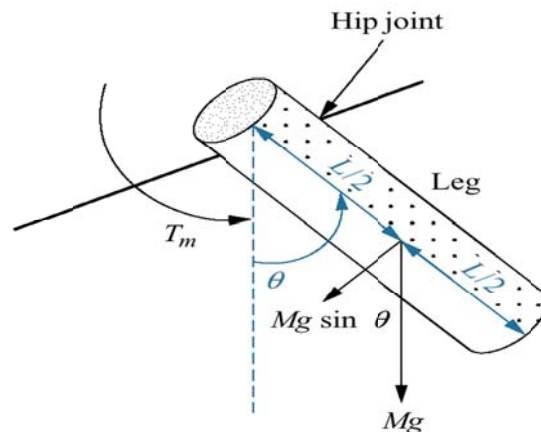


Figure 3.1 Cylindrical model of a Robotic Human leg

Summing the torques, the dynamic model of the robotic human leg can be obtained which is as follows:

$$J \frac{d^2\theta}{dt^2} + D \frac{d\theta}{dt} + Mg \frac{L}{2} \sin \theta = T_m(t) \quad (3.1)$$

### 3.1.1 Modeling of the DC motor used to generate the Torque.

The torque will be supplied by a DC motor and hence an appropriate DC motor capable of rotating the leg from 0 degree to 90 degree is the next step for controlling this robotic leg.

A DC motor with armature control and a fixed field is considered. The electrical model of such a DC motor is illustrated in Figure 3.2. The armature voltage,  $e_a(t)$  is the voltage provided by an amplifier to control the motor. The motor has a resistance  $R_a$ , inductance  $L_a$  and back electromotive force constant,  $K_b$ . The back emf voltage,  $V_b(t)$  is induced by the rotation of the armature windings in the fixed magnetic field. The counter emf is proportional to the speed of the motor with field strength fixed. The governing equations are as follows:-

$$V_b(t) = K_b \frac{d\theta}{dt} \quad (3.2)$$

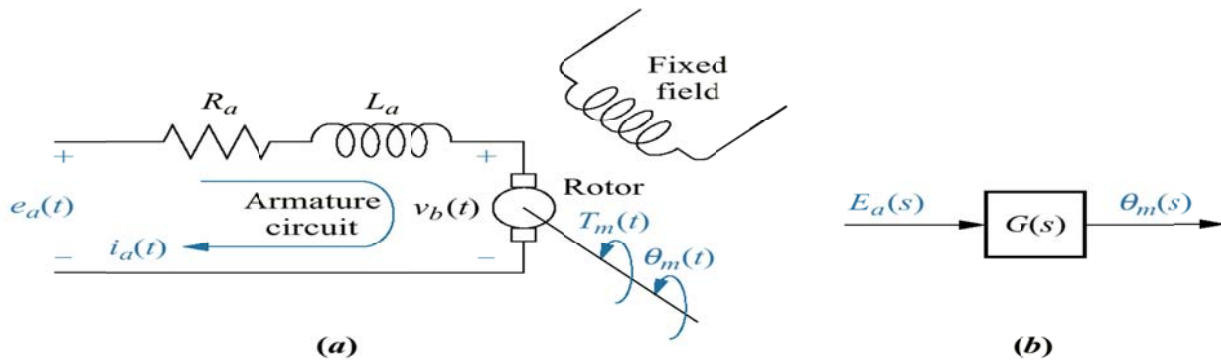


Figure 3.2 DC motor (a) Circuit diagram (b) Block diagram

Taking the Laplace transform of equation 3.2 gives

$$V_b(s) = sK_b\theta \quad (3.3)$$

The circuit equation for the electrical section of the motor can be written as

$$E_a(s) = R_a I_a(s) + L_a s I_a(s) + V_b(s) \quad (3.4)$$

The equation can also be written as:

$$I_a(s) = \frac{E_a(s) - K_b s \theta(s)}{L_a s + R_a} \quad (3.5)$$

The torque developed by the motor is proportional to the armature current and the equation is as follows

$$T_m(s) = K_t I_a(s) \quad (3.6)$$

Using the torque equation and the current equation a Simulink model of the DC motor operated robotic arm can be obtained.

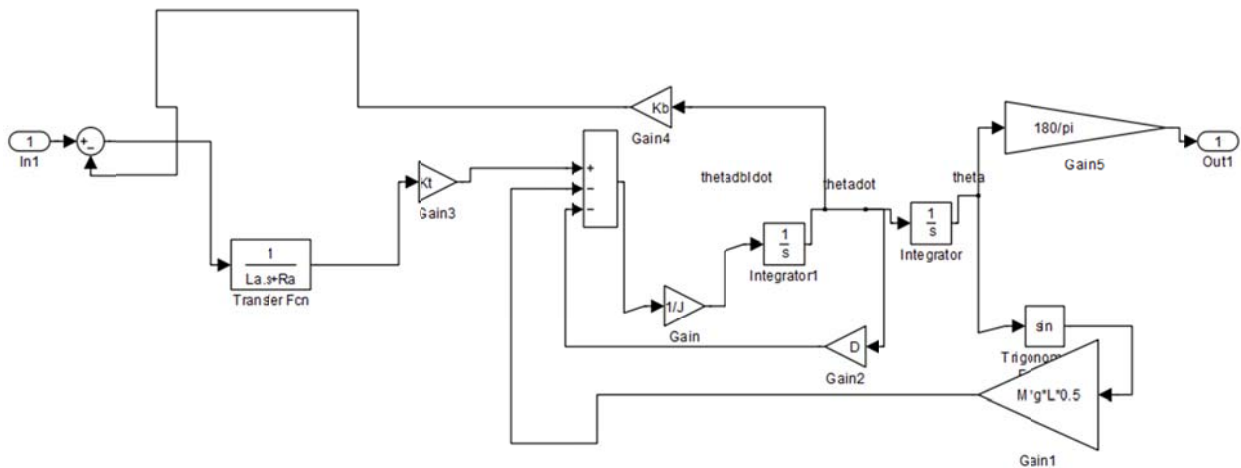


Figure 3.3 DC Motor and the Nonlinear Robotic Human Leg Combined

To control the robotic leg such that the DC motor can rotate it from 0 degrees to 90 degrees, a PID controller is first of all installed so that it can give the accurate actuating signal for the desired response of the DC motor operated robotic leg model. The PID controller used for this purpose is an adaptive PID controller which also includes a filter block to obtain the most efficient response. The PID block uses the compensator formula which is:

$$Kp + \frac{K_i}{s} + K_d \frac{N}{1+\frac{N}{s}} \quad (3.7)$$

where  $K_p$  is the proportional constant,  $K_i$  is the integral constant,  $K_d$  is the derivative constant and  $N$  is known as the filter coefficient.

The Simulink model of the PID controller is as follows:

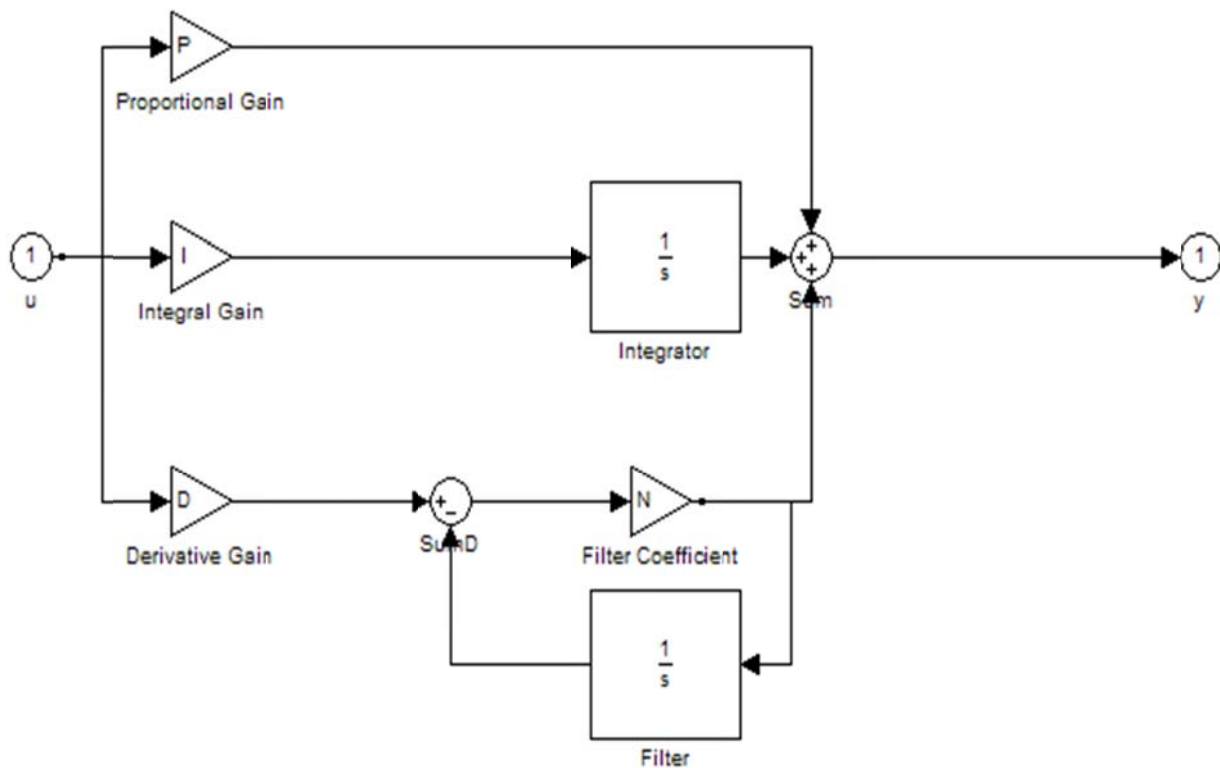


Figure 3.4 Simulink Representation of the PID Controller



The optimized values used for the PID controller is tabulated as follows:

Table 3.1 Control Parameters of the PID controller for Robotic leg

Parameters	Values
Proportional constant ( $K_p$ )	6.9
Integral constant ( $K_i$ )	8.0
Derivative constant ( $K_d$ )	1.4
Filter coefficient (N)	46.7

The Simulink model incorporating the PID controller is shown below:

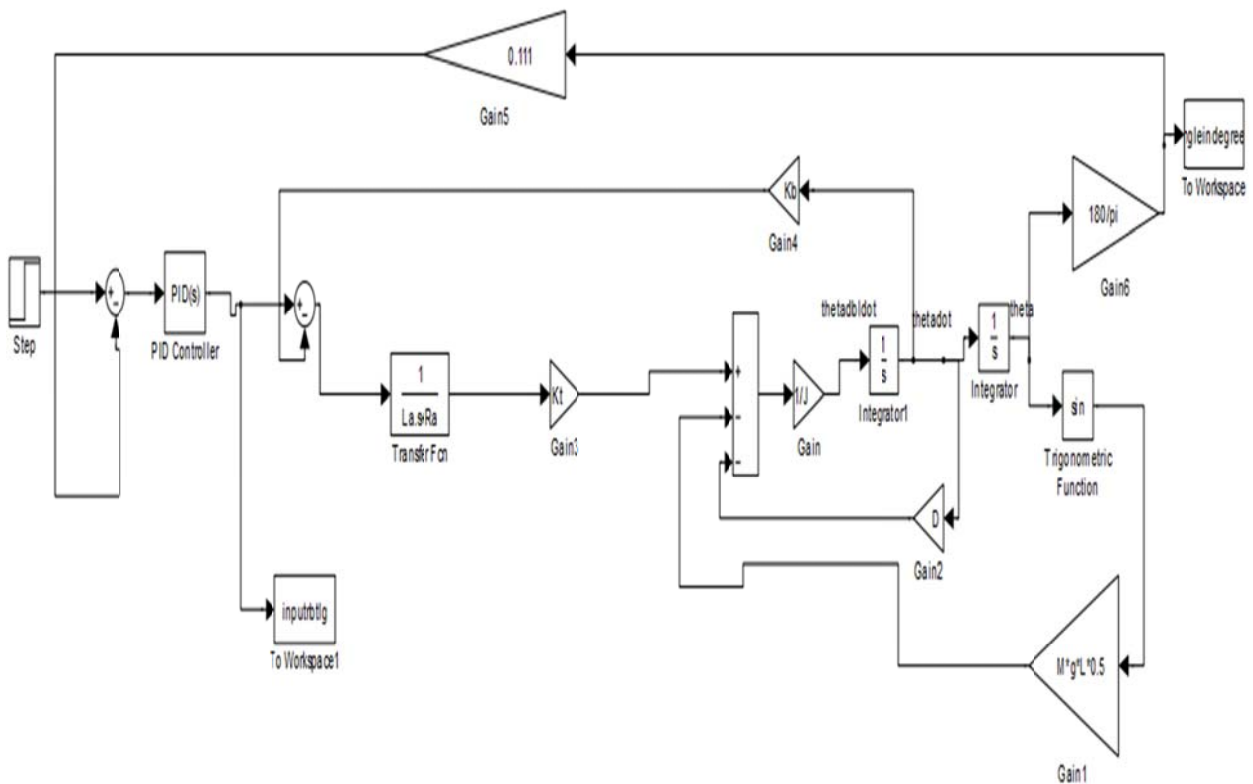


Figure 3.5 Simulink model incorporating the PID controller

The system input is a voltage signal with a range from 0 to 10 V. This signal is used to provide the control voltage and current to the DC motor. The goal is to design a controller so that a voltage ranging from 0 to 10 volts corresponds linearly to an angular rotation of a robotic arm from 0 to 90 degree respectively. Since we want to move the robotic human leg to a proper angular position corresponding to the input, a positional servomechanism will be needed to convert the angular position information into corresponding voltage and negatively feedback the signal back into the system so that it can be compared with the input voltage signal and fed to the input of the controller. The feedback signal in voltage is  $E_f = \theta_L \times K_p$  where  $K_p$  is the proportional constant and is equal to the ratio of the input to the desired position output. In our case 10V should correspond to 90 degree [36]. Hence  $K_p$  which also known as the Load angle Velocity feedback will be equal to  $10/90 = 0.1111$ .

The same procedure is carried out using the MPC controller and the Simulink model is shown as follows

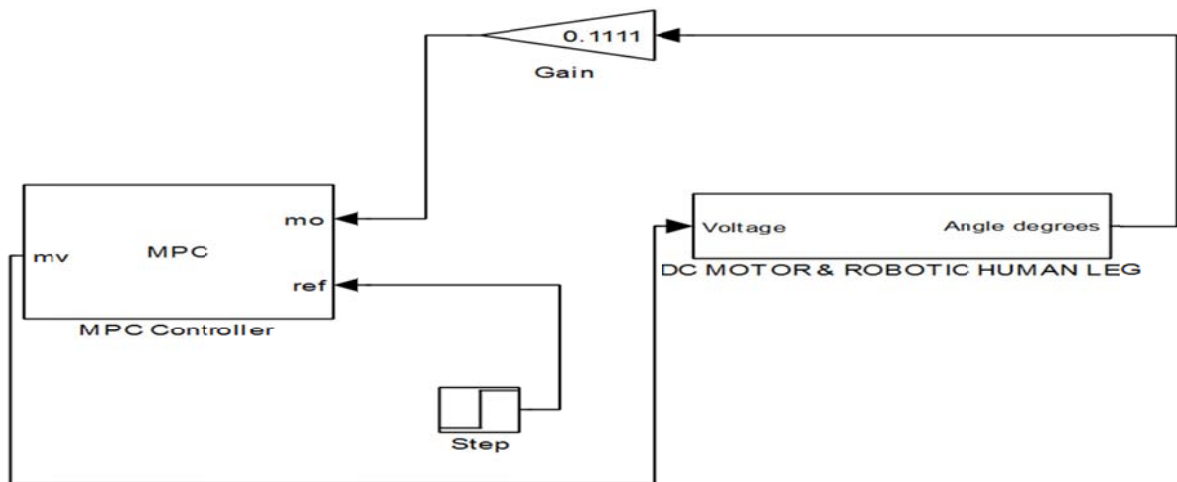


Figure 3.6 Simulink Model of the MPC Controller for the DC MOTOR OPERATED ROBOTIC LEG

Finally a comparative analysis of the performance of the robotic leg by both MPC and PID controller is obtained by undergoing simulations in Matlab. Signal values ranging from 10V to 4V is chosen and the desired output for such actuating signals should be from 90 to 30 degree respectively. The model predictive controller is designed such that the parameters chosen are shown in the tabular format as follows:

Table 3.2 Control Parameters of the MPC Controller for the Robotic Leg

Parameters	Values
Control Interval	0.1
Prediction Horizon	10
Control Horizon	2

The response of the system using the PID controller for an input of 10 volts is shown below:

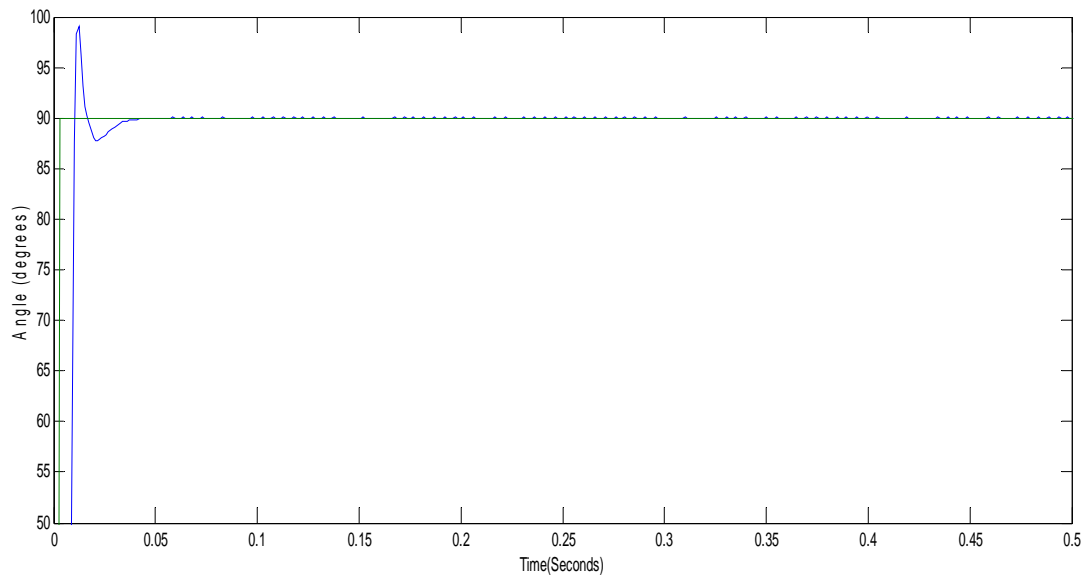


Figure 3.7 Angular Response using Reference Voltage of 10 V corresponding to an angle of  $90^{\circ}$  using PID Controller

The settling time for the system is 0.04 seconds but the overshoot is around 8%.

The response of the system using the MPC controller for an input of 10 volts is shown below:

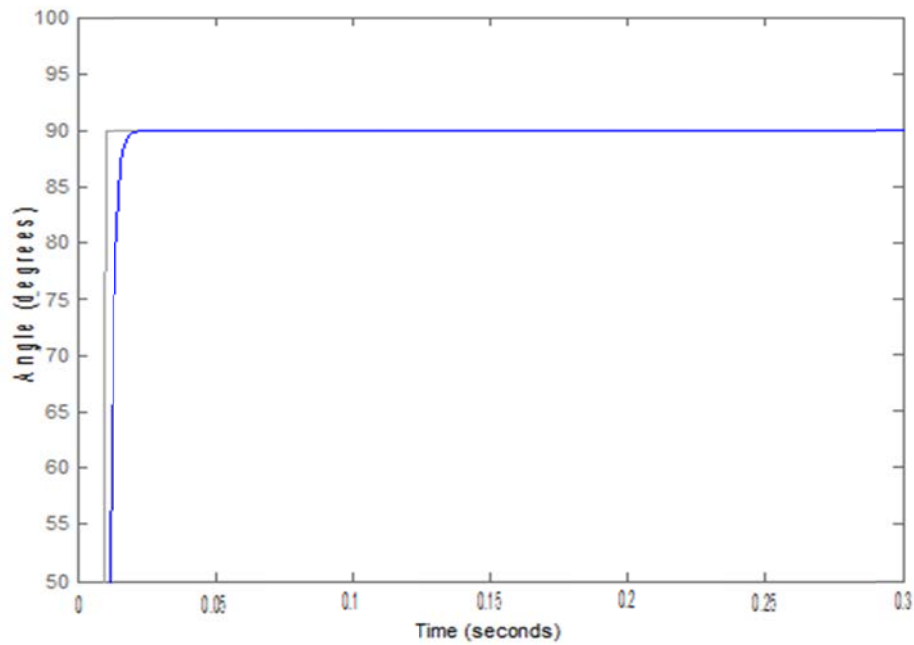


Figure 3.8 Angular Response Using MPC Controller

Settling time was reduced to 0.037s and overshoot was eliminated using the MPC controller

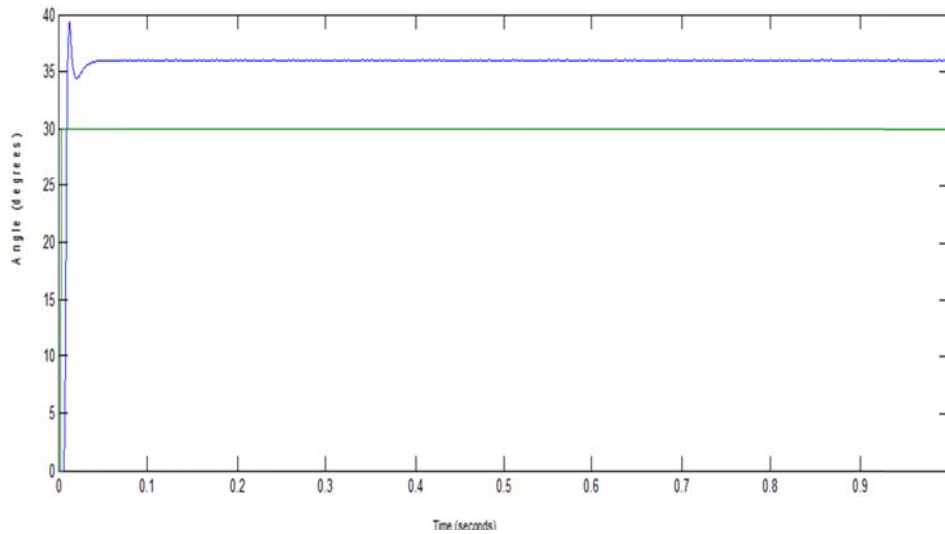


Figure 3.9 Angular response for an input voltage of 4 V using PID controller

The output was way beyond the desired angle of 30 degrees. A steady state error of 5% was obtained. The response was very poor.

Carrying out the same operation using MPC controller we got a far better response as shown below:

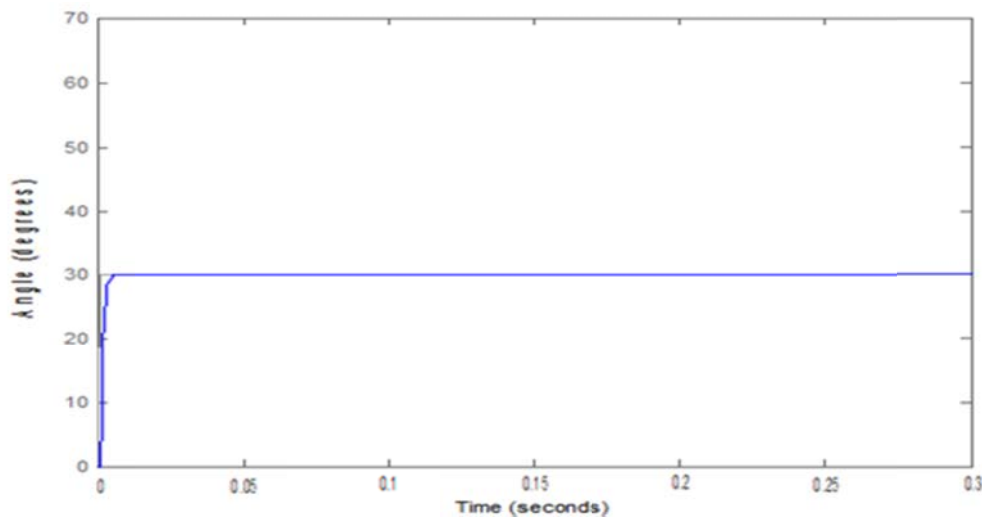


Figure 3.10 Angular response for a input voltage of 4 V using MPC controller

In this case we obtained a settling time of 0.025 seconds and no overshoot at all.

This simple nonlinear model was linearized using Taylor series method and the state space model used by the MPC controller was

$$\begin{bmatrix} \dot{x}_1 \\ \dot{x}_2 \end{bmatrix} = \begin{bmatrix} 0 & 1 \\ -11.73 & -2.657 \end{bmatrix} \begin{bmatrix} x_1 \\ x_2 \end{bmatrix} + \begin{bmatrix} 0 \\ 2.394 \end{bmatrix} E_a \quad (3.8)$$

$$y = 6.363x_1 \quad (3.9)$$

where  $x_1 = \theta$ .

The corresponding transfer function of the linear model is described as follows:

$$\frac{\theta(s)}{E_a(s)} = \frac{15.24}{s^2 + 2.657s + 11.73} \quad (3.10)$$

The eigenvalues of the system matrix were  $-1.3285 + 3.1568i$  &  $-1.3285 - 3.1568i$  showing that the system is stable because the real parts of the eigenvalues are negative.

### 3.1.2 Summary of the Result

From the simulation result we see that the MPC not only did improve the performance of the rotational control of the Robotic leg but also ensured a fast reponse which makes the system a very effective stepping stone for analyzing more complex model of the Robotic leg using MPC.

## 3.2 Modeling of a Stirred Tank Heater

Stirred tank heater is used in many chemical processes. Often tank is heated, either by a coil or a jacket surrounding the tank. The temperature in the tank is maintained by the flow rate

of a fluid through the jacket and can also be controlled by the temperature of the fluid in the jacket. The model obtained involves four state variables in which only two variables mainly the temperature of the fluid through the jacket and the flow rate of the fluid through the jacket are taken as the two manipulated variables and the other variables are considered as unmeasured disturbances. The objective is to maintain the temperature of the tank for optimum yield of the chemical process taking place in the tank at multifarious operating conditions. Moreover the parameters for the model are taken as standardized values of a certain chemical process where the temperature of the tank needs to be maintained at a certain optimum temperatures.

The assumptions taken to develop the mathematical dynamic model of the stirred tank heater are as follows [35]:

1. A constant volume with constant liquid density and heat capacity
2. Perfect Mixing in both Tank and Jacket
3. Inflow and outflow of the fluid in the Jacket and Tank is assumed to be constant.

A pictorial representation of a typical Stirred Tank heater is illustrated as follows

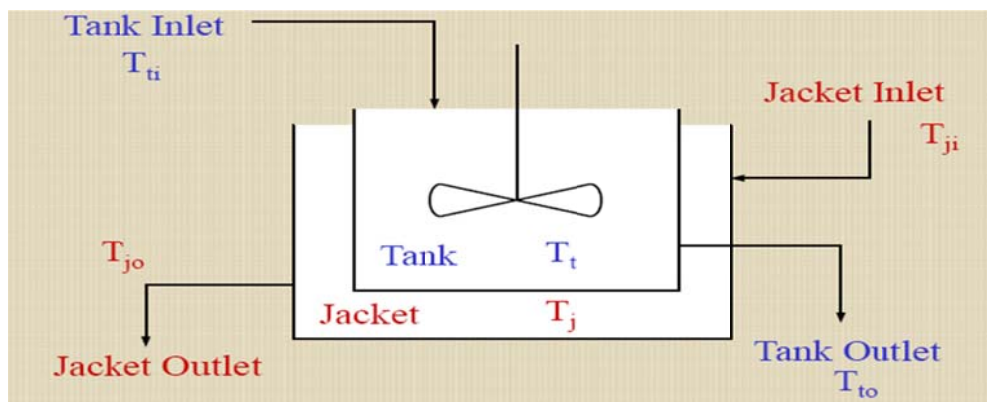


Figure 3.11 Stirred Tank Heater

The governing mathematical equation can be represented as follows:

1. Conservation of Mass around the Tank and Jacket gives:

$$\frac{d}{dt}(\rho_t V_t) = \rho_t \dot{V}_{ti} - \rho_t \dot{V}_{to} \quad (3.11)$$

$$\frac{d}{dt}(\rho_t V_t) = \rho_t \dot{V}_{ti} - \rho_t \dot{V}_{to} \quad (3.12)$$

Since constant volume is assumed hence both the equations will yield zero.

2. Conservation of Energy around the Tank and Jacket gives [35][48]:

$$\frac{dT_t}{dt} = \frac{\dot{V}_t}{V_t} (T_{ti} - T_{to}) + \frac{\dot{Q}}{\rho_t V_t c_{pt}} \quad (3.13)$$

$$\frac{dT_j}{dt} = \frac{\dot{V}_j}{V_j} (T_{ji} - T_{jo}) + \frac{\dot{Q}}{\rho_j V_j c_{pj}} \quad (3.14)$$

$$\dot{Q} = hA(T_j - T_t) \quad (3.15)$$

From the above equations a dynamic model of a stirred tank heater can be obtained. The Simulink model of the stirred water tank heater is shown below.

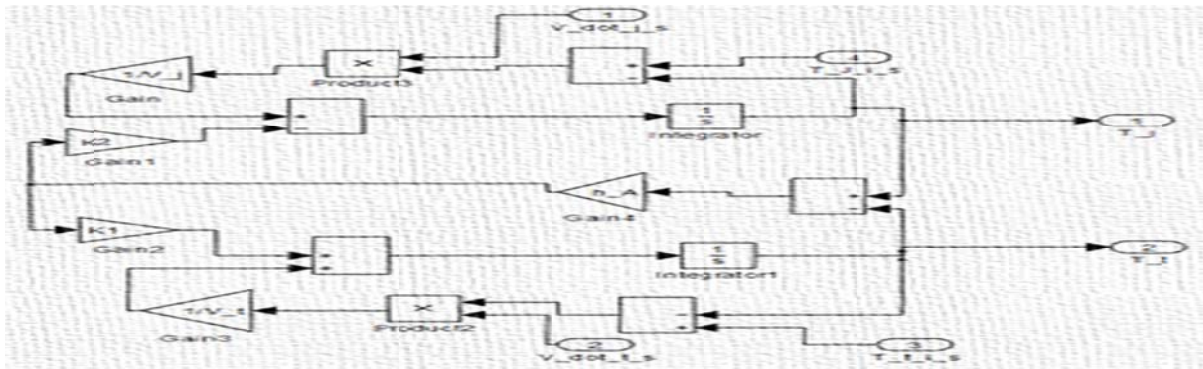


Figure 3.12 Total Simulink Representation of the Stirred Tank Heater



The input-output Simulink model of the stirred water tank heater is shown below.

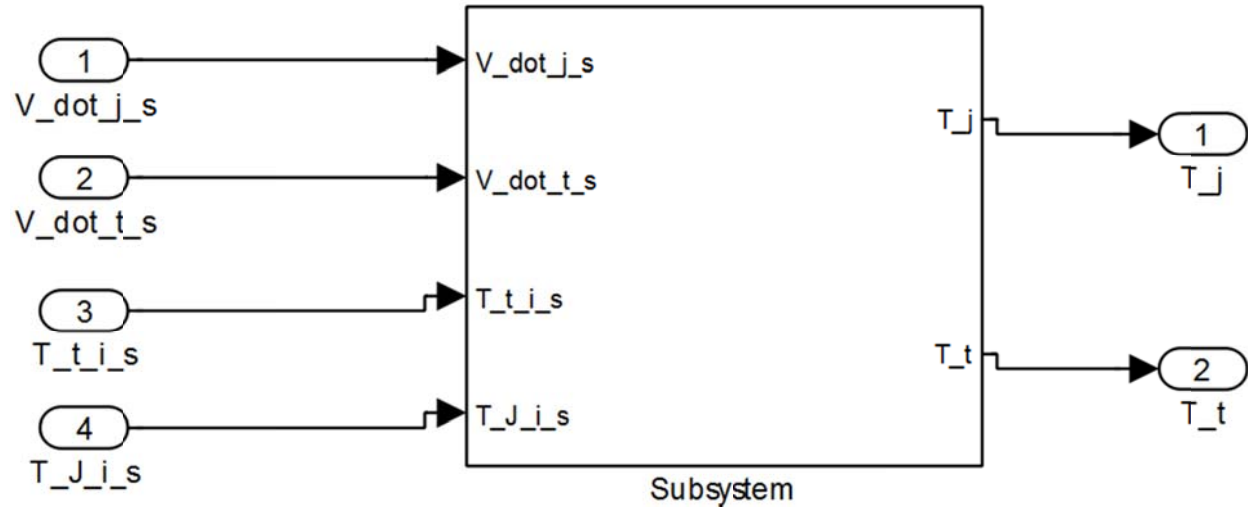


Figure 3.13 Input - Output Simulink Model of the Stirred Water Tank Heater

Since it is convenient and necessary for the model predictive controller to be able to process a linear model, the linearized model is obtained via the linmod command in Matlab. The obtained LTI State Space equation for the nonlinear Stirred Water Tank Heater model is as follows:

$$\begin{bmatrix} \dot{x}_1 \\ \dot{x}_2 \end{bmatrix} = \begin{bmatrix} -4.5 & 3 \\ 0.3 & -0.4 \end{bmatrix} \begin{bmatrix} x_1 \\ x_2 \end{bmatrix} + \begin{bmatrix} 50 & 0 & 0 & 1.5 \\ 0 & -7.5 & 0.1 & 0 \end{bmatrix} \begin{bmatrix} \dot{V}_j \\ \dot{V}_t \\ T_{ti} \\ T_{ji} \end{bmatrix} \quad (3.16)$$

$$\begin{bmatrix} y_1 \\ y_2 \end{bmatrix} = \begin{bmatrix} 1 & 0 \\ 0 & 1 \end{bmatrix} \begin{bmatrix} x_1 \\ x_2 \end{bmatrix} + \begin{bmatrix} 0 & 0 & 0 & 0 \\ 0 & 0 & 0 & 0 \end{bmatrix} \begin{bmatrix} \dot{V}_t \\ \dot{V}_j \\ T_{ti} \\ T_{ji} \end{bmatrix} \quad (3.17)$$

where  $x_2$  is the temperature of the tank  $T_t$  to be controlled.

Now our objective is to keep the temperature of the tank at 150 °F under different operating conditions. Initially only the flow rate of the fluid through the jacket was used as the manipulated

variable while the other variables were kept constant and considered as unmeasured disturbances. Taking the values of the disturbances as:

- Tank inlet flow rate ( $\dot{V}_t$ ) = 1 ft<sup>3</sup>/min
- Tank inlet temperature ( $T_{ti}$ ) = 50 °F
- Jacket inlet temperature ( $T_{ji}$ ) = 200 °F

we finally simulate the model with all the specifications using first of all using the PID controller. The Simulink model for this purpose is shown below:

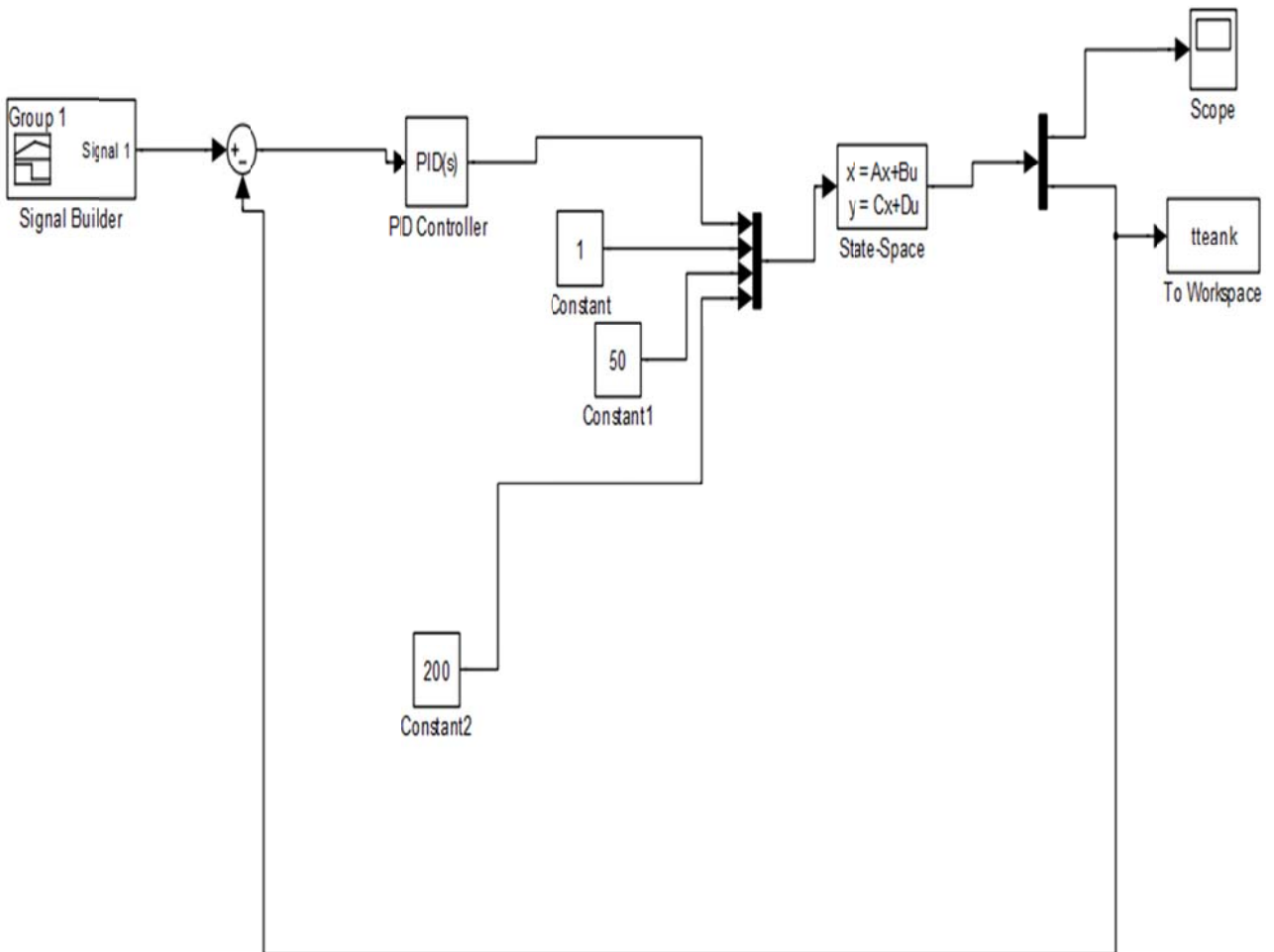


Figure 3.14 PID Control of the STH with  $\dot{V}_j$  as the manipulated variable

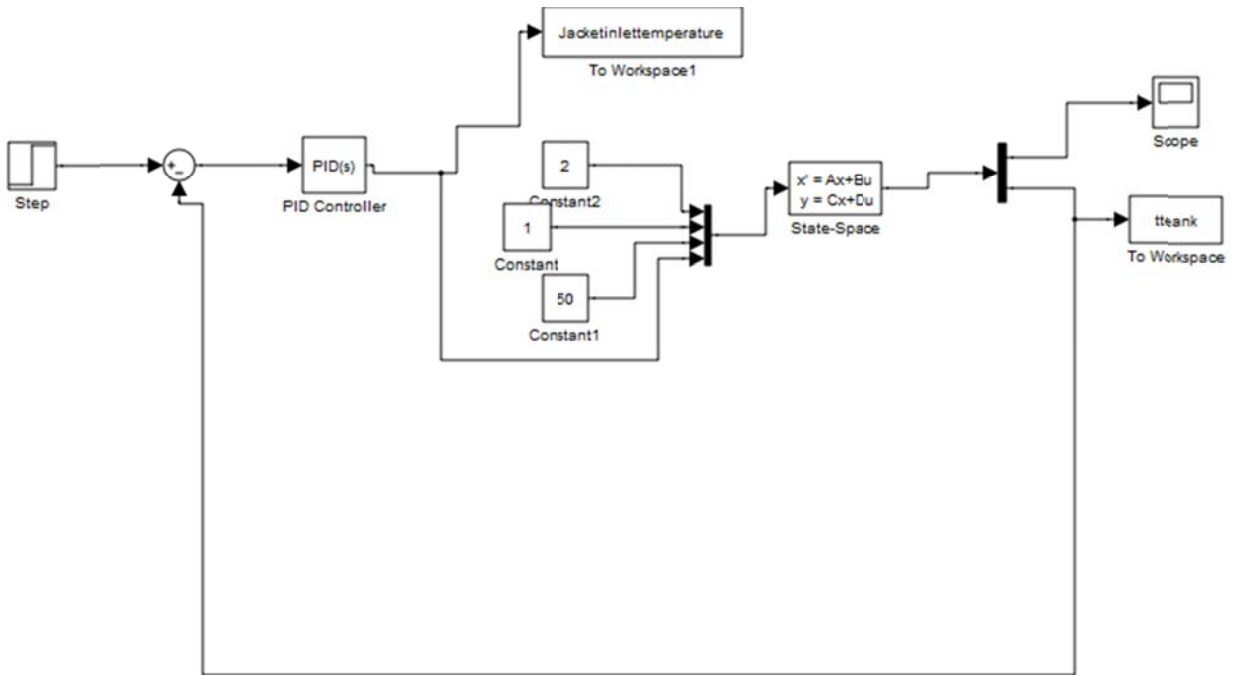


Figure 3.15 PID control of the STH with  $T_{ji}$  as the manipulated variable

During simulation with the PID controller the input disturbance values were initially set to 1 ft<sup>3</sup>/min (Tank inlet flow rate  $\dot{V}_t$ ), 50 °F (Tank inlet temperature  $T_{ti}$ ) and 200 °F (Jacket inlet temperature  $T_{ji}$ ) and then altered. In this case Jacket inlet flow rate ( $\dot{V}_j$ ) is the manipulated variable. The same process was carried out but the manipulated variable was considered to be the Jacket inlet temperature ( $T_{ji}$ ). Under such a scenario the input disturbances were initially set to 50 °F (Tank inlet temperature  $T_{ti}$ ), 1 ft<sup>3</sup>/min (Tank inlet flow rate  $\dot{V}_t$ ) and 2 ft<sup>3</sup>/min (Jacket inlet flow rate  $\dot{V}_j$ ). The results obtained from the simulations are shown below:

### Simulation Results for the PID Controller in STH

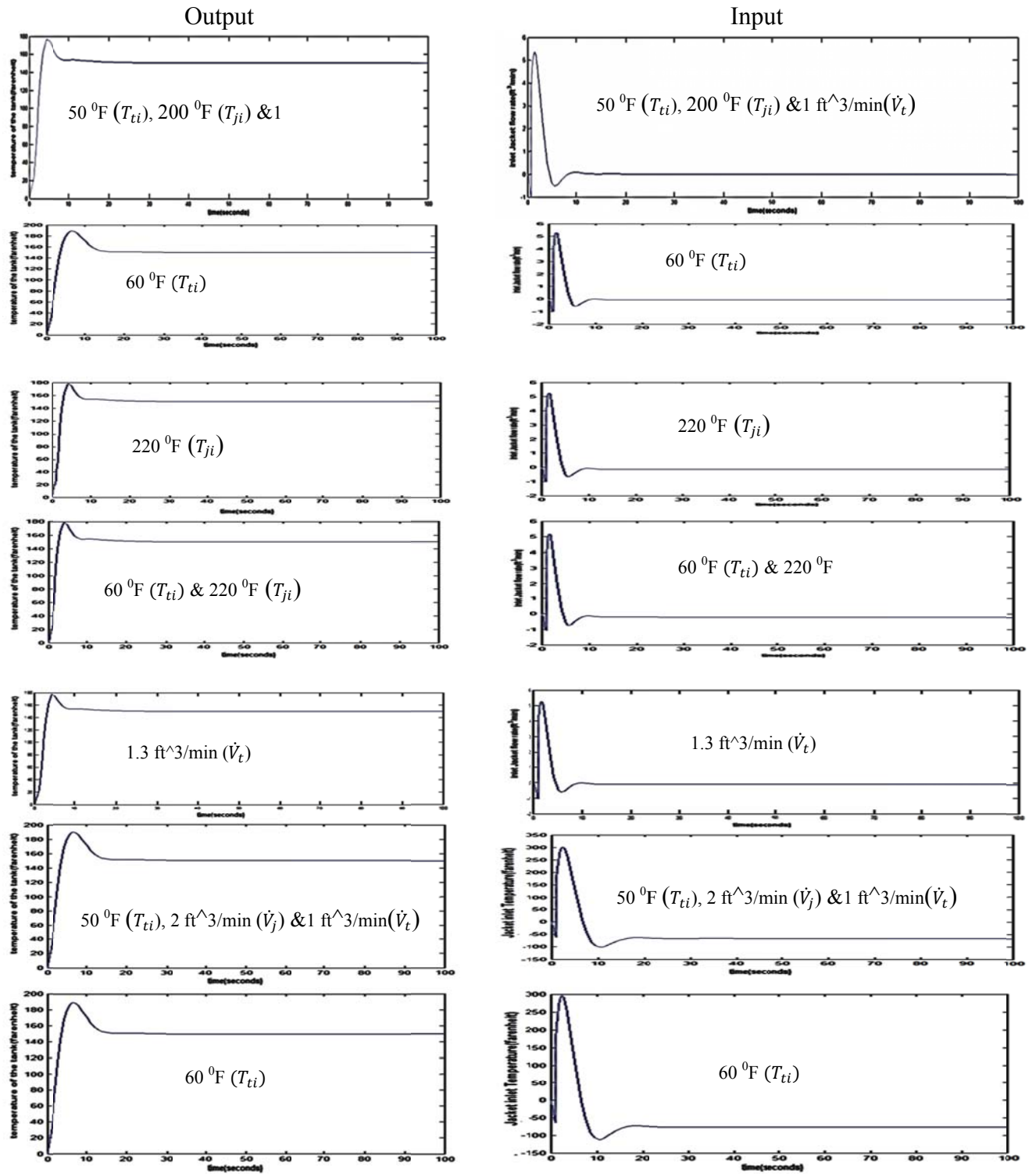


Figure 3.16 Simulation results using the PID controller for STH

The Model Predictive Controller Block used to carry out the simulations under different operating conditions with  $\dot{V}_j$  as the manipulated variable is shown below:

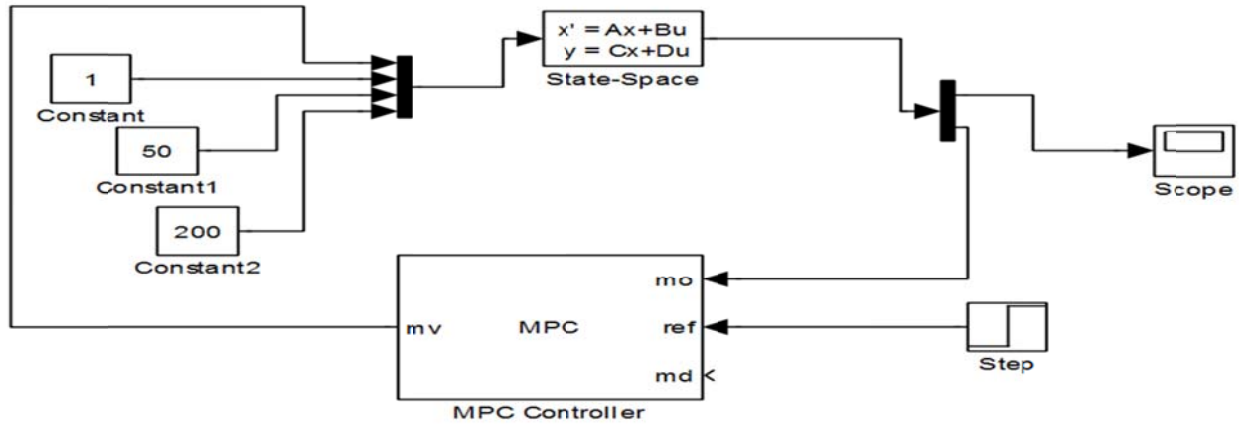


Figure 3.17 MPC Simulink block for controlling STH with  $\dot{V}_j$  as the manipulated variable

The Model Predictive Controller Block Diagram used to carry out the simulations under different operating conditions with the Jacket Inlet temperature  $T_j$  as the manipulated variable is shown below:

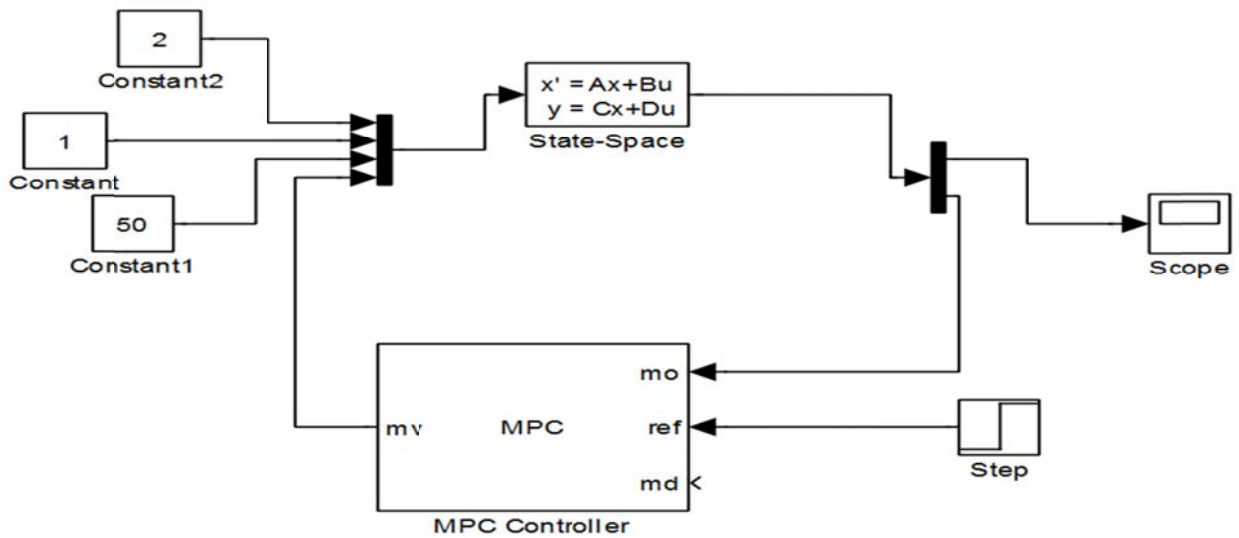


Figure 3.18 MPC of the Stirred Water Tank Heater with  $T_j$  as the manipulated variable

The same simulation is carried out with MPC and the results obtained are shown below:

### Simulation Results for the SISO MPC Controller in STH

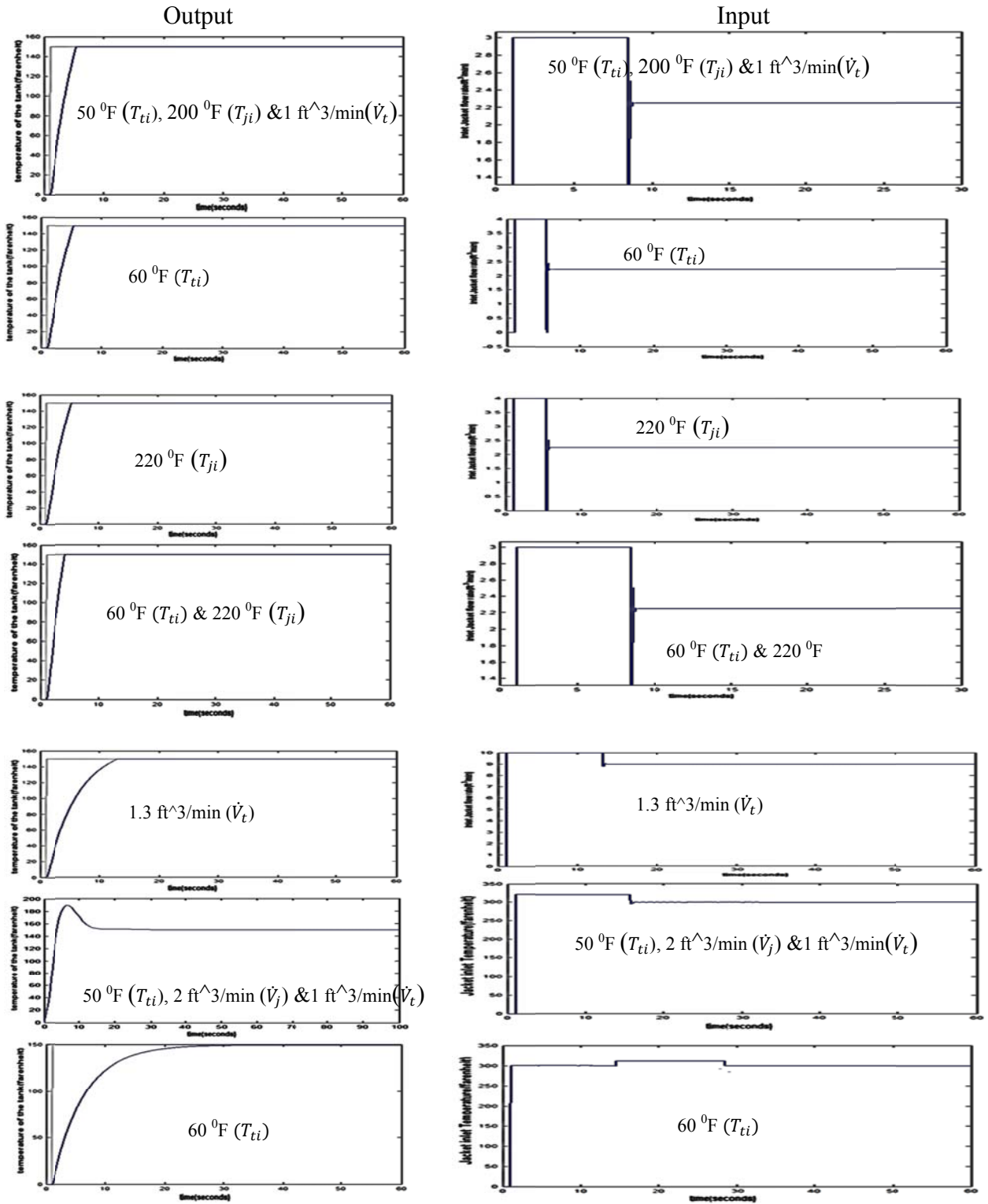


Figure 3.19 Simulation Results for the SISO MPC control of STH

Finally two manipulated variables which are the Jacket inlet flow rate  $\dot{V}_j$  and Jacket inlet temperature ( $T_j$ ) are considered for maintaining the temperature of the tank at 150 °F while keeping the other variables constant at 1 ft<sup>3</sup>/min (Tank inlet flow rate  $\dot{V}_t$ ) and 50 °F (Tank inlet temperature  $T_{ti}$ ) respectively (Case 15). MPC controller is designed to carry out this operation while the PID controller is rendered quite unworthy because it is generally applicable for Single-Input Single-Output (SISO) systems but not for a Multiple-input Single-Output (MISO) systems.

The block diagram of the system utilizing the MPC controller is shown below:

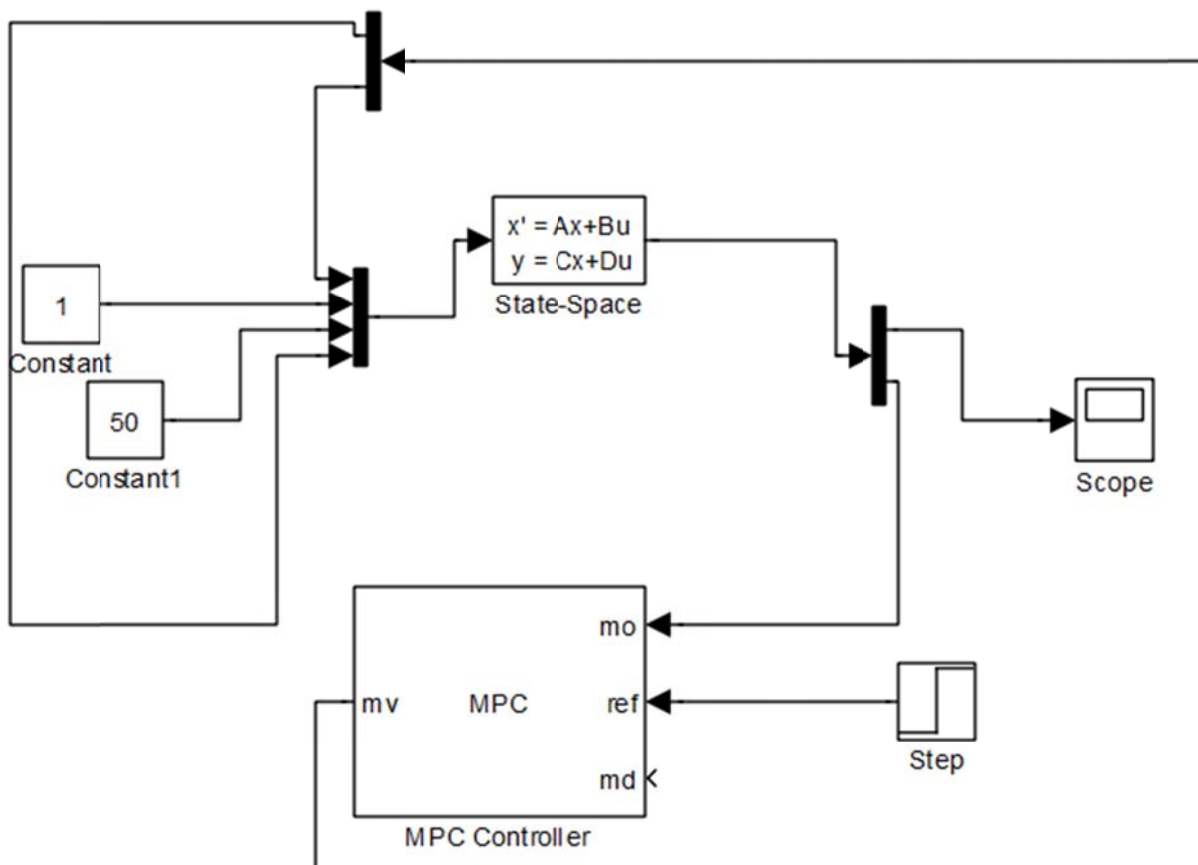


Figure 3.20 MISO MPC Representation of the Stirred Water Tank Heater

The simulation results obtained for this MISO system are shown below.

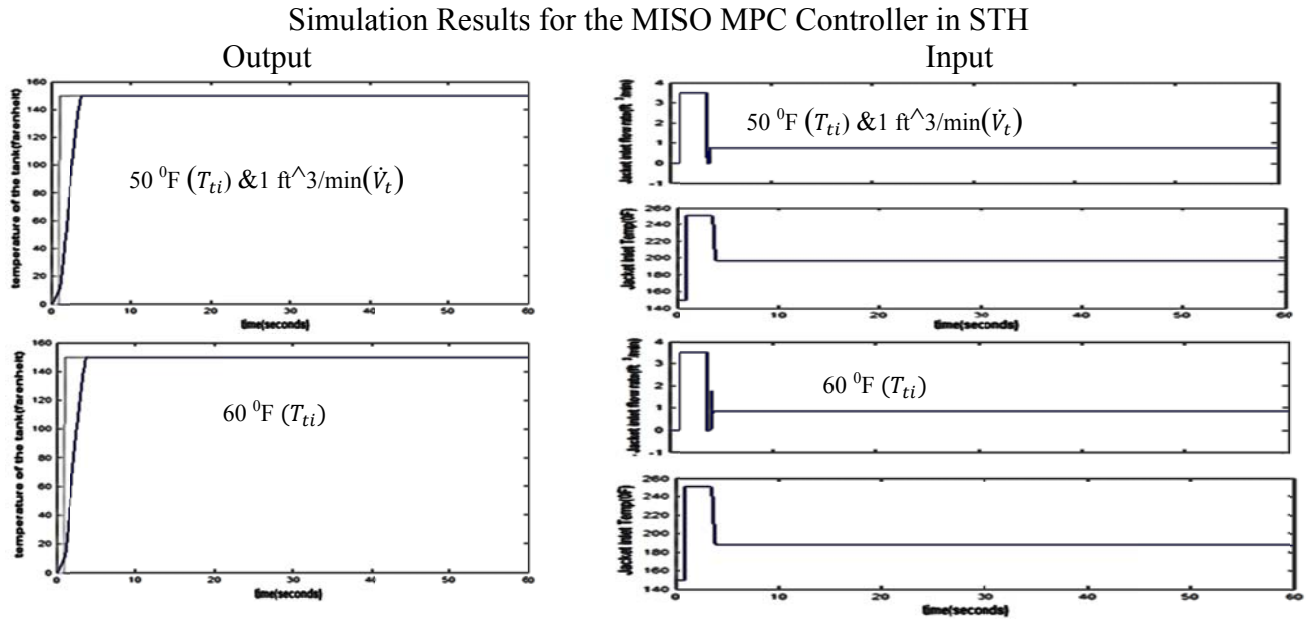


Figure 3.21 Simulation results using the MISO MPC control of STH.

All the simulations done with the MPC controller was carried out with the parameters of the MPC controller fixed to:

Table 3.3 Control Parameters of the MPC controller for STH

Parameters	Values
Control Interval	0.05
Prediction Horizon	20
Control Horizon	5



The PID controller with the input variable as the (Jacket inlet flow rate  $\dot{V}_j$ ) was adaptively tuned to:

Table 3.4 Control Parameters of the PID controller for STH

Parameters	Values
Proportional Constant ( $K_p$ )	0.07
Integral Constant ( $K_i$ )	0.012
Derivative Constant ( $K_d$ )	-0.054
Filter Coefficient (N)	0.78

While undergoing the control of temperature of the tank it was necessary to maintain the inputs to non-negative value because under no circumstances would the fluid through the jacket be drawn out of the system and the temperature of the fluid in the Jacket cannot be decreased to a temperature below 0 °F because it would require a complicated actuator to undergo a negative change. The temperature of the tank was required to be maintained at 150 °F which is the optimum temperature for wet process chemical plants such as Warewashing and food processing operations.

### 3.2.1 Linearization of the STH system

The linearization was carried out using the Matlab command `linmod` and the linearization block present in the Simulink environment. The state space model obtained is shown below

$$\begin{bmatrix} \dot{x}_1 \\ \dot{x}_2 \end{bmatrix} = \begin{bmatrix} -3.296 & 3 \\ 0.3 & -0.4 \end{bmatrix} \begin{bmatrix} x_1 \\ x_2 \end{bmatrix} + \begin{bmatrix} -0.598 & 0.2962 \\ 0 & 0 \end{bmatrix} \begin{bmatrix} u_1 \\ u_2 \end{bmatrix}$$

$$y_1 = \begin{bmatrix} 0 & 1 \end{bmatrix} \begin{bmatrix} x_1 \\ x_2 \end{bmatrix}$$

where  $u_1$  and  $u_2$  represents  $T_j$  and  $\dot{V}_j$  respectively and the output  $y_2$  represents  $T_t$  which is the temperature of the tank

The corresponding transfer function representation of the state space model was obtained and is shown below:

$$\frac{T_t(s)}{T_j(s)} = \frac{0.1794}{s^2 + 3.696s + 0.4185}$$

$$\frac{T_t(s)}{\dot{V}_j(s)} = \frac{0.08886}{s^2 + 3.696s + 0.4185}$$

The system was stable because the real part eigenvalues of the system matrix was **-3.5793** and **-0.1169** respectively which are negative and hence all trajectories in the neighborhood of the fixed point will be directed towards the fixed point.

### 3.2.2 Tabulation of the Simulated Results

The simulated results obtained can be tabulated to delineate the comparison of the performance using both MPC and PID controllers.

Table 3.5 Tabulated summary of the simulated results of the STH System.

Controllers	Input Variables				Settling Time	Overshoot %	Manipulated variable	
	$(\dot{V}_T)$	$(\dot{V}_j)$	$(T_{ji})$	$(T_{ti})$			Min	Max
<b>PID</b>	1	Manipulated	200	50	36	26	-0.97	5.4
	1	Manipulated	200	60	33	29	-1.1	5.2
	1	Manipulated	220	50	31	29	5.15	-1.0
	1	Manipulated	220	60	29	30	-1.2	5.1
	1.3	Manipulated	200	50	40	29.5	-1.03	5.24
	1	2	Manipulated	50	20	38	-128	300
	1	2	Manipulated	60	22	38	-124	300
<b>MPC</b>	Input Variables				Settling Time	Overshoot %	Manipulated variable (1/2)	
	$(\dot{V}_T)$	$(\dot{V}_j)$	$(T_{ji})$	$(T_{ti})$			Min	Max
	1	Manipulated (1)	200	50	9	0	0 (1)	3 (1)
	1	Manipulated (1)	200	60	7	0	0 (1)	4 (1)
	1	Manipulated (1)	220	50	8	0	0 (1)	4 (1)
	1	Manipulated (1)	220	60	5	0	0 (1)	2.9(1)
	1.3	Manipulated	200	50	13	0	0 (1)	10 (1)
	1	2	Manipulated (2)	50	17	0	0 (1)	319 (2)
	1	2	Manipulated (2)	60	34	0	0 (1)	311 (2)
	1	Manipulated (1)	Manipulated (2)	50	3	0	0 (1) 150 (2)	3.3 (1) 250 (2)
	1	Manipulated (1)	Manipulated (2)	60	3.1	0	0 (1) 150 (2)	3.5 (1) 250 (2)

### 3.2.2 Summary of the Simulated Results for the STH system

From the tabulated data showing all the data's obtained from the simulation results, it is quite apparent that the performance of MPC completely overhauls the performance of the adaptive PID controller. In the case of controlling the Stirred Tank Heater with a single input, it was observed that the input values had gone negative at certain time intervals while using PID controller. This is derogatory for maintaining STH temperature of the tank because it will lead to

a complicated and a costly actuator for controlling the temperature of the tank. It is also necessary to eliminate any presence of overshoot responses while controlling STH. This was not possible with the PID controller. All of these negative impacts while using the PID controller were totally eliminated when MPC was used. It was also possible to control the temperature of STH by manipulating both the Jacket Inlet flow rate and Jacket Inlet Temperature with the MPC controller. Moreover the input controlling signals were also constrained for optimum performance of STH. Hence the temperature control of STH has been quite remarkably improved by using the Model Predictive Controller.

### **3.3 Modeling of a single phase Speed Controller and a Current Controller for a Linearized Small Signal model of a Switched Reluctance Motor (SRM)**

The design of the speed controller is an integral part of any drive system development. Due to the nonlinear nature of the SRM, the development of a block diagram is not as straightforward as in the case of the dc motor. Realizing that the SRM is very much similar to the series-excited dc machine (as seen from the torque and equivalent circuit development earlier in our text), it is feasible to proceed with linearization of the system equations to obtain a small signal model and a block diagram from which the transfer functions are developed. The linearized mechanical equation can also be written as

$$\frac{1}{2} i^2 \frac{dL(\theta, i)}{d\theta} - T_e = J \frac{d\omega_m}{dt} + B \omega_m \quad (3.18)$$

Where B is the rotor friction constant and  $\omega_m$  is the mechanical speed. The linearized voltage equation is written as:

$$v = R_s i + \frac{d[L(\theta, i)i]}{dt} = R_s i + L(\theta, i) \frac{di}{dt} + \frac{dL(\theta, i)}{d\theta} \omega_m i \quad (3.19)$$

The states of the SRM plant are the rotor speed,  $\omega_m$ , and the phase current,  $i$ . By examining the SRM voltage and torque equations, there are terms where states are multiplied together resulting in a nonlinear system. It is desirable to derive a linearized model to utilize a vast amount of knowledge on linear systems to synthesize the current and speed controllers. This section contains the derivation of a linearized model of the SRM. The inductance is assumed to be constant for the sake of simplification. The inductance is chosen as the mean value between the aligned inductance and the unaligned inductance at the rated current. The derivative of inductance with respect to rotor position is also assumed to be a constant and calculated between the conduction angles at the rated current value. This derivative has only a small change over the operating range of the motor.

Perturbing the system around a steady-state operating point with small signals, the new system states and inputs are-

$$i = i_o + \delta i \quad (3.20)$$

$$\omega_m = \omega_{mo} + \delta \omega_m \quad (3.21)$$

$$v = v_o + \delta v \quad (3.22)$$

$$T_l = T_{lo} + \delta T_l \quad (3.23)$$

where the extra subscript  $o$  indicates steady-state values of the states and inputs, and the small signals are indicated by  $\delta$  preceding the variables. Substituting the perturbed variables in the

system equations, it is seen that the steady-state terms cancel and the residual of these equations gives:

$$\frac{d\delta i}{dt} = \left( -\frac{R_s}{L} - \frac{1}{L} \frac{dL}{d\theta} \omega_{mo} \right) \delta i - \frac{1}{L} \frac{dL}{d\theta} i_o \delta \omega_m + \frac{\delta V}{L} \quad (3.24)$$

$$\frac{d\delta \omega_m}{dt} = \left( +\frac{1}{J} \frac{dL}{d\theta} i_o \right) \delta i - \frac{B}{J} \delta \omega_m - \frac{\delta T_e}{J} \quad (3.25)$$

Hereafter, the following substitutions are used:

$$R_{eq} = R_s + \frac{dL}{d\theta} \omega_{mo} \quad (3.26)$$

$$K_b = \frac{dL}{d\theta} i_o \quad (3.27)$$

$$\delta e = \frac{dL}{d\theta} i_o \delta \omega_m \quad (3.28)$$

where  $R_{eq}$  is the equivalent resistance,  $K_b$  is the emf constant, and  $\delta e$  is the induced emf. By using the small signal voltage and torque equations, the following block diagram is derived for the linearized SRM plant model. Note that this model is similar to the separately excited dc machine model. The block diagram of the linearized SRM is shown in Figure 4.1. The load is assumed to be frictional; that way, the load torque is treated as an integral component of the system but not as a disturbance. For the sake of simplicity, only one current feedback loop is shown in Figure 4.1, even though for a q-phase SRM there will be q current feedback loops.

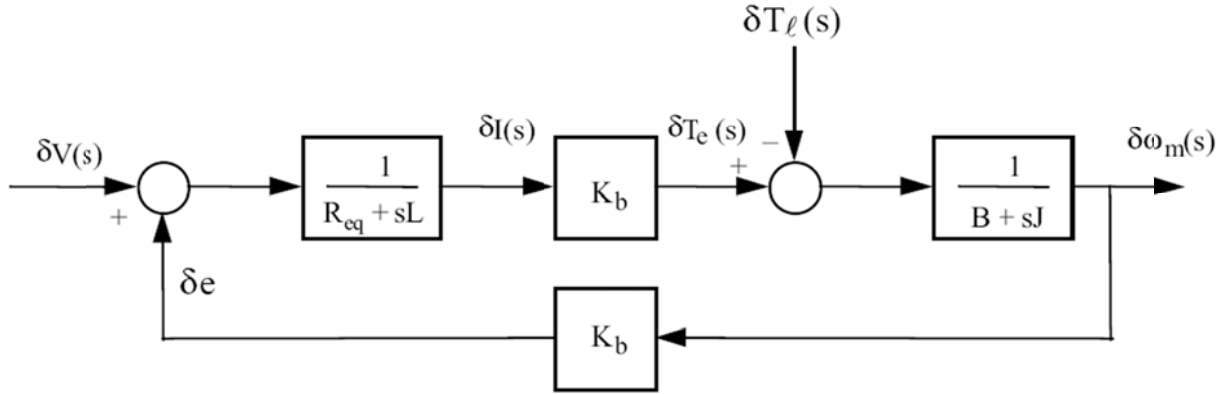


Fig. 3.22 Block diagram of the linearized SRM.

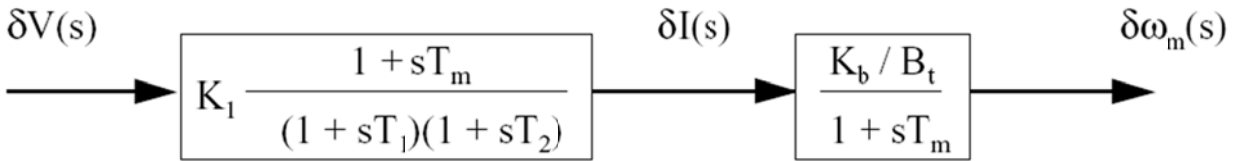


Figure 3.23 Reduced block diagram of the SRM.

These current loops are identical but shifted in phase, so there is no need to consider more than one phase for control modeling, analysis, and design. The back emf and current feedback loops cross each other, resulting in cross coupling of these loops. Further, it makes the task of designing a current controller and later the speed controller very difficult. For this reason, the SRM block diagram is cast in a different form by removing the back emf feedback loop but absorbing it in a form which leads to a two-stage transfer function as shown in Figure 3.52, very much similar to dc machines, where

$$B_t = B + B_e \quad (3.29)$$

$$K_1 = \frac{B_t}{K_b^2 + R_{eq}B_t} \quad (3.30)$$

$$T_m = \frac{J}{B_t} \tag{3.31}$$

$$-\frac{1}{T_1}, -\frac{1}{T_2} = -\frac{1}{2} \left[ \frac{B_t}{J} + \frac{R_{eq}}{L} \right] \pm \sqrt{\frac{1}{4} \left( \frac{B_t}{J} + \frac{R_{eq}}{L} \right)^2 - \frac{K_b^2 + R_{eq} B_t}{JL}} \tag{3.32}$$

The design of the current controllers is an integral part of any drive system development. Due to the nonlinear nature of the SRM, the development of a block diagram is not as straightforward as in the case of the dc motor. Realizing that the SRM is very much similar to the series-excited dc machine (as seen from the torque and equivalent circuit development earlier in our text), it is feasible to proceed with the linearized small signal model of the Switched Reluctance Motor (SRM)

A speed-controlled SRM drive system is shown in Figure 5.1. Rotor speed is converted to a voltage signal through a tachogenerator which then is filtered to provide  $\omega_r^*$ , which is then compared with its reference. The speed error signal is amplified and conditioned with the speed controller. The output of this speed controller is a voltage signal proportional to current command signal  $I^*$ . A current feedback signal in volts is compared with this command signal to generate a current error. The current error is processed through a current controller to produce a command signal for the power converter. The power converter is

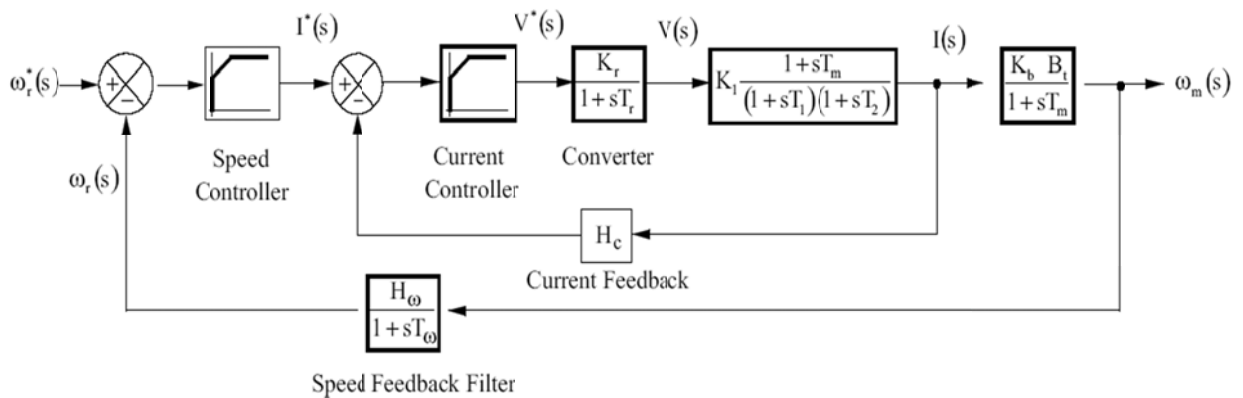


Figure. 3.24 Block diagram of the SRM drive.



Modeled as a gain with a first-order lag, and both of these constants maybe measured or evaluated in the design stage. The power converter gain is

$$K_r = \frac{V_{dc}(\text{nominal})}{V_{cm}} \quad (3.33)$$

where  $V_{cm}$  is the maximum control voltage.

The time constant of the converter,  $T_r$ , assuming PWM control of the converter with a carrier frequency of  $f_c$ , is given by:

$$T_r = \frac{T_c}{2} = \frac{1}{2f_c} \quad (3.34)$$

To validate the design technique using the linearized model, a 5-hp SRM is considered for the current and speed controller designs [38].

### 3.3.2 Single Phase Current Control of the Linearized Small Signal SRM

Based on the linearized Small Signal Model of the Switched Reluctance Motor (SRM), it is possible to use a PID controller to control the current signal of SRM. The PID controller used in this case is an adaptive PID controller and the block diagram of the controller is shown below:

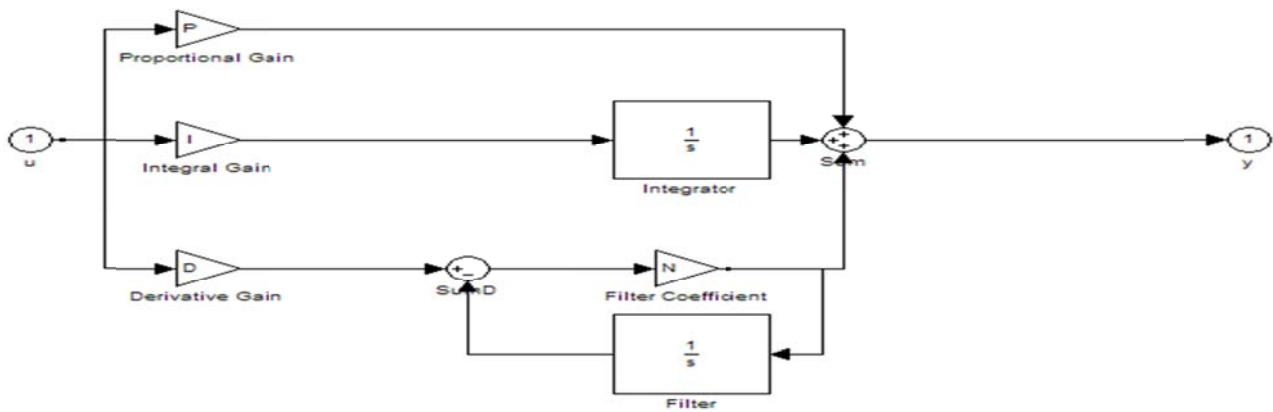


Figure 3.25 Simulink Model of the PID Controller

Incorporating the PID controller in the form of a subsystem in the current controller loop of the SRM drive, the Block diagram [31][37] of the current loop is shown below:

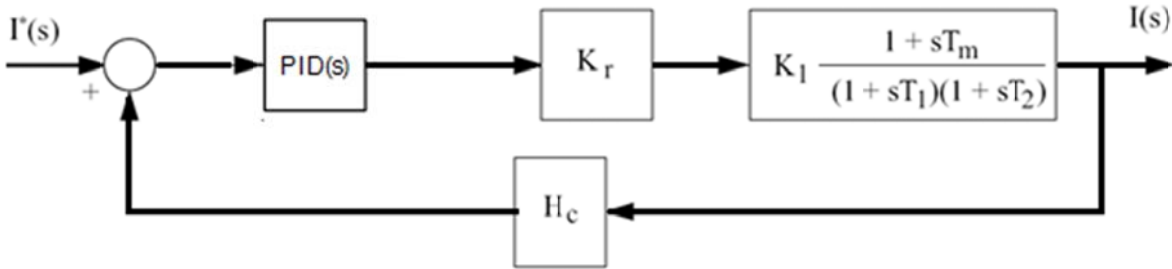


Figure 3.26 Block Diagram of the Current Control Loop

The representation of the Block diagram as a simulink model for carrying out simulation is shown below:

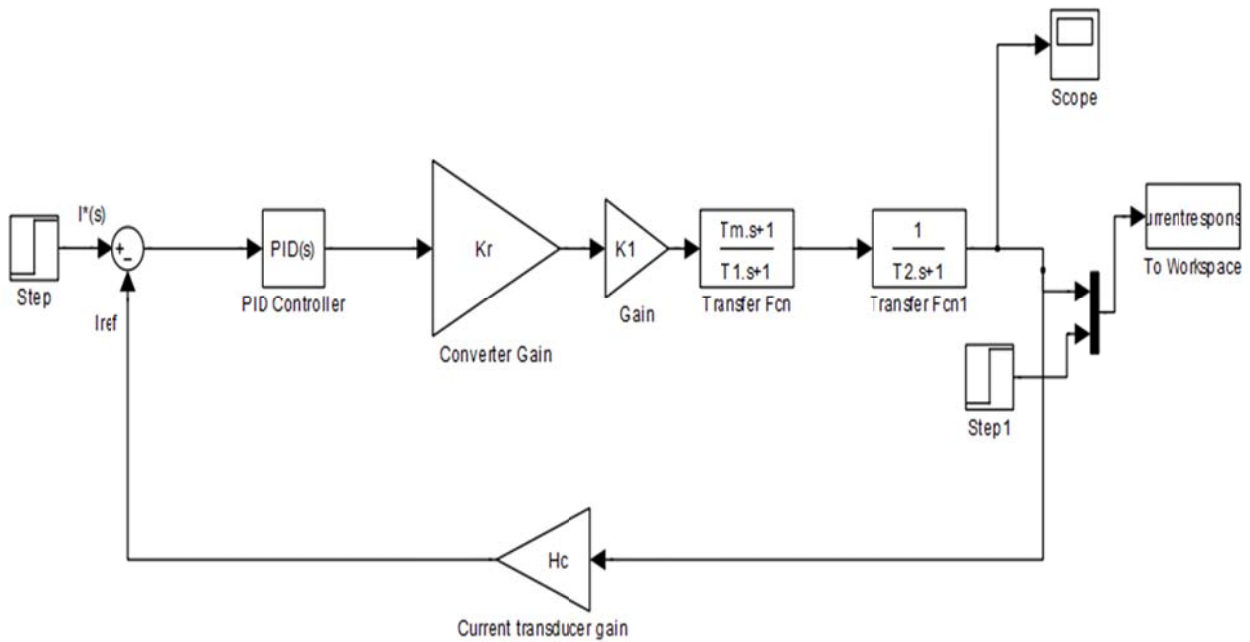


Figure 3.27 Simulink Model of the Current Control Loop using PID

The simulation result obtained for the step response of 1.5 p.u of the current control loop using the PID controller is shown below:

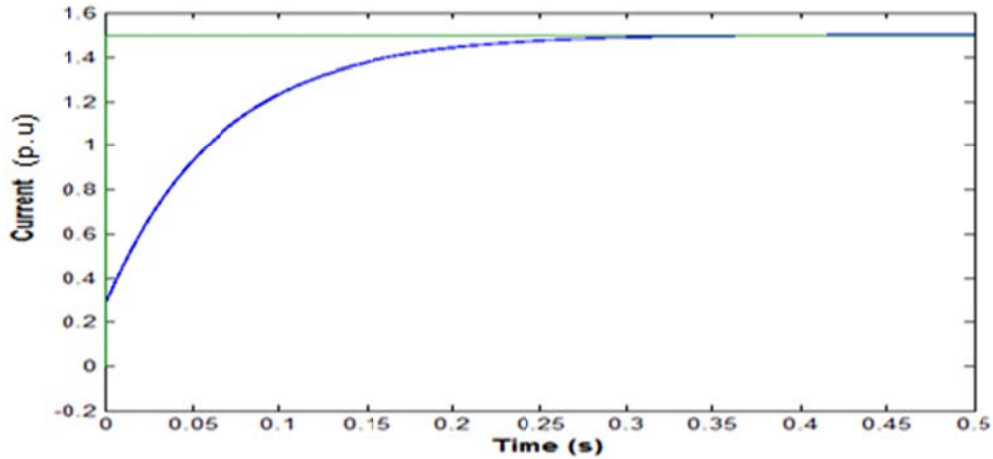


Figure 3.28 Step Response for a reference current of 1.5 p.u

The settling time is 0.32 seconds and the overshoot percentage is zero.

Using Model Predictive Controller as the current controller in the current loop and representing the current controlled loop in the form of a Simulink model for carrying out simulations is shown below:

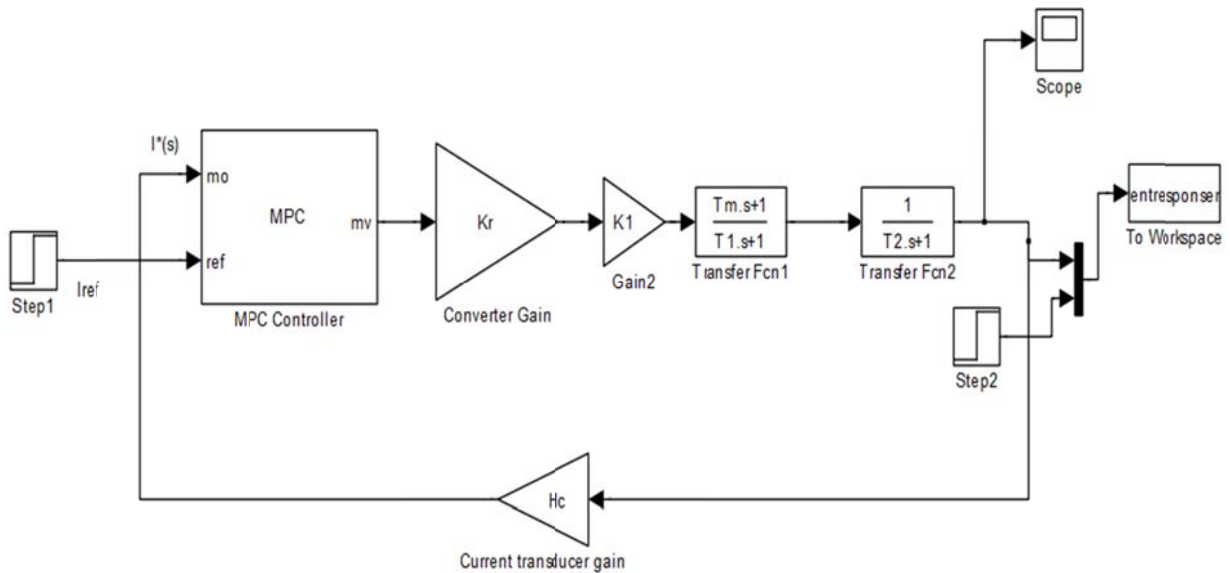


Figure 3.29 Simulink Model of the Current Control Loop using MPC.

The simulation result obtained for the step response of 1.5 p.u using the MPC controller is shown below:

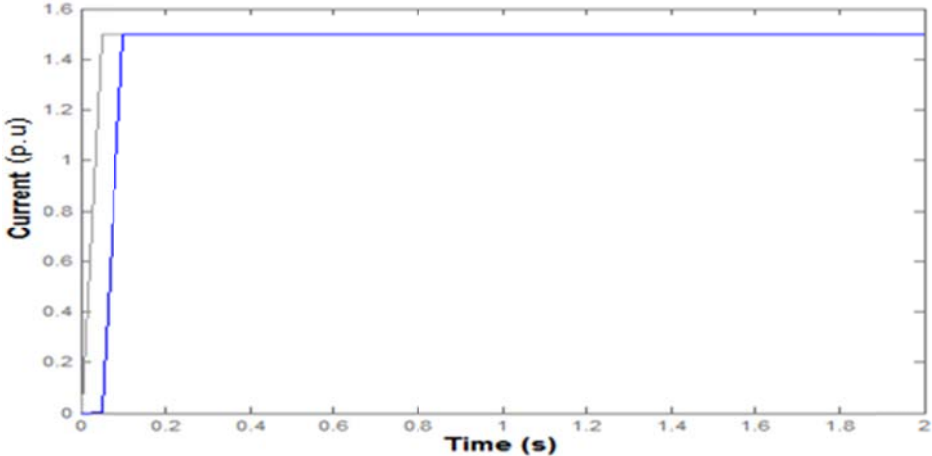


Figure 3.30 Step Response for a reference current of 1.5 p.u

The settling time is 0.1 seconds and the overshoot percentage is zero.

The simulation result carried out with a ramp response of a slope of 1.5 on the PID controlled current loop is shown below:

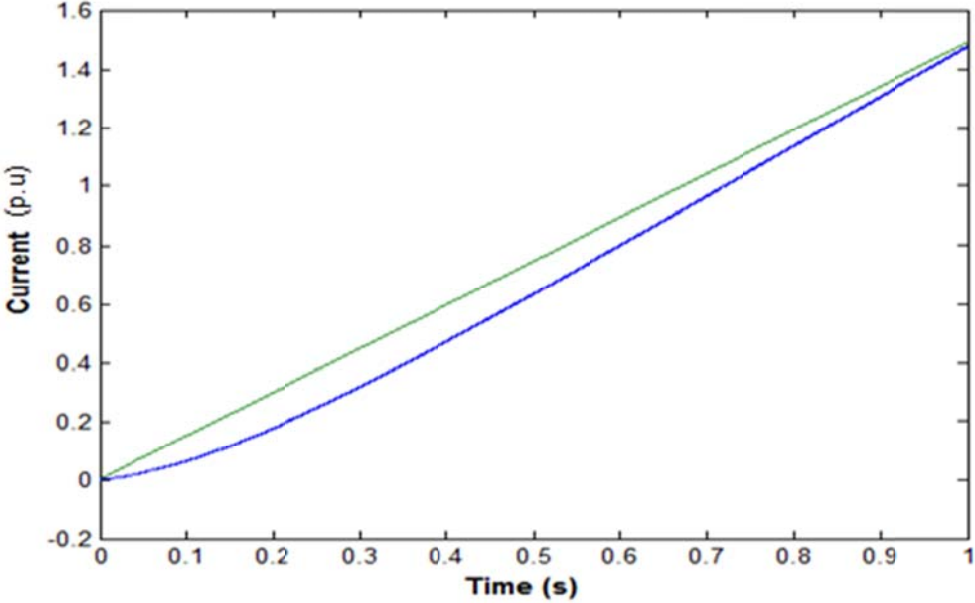


Figure 3.31 Ramp response for a reference ramp current of slope 1.5 using PID

The output has just been able to track the reference ramp current signal showing a decline in the performance with the PID controller.

The simulation results obtained for the same ramp signal using the MPC controller in the SRM current loop is shown below:

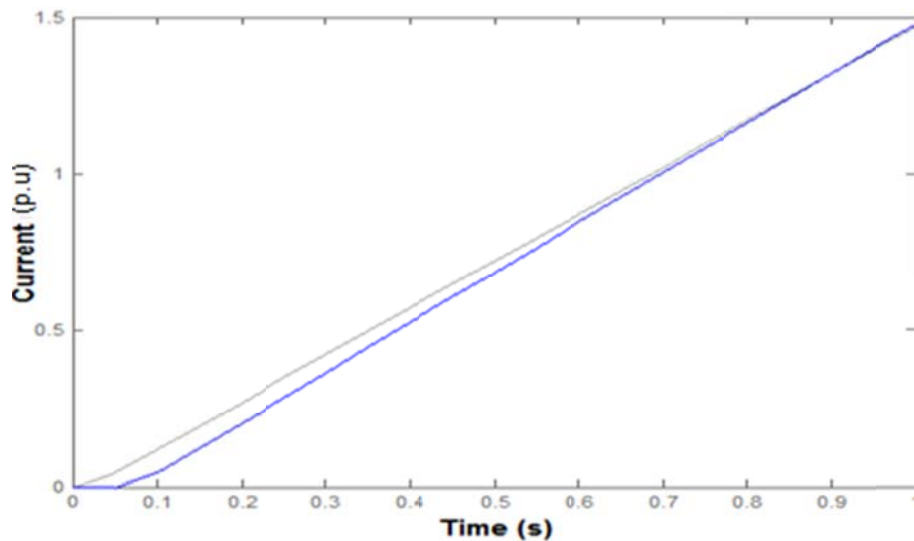


Figure 3.32 Ramp response for a reference ramp current of slope 1.5 using MPC

The output has been able to settle at 0.85seconds with no steady state error or overshoot.

### 3.3.3 Single Phase Speed Control of the Linearized Small Signal SRM

To simplify the design of the speed control loop, it is assumed that the delay of the current loop is negligible due to the fact that usually the speed of response of the current loop is at least ten times faster than the response of the speed loop. To further simplify the design equations, the current loop gain is approximated as unity and its time delay is neglected as it is very, very small compared to all other time constants. Normally, the delay due to the speed feedback may be neglected, which would reduce the system to a second-order system, but when

the speed feedback delay is comparable to the delay of the other subsystems it must be considered in the design process [39][42]. The block diagram of the approximatedSpeed Control loop is shown below.

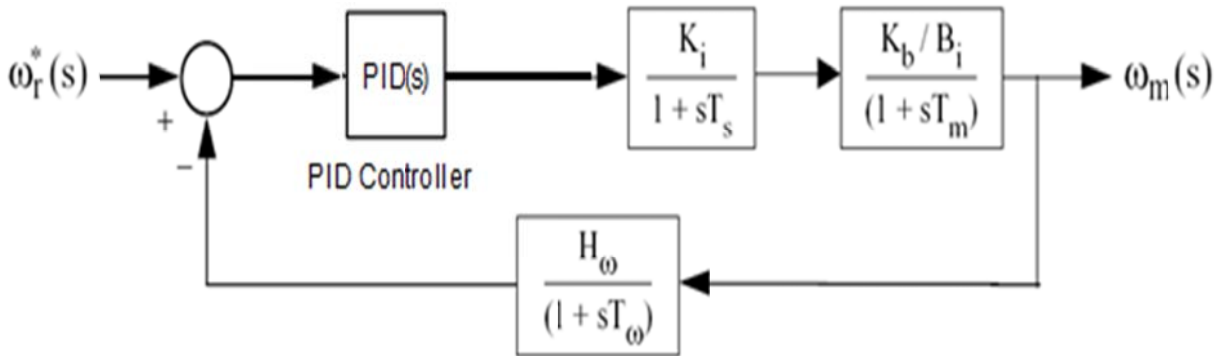


Figure 3.33 Approximated speed loop block diagram.

The representation of the speed control loop with a Simulink model using PID as the speed controller is shown below:

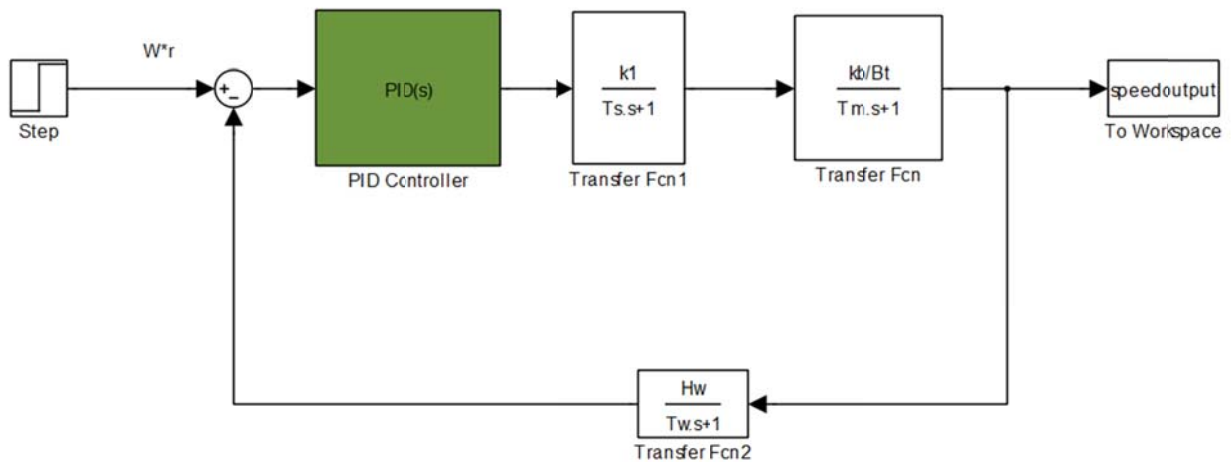


Figure 3.34 Simulink model of the Speed Control Loop using PID

The simulation result obtained for the step response of 1 p.u speed using the PID controller is shown below:

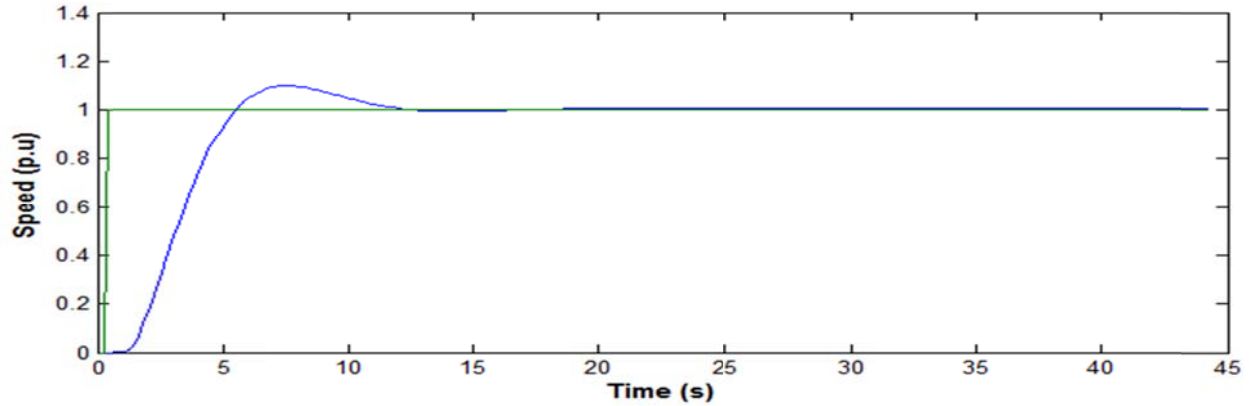


Figure 3.35 Step Response for a reference speed of 1.pu using PID

The settling point is 14 seconds and the overshoot percentage is 10.2%.

Using Model Predictive Controller as the speed controller in the speed loop and representing the speed controlled loop in the form of a Simulink model for carrying out simulations is shown below:

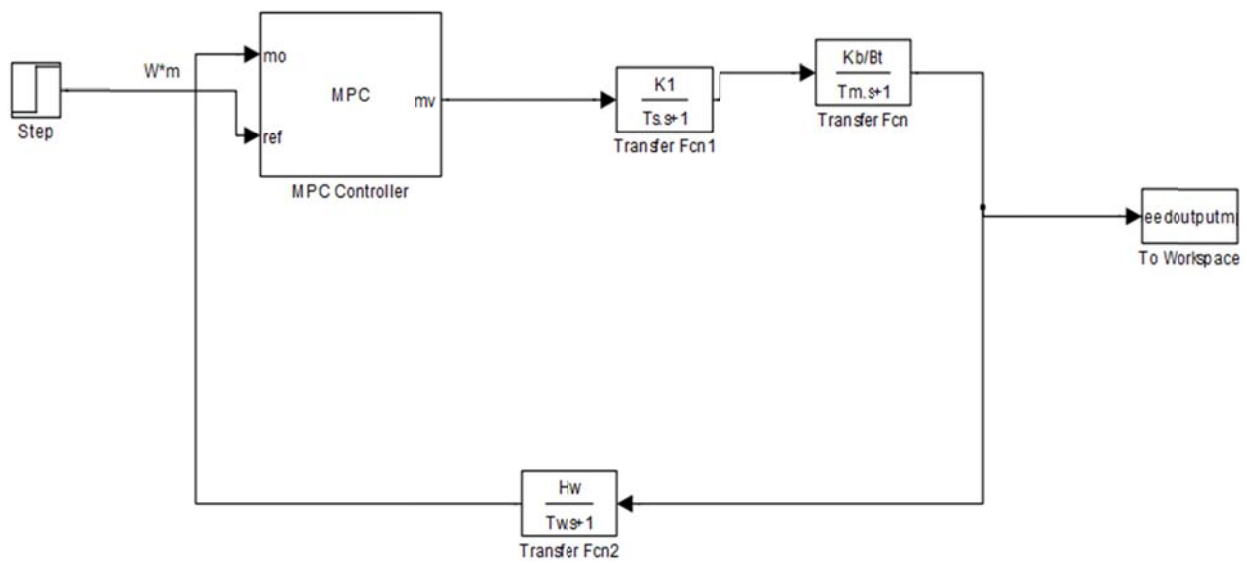


Figure 3.36 Simulink Model for the Speed Control Loop using MPC

The simulation result obtained for the step response of 1 p.u speed using the MPC controller is shown below:

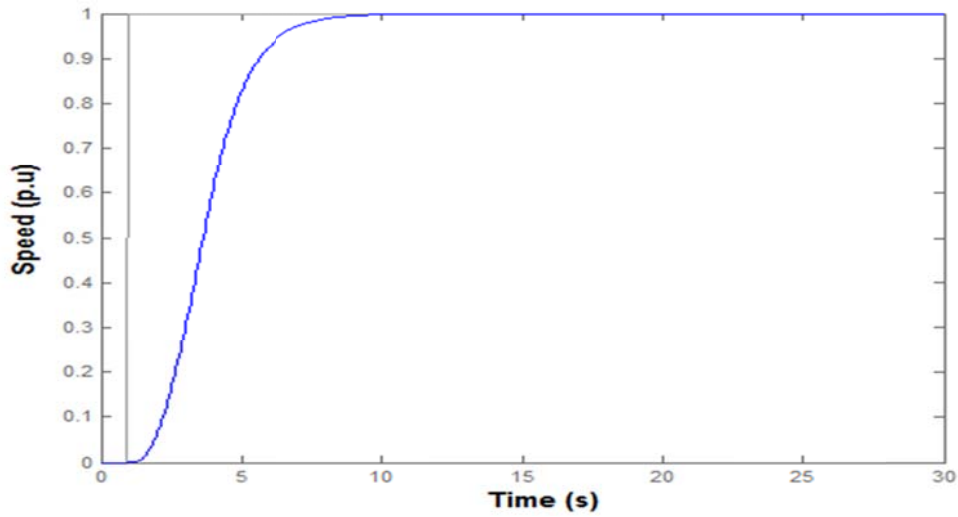


Figure 3.37 Step Response for a reference speed of 1.pu using MPC

The settling time is 9.2 seconds and the overshoot percentage is zero.

### 3.3.4 Tabulated results obtained from simulations:

Table 3.6 Result Comparison Using the Simulated results tabulated for the SRM system

System	Overshoot (%)		Settling time (sec)	
	MPC Controller	Only adaptive PID controller	MPC Controller	Only adaptive PID controller
Speed control loop	0	10	9.2	14
Current control loop	0	0	0.1	0.32
Current Control Loop with ramp signal	0	Damping was present	0.85 and the tracking ability was very satisfactory	Very bad tracking ability



From the tabulated results we can clearly say that the performance of the responses of the speed control loop and current control loop of the Switched Reluctance Motor has been significantly improved using MPC as the controller. Moreover the tracking of the ramp reference current signal has also been very satisfactory which thereby clearly shows the superlative performance of MPC over the PID controller.

### 3.3.5 Stability analysis of the SRM system.

The state space model of the current control loop of SRM with all the parameters taken from table 3.8 is shown below:

$$\begin{bmatrix} \dot{x}_1 \\ \dot{x}_2 \end{bmatrix} = \begin{bmatrix} -14.97 & 0 \\ -1330 & -2793 \end{bmatrix} \begin{bmatrix} x_1 \\ x_2 \end{bmatrix} + \begin{bmatrix} 0.00728 \\ 0.6539 \end{bmatrix} I^* \quad (3.35)$$

$$y = 1863x_2 \quad (3.36)$$

where  $y = I$

The corresponding transfer function of the current control loop is shown below:

$$\frac{I(s)}{I^*(s)} = \frac{1218s+203}{s^2+2808s+41820} \quad (3.37)$$

The eigenvalues of the system matrix are  $-2793.3$  and  $-0.0150$  respectively and since the values are negative the current loop of the Switched Reluctance motor is stable.

The state space model of the speed control loop of the Switched Reluctance Motor is shown below:

$$\begin{bmatrix} \dot{x}_1 \\ \dot{x}_2 \\ \dot{x}_3 \end{bmatrix} = \begin{bmatrix} -0.1667 & 0.000455 & 0 \\ 0 & -2.5 & 0 \\ 390 & 0 & -10 \end{bmatrix} \begin{bmatrix} x_1 \\ x_2 \\ x_3 \end{bmatrix} + \begin{bmatrix} 0 \\ 1 \\ 0 \end{bmatrix} \omega^* \quad (3.38)$$

$$y = 0.383x_3 \quad (3.39)$$

where  $y = \omega$

The corresponding transfer function is shown below:

$$\frac{\omega(s)}{\omega^*(s)} = \frac{0.06796}{s^3 + 12.67s^2 + 27.08s + 4.167} \quad (3.40)$$

The eigenvalues of the system matrix are  $-10$ ,  $-0.1667$  and  $-2.5$  respectively. Since the values are negative the speed control loop of the Switched Reluctance Motor is stable.

# Chapter 4

## Ornithopter, its Dynamics and Flight Control Model

### 4.1 Introduction to Ornithopter

Natural fliers like birds have mesmerized and captured the inquisitive minds of inventors through ages. The ease and grace with which they fly in the air is really amazing and it quite remarkably and significantly surpasses the complicated dynamics and control mechanism of the aircrafts of today. Several attempts at imitating the natural agility and nonchalant ease of flight of the birds have been carried out. Amongst many truly groundbreaking works a flapping wing vehicle commonly known as an ornithopter has been brought to the illuminating canvas of recent research works. The aircraft mechanism involves separating the flight mechanism into two different forces of action [26]. The lift mechanism which involves the wing surfaces of the aircraft are totally separated from the mechanism of thrust [26]. But in the control mechanism of the ornithopter both the lift and thrust mechanism are integrated together [2] [7]. This intricate nature of control of the birds is only possible to be materialized by human beings if the complicated dynamics of the birds of wings can be unraveled with complete mathematical modeling. The mechanical, aerodynamics and structural aspects of the flapping wing motion control is the key to developing an adequate and comprehensive model of the ornithopter [1][11] [5] [6] which can be launched in real life, thus expanding the horizon of human imagination and make human beings that closer to accomplish a victory over the nature itself. Attempts to incorporate all the complex motions of a bird for developing a flying vehicle has never stopped

short of research ever since the aspect of flying with the grace of a bird had caught the human imagination. Reality has interestingly deceived the human's attempts for achieving this tremendous fit. The best groundbreaking attempts so far has been significantly done in the relentless research on the dynamics of the ornithopter which is different from the birds in that it does not have the complex motions such as feather spreading, fore-and-aft swinging, semispan variations quite vividly present in the bird's motion.

Although rubber-powered and human-powered ornithopters have existed, successful examples of motorized flapping-wing aircraft are few with the notable exception of the 18 ft span robot pterosaur built by AeroVironment Inc. of Monrovia California [1]. However, this model was not able to sustain flight. The first successful flight of a motorized radio-controlled flapping-wing aircraft, known as 'Mr.Bill', was made on September 4,1991 by Dr. James De Laurier and Mr. Jeremy Harris at the University of Toronto. This model aircraft was able to sustain flight for about 3 minutes and was landed successfully. This ornithopters wing design is different from that for birds in that it does not have the complex motions [7] such as feather spreading, fore-and-aft swinging, semispan variation, etc.

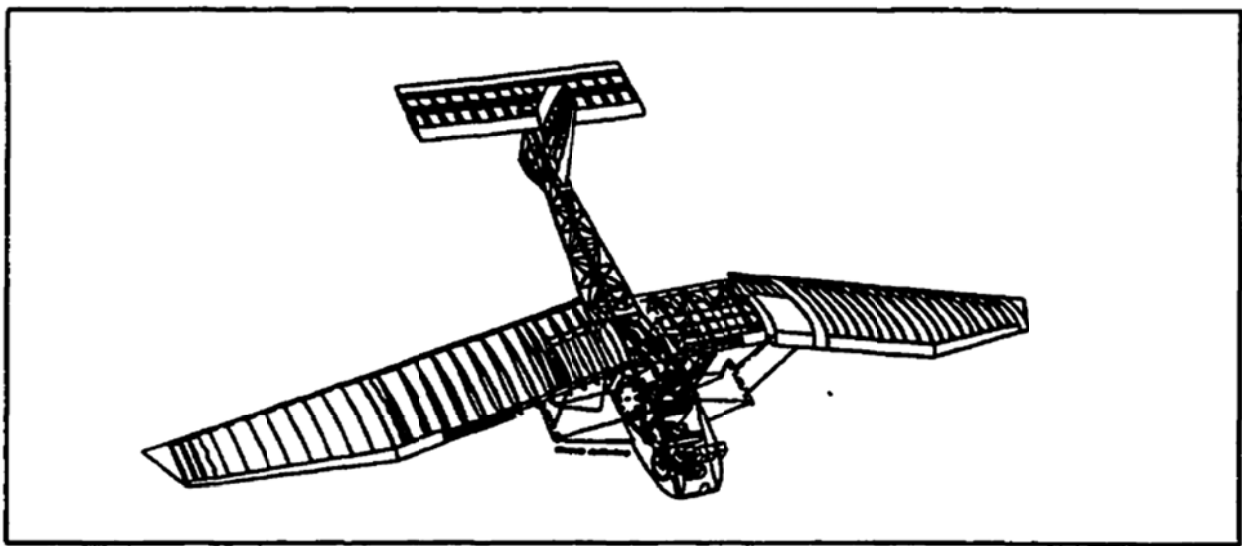


Figure 4.1 Mr. Bill Ornithopter

The motion is such that the center panel moves in a direction which is opposite to the flapping of the outer panels. This three-panel design serves to balance the time-varying lift seen by the fuselage and evens out the power required from the engine during the flapping cycle. With the two-panel design, the power required for the downstroke [5] is greater than for the upstroke. The flapping is a simple harmonic motion driven by a lightweight transmission which reduces the high rotational speed of the engine down to the low flapping frequencies which are required. A linear twist is experienced by the wing and is 90 degrees out of phase with the flapping. No ailerons are present, thus turning is accomplished by yaw & roll coupling produced by the rudder deflection in conjunction with the wing's average dihedral angle. The dihedral angle is accomplished by making the upstroke flapping angle larger than the downstroke angle.

#### **4.2 Recent Applications of Ornithopter**

Research is now continuing into constructing a full-scale motorized ornithopter capable of carrying a human being. This enormous task can be divided into several different sub-areas some of which include: wing design, landing and take-off simulations, drive mechanism design, and flight dynamic analysis [4] [6].

Recently the earnest interest for ornithopters has grown in the area of Micro Aerial Vehicles (MAV). These miniature flying objects of such agility will indeed be the ultimate platform for a diversified area of tasks including systems monitoring and surveillance where a swarm of tiny agents would be unobtrusive and have better access to confined areas than large flying vehicles.

The most recent realizable (MAV) based ornithopter of such kind is the Kestrel ornithopter [5].



Figure 4.2 Kestrel Ornithopter

This thesis will mainly focus on the flight dynamics of such an ornithopter in a small scale amongst other concerning subjects' necessary for a realizable ornithopter.

### **4.3 Flight Dynamics and modeling of the Ornithopter**

The flight dynamics of the ornithopter are basically organized into three different dimensions each being more complex than the other. The simplest amongst them is the one dimensional flight dynamics. The 3D dynamics and modeling is far more complex [1] [4] [16] [18] and thus requires lengthy procedures and eventually loses the simplistic approach for obtaining an accurate mathematical model [4] [10] [15].

In this thesis only the two dimensional modeling of the dynamics will be taken into consideration which works as a model not too sophisticated and not too simple as well. This model thus represents a rather less complicated model which doesn't lose all the details necessary for forming a realistic dynamic system [1] [4] [18].

### 4.3.1A General Two Dimensional Model of the Ornithopter

A general free body diagram of the ornithopter in flight is shown in Figure 4.3. The following notation applies to Figure 4.3.

$x$  the horizontal axis.

$y$  the vertical axis.

$\hat{x}$  the horizontal body axis.

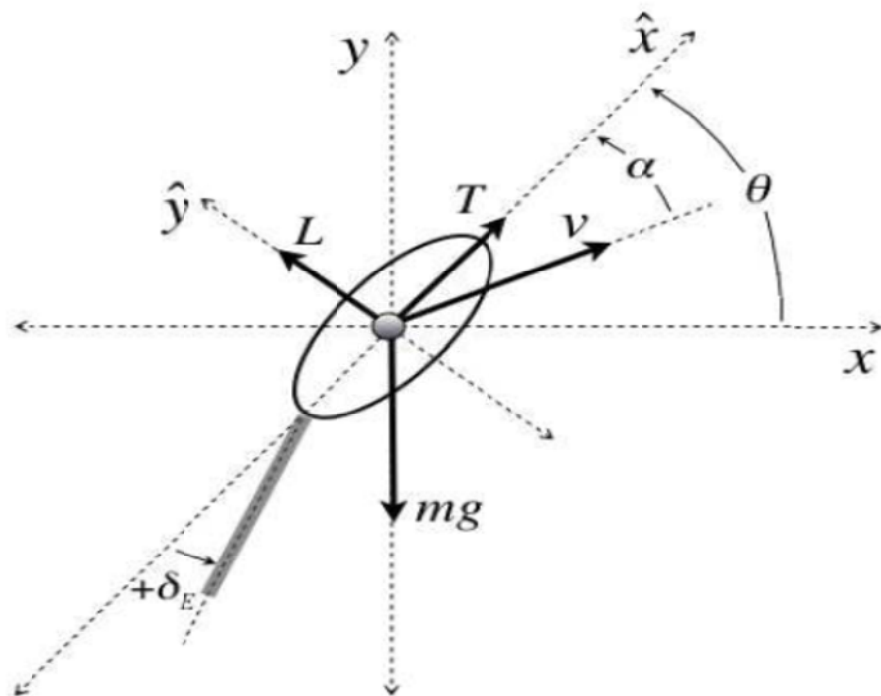


Figure 4.3 Two Dimensional Model of the Ornithopter

$\hat{y}$  the vertical body axis.

$\theta$  the angular position of the ornithopter.

$\alpha$  the angle of attack of the ornithopter and angle between the velocity vector and

horizontal body axis.

$\delta_E$  the angle of the tail (or elevator).

$m$  the mass of the ornithopter.

$g$  Earth's gravity:  $g \approx 9.81 \text{ m/s}^2$ .

$v$  the velocity of the ornithopter:  $v = \sqrt{v_x^2 + v_y^2} = \sqrt{\dot{x}^2 + \dot{y}^2}$

$T$  the thrust produced by the wings, which is assumed to be parallel to the body axis.

$L$  the lift generated by oncoming air flow.

The equations of motion for this case can be summarized as [4] [5]:

$$m\ddot{x} + b_x\dot{x} = T \cos \theta - L \sin \theta \quad (4.1)$$

$$m\ddot{y} + b_y\dot{y} = T \sin \theta + L \cos \theta - mg \quad (4.2)$$

$$\ddot{\theta}I + b_\theta\dot{\theta} = -K_t\delta_E \quad (4.3)$$

where  $b_x$ ,  $b_y$ , and  $b_\theta$  are horizontal, vertical, and rotational damping of the ornithopter,  $I$  is the moment of inertia of the ornithopter, and  $K_t$  is a torque constant relating the total torque, of which the ornithopter is subject, to the angle of the tail. From the free-body diagram, we can also conclude that

$$\dot{x} = v \cos(\theta - \alpha) \quad (4.4)$$

&

$$\dot{y} = v \sin(\theta - \alpha). \quad (4.5)$$



An approximation of the moment of inertia is made using the following equation for the moment of inertia for a solid cuboid [4]:

$$I = \frac{1}{2}m(h^2 + l^2) \quad (4.6)$$

where  $h$  = height and  $l$  = length. For  $h \approx 4 \text{ in.} = 0.1016 \text{ m}$ ,  $l \approx 6 \text{ in.} = 0.1524 \text{ m}$ , and  $m = 0.096 \text{ kg}$ , we find that  $I \approx 2.6839 \text{E} - 4 \text{ kg} \cdot \text{m}^2$ . An estimate of the rotational damping and torque constant can be made by considering two cases for the equation  $\ddot{\theta}I + b_{\theta}\dot{\theta} = -K_t\delta_E$ . In the first case, the ornithopter is at rest and a maximum step in angular acceleration,  $\ddot{\theta}_{max}$ , is applied to the system. At this point  $\dot{\theta} = 0$  and  $\delta_E = \delta_{E,max}$ . From observation,  $\delta_{E,max} \approx \pm 45^\circ$  and  $\dot{\theta}_{max} \approx \pm 540^\circ/\text{s}^2 \approx \pm 9.43 \text{ rad/s}^2$ . We can then solve for  $K_t \approx 0.0032$ . In the second case, the ornithopter is in steady rotation. Here  $\dot{\theta} = \dot{\theta}_{max} = 180^\circ/\text{s}$  and  $\ddot{\theta} = 0$ . We can then solve for  $b_{\theta} \approx 8.0516 \text{E} - 4 \text{ N} \cdot \text{s/m}$ .

The system parameters were approximately estimated for an ornithopter in steady state motion/rotation with its velocity increasing from the moment of flight to the point it starts to hover at the cruise altitude. The complex differential equations describing the equation of motion of an ornithopter was simulated in Simulink.

The Simulink model of the ornithopter representing the two dimensional flight control is shown below.

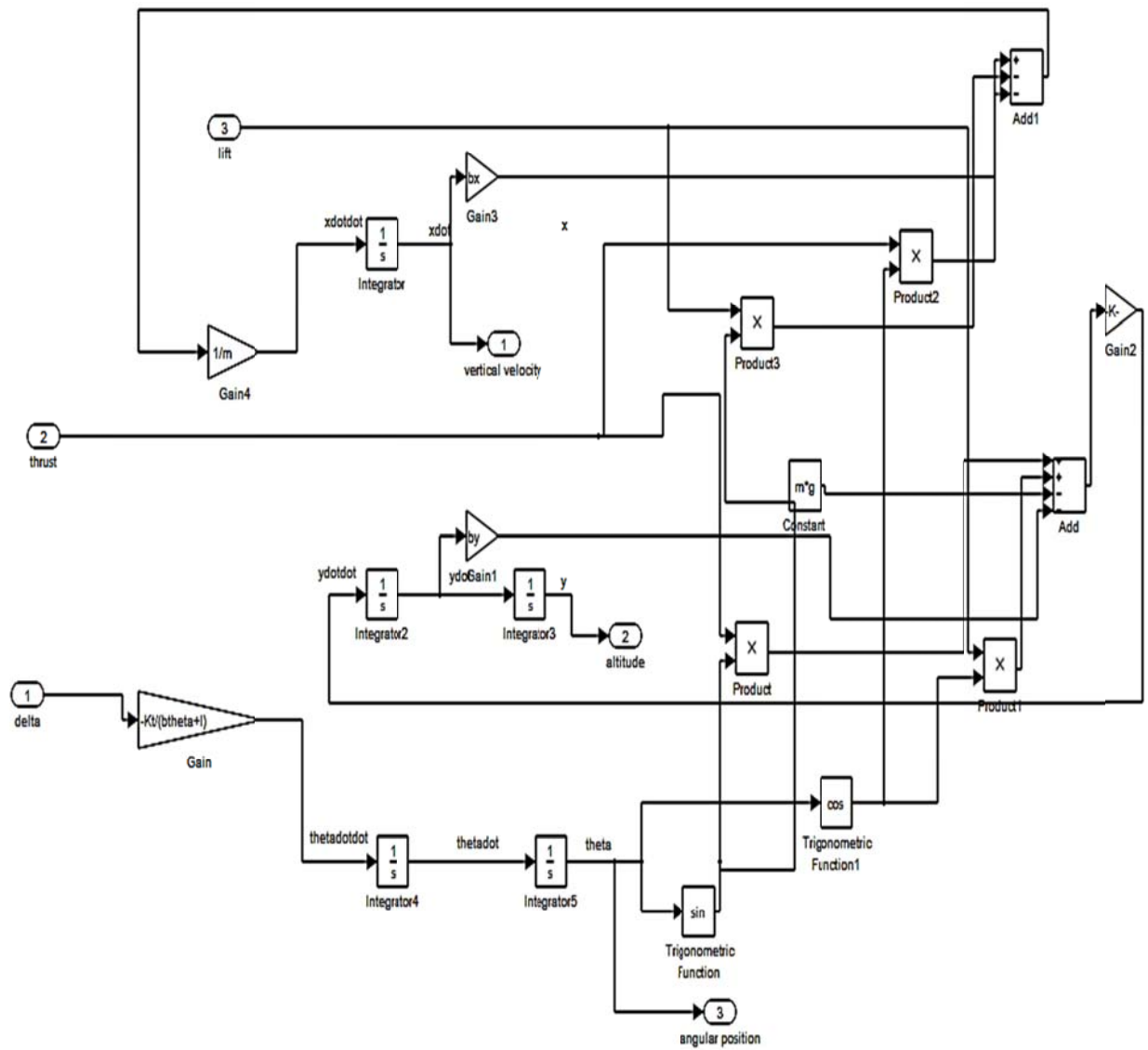


Figure 4.4 Total Nonlinear Simulink Representation of the Ornithopter

Now the major problem is the designing of such ornithopter model in the two dimensional model because it also incorporates lift, thrust and taii command. In most cases only the thrust and tail command angle are considered to be the manipulated variable. This general approach follows a

similar method employed in aircraft dynamic modeling where the lift is separately considered and the mechanism is totally detached from the thrust mechanism.

A typical subsystem that incorporates both the thrust and lift mechanism of the ornithopter was simulated in Simulink as shown below:

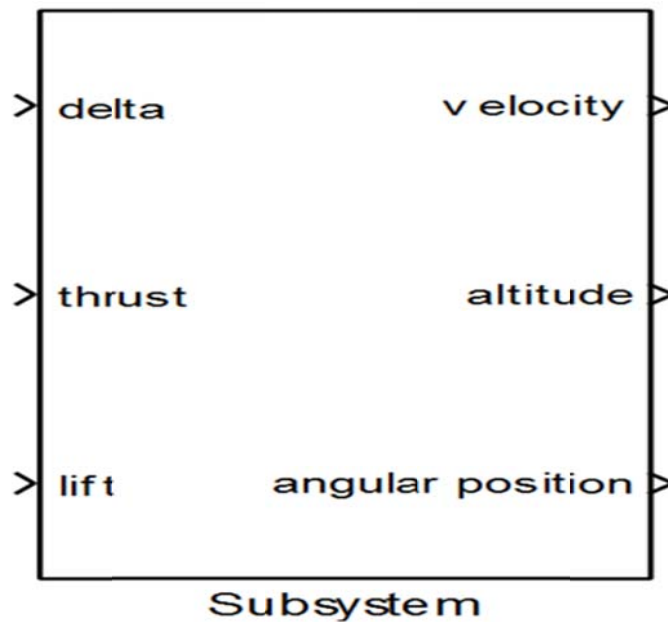


Figure 4.5 Ornithopter Simulink Model

#### 4.4 Flight Control of the Ornithopter

The 2D model is designed with parameters representing steady motion of the ornithopter. Thus the system lacks the acceleration motion after the point of cruise holding altitude but yet again the most essential mechanism of control is the steady state motion because in most period of operation the ornithopter will have to stay in steady motion [7][8][10]. Moreover this model also truncates the aspects of rotational acceleration and rotational velocity because such directions of motion are best described in 3D dynamic modeling of the ornithopter [6] [18].

#### 4.4.1 Flight Control of the Ornithopter using the PID Controller

The three output variables are taken to be the key exponents of control in this thesis. The PID controller is utilized in a step by step SISO modeling of the nonlinear 2D dynamic model of the ornithopter. Linearization of this complex system was carried out using the Matlab command `linmod`. Initially only the thrust was taken as the manipulated variable for controlling only the vertical velocity of the ornithopter.

The PID controller used for this purpose is an adaptive PID controller which also includes a filter block to obtain the most efficient response. The PID block uses the compensator formula which is:

$$Kp + \frac{K_i}{s} + K_d \frac{N}{1+\frac{N}{s}} \quad (4.7)$$

where  $K_p$  is the proportional constant,  $K_i$  is the integral constant,  $K_d$  is the derivative constant and  $N$  is known as the filter coefficient. The Simulink model of the PID controller is as follows:

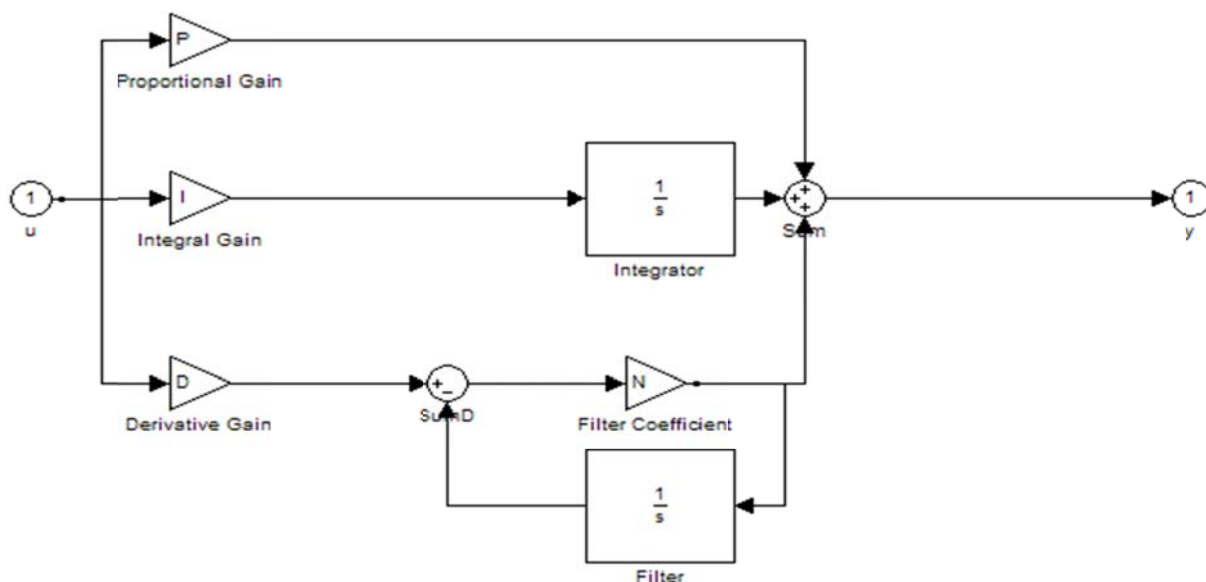


Figure 4.6 The internal Simulink Representation of the PID Controller

The Simulink model for such representation is shown below:

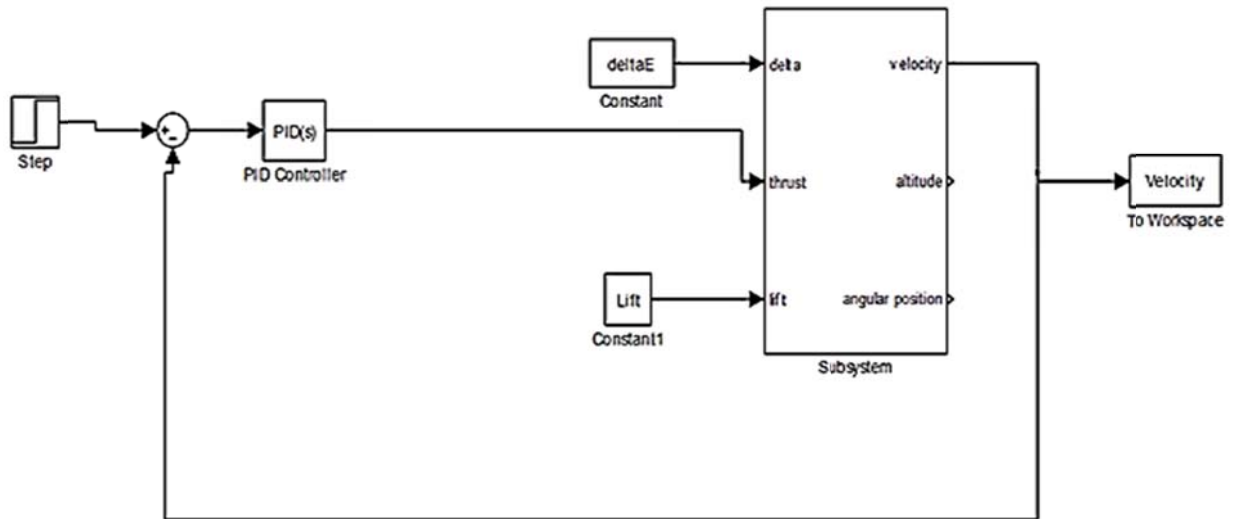


Figure 4.7 PID controller using thrust as the only Manipulated Variable and Velocity as Output

The same approach was carried out with the thrust as the manipulated variable for controlling the angular position and finally the altitude.

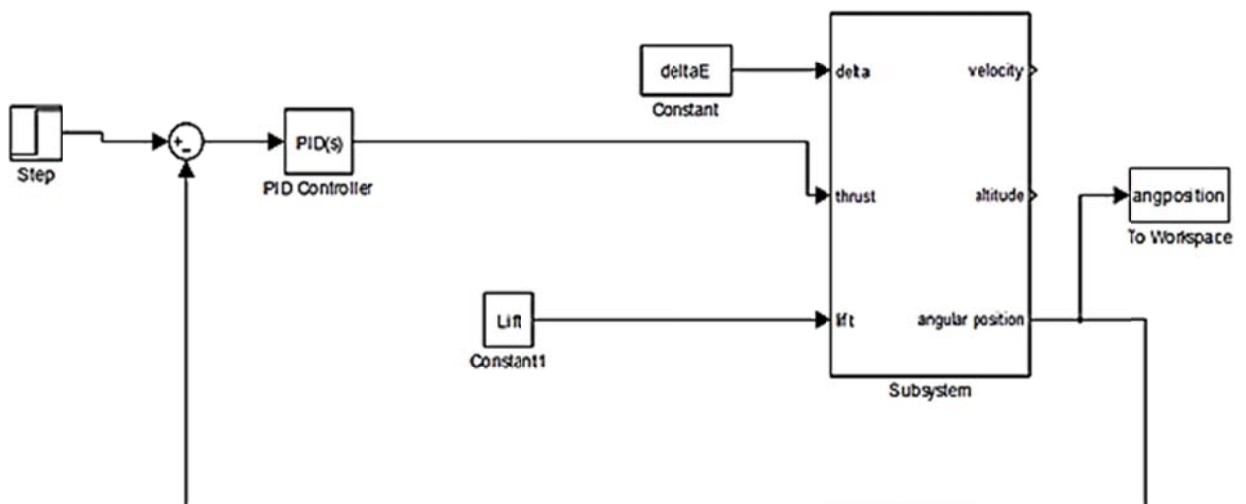


Figure 4.8 Continuation of the Previous Figure with Angular Position as the output

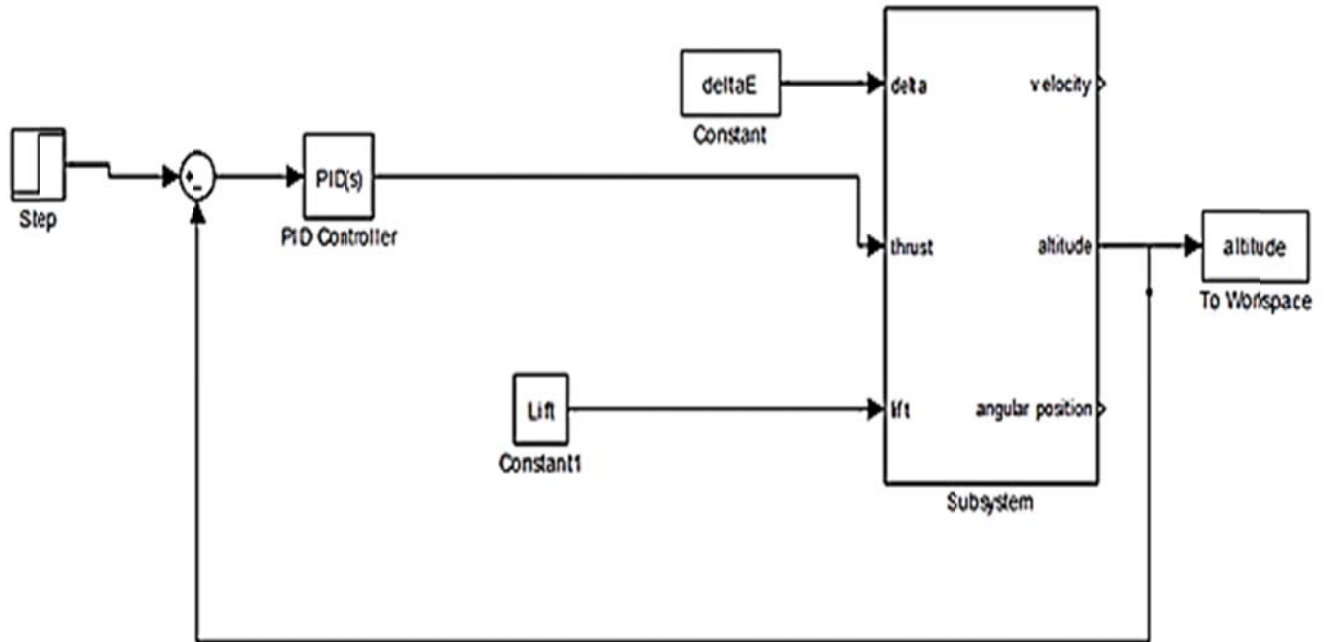


Figure 4.9 Continuation of the previous Figure with altitude as the output

However the thrust is the controlling variable possible for only controlling the vertical velocity [5][16]. Thus the results completely obeyed this theoretical aspect of ornithopter.

In the same way tail angle command  $\delta_E$  was taken as the manipulated variable for controlling the outputs using PID controller. However the outputs obtained were really unsatisfactory and evidently approves the theoretical concept of controlling the ornithopter since  $\delta_E$  is only considered for controlling the angular position. Again when lift was taken to be the commanding variable, it followed the theoretical aspect [10] once again and only the altitude was able to be controlled.

The corresponding Simulink model of such control scheme is shown below:

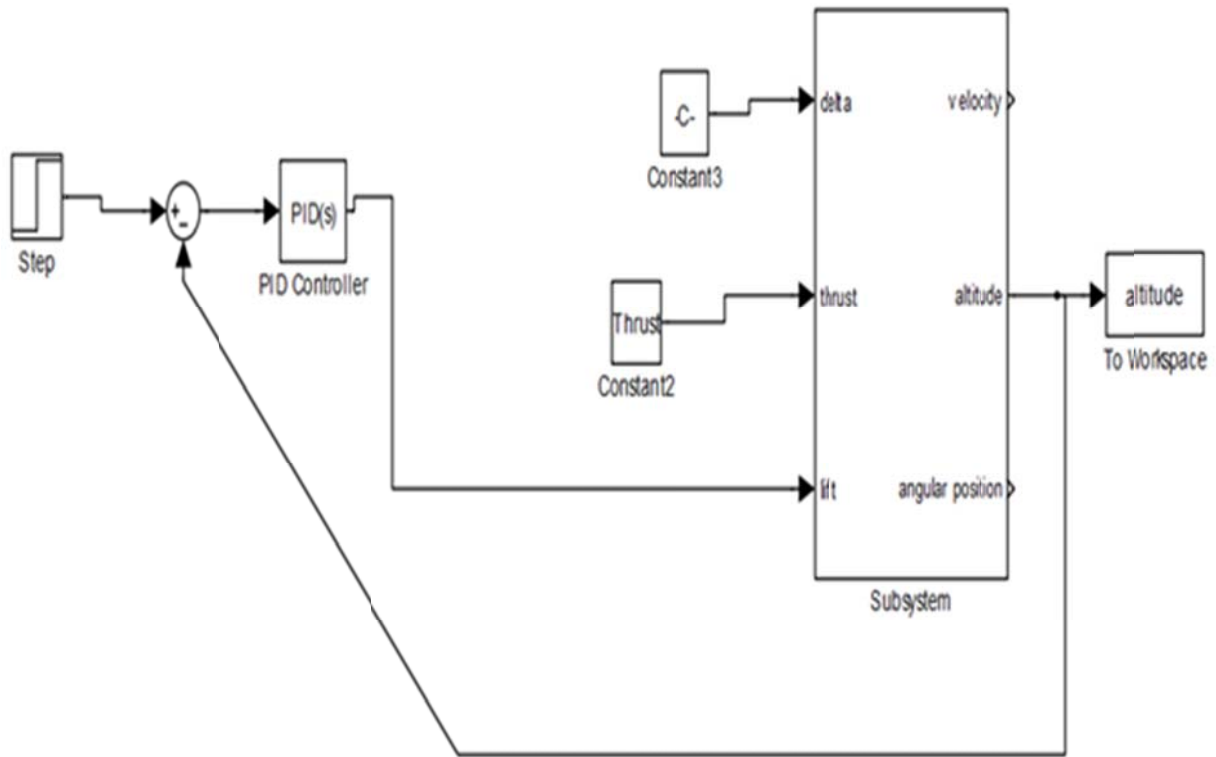


Figure 4.10 PID controller with Lift as the Manipulated Variable and the output as the altitude.

#### 4.4.2 SISO, MISO Model Predictive Controller in the Flight Control of the Ornithopter

The whole process was carried out using MPC Model Predictive Controller taking only one manipulated variable at a time to control the output variables.

The Simulink Models representing such Single Input Single Output (SISO) control schemes and also with the theoretical aspect taken into consideration are shown below:

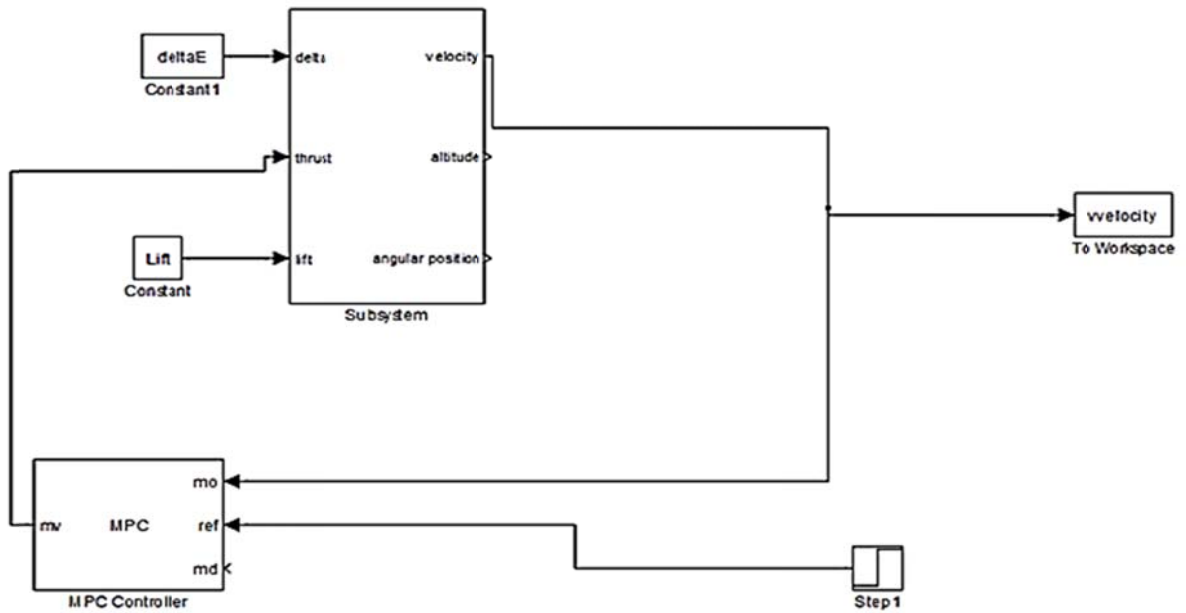


Figure 4.11 MPC Controller scheme for controlling the velocity with the manipulated variable as Thrust

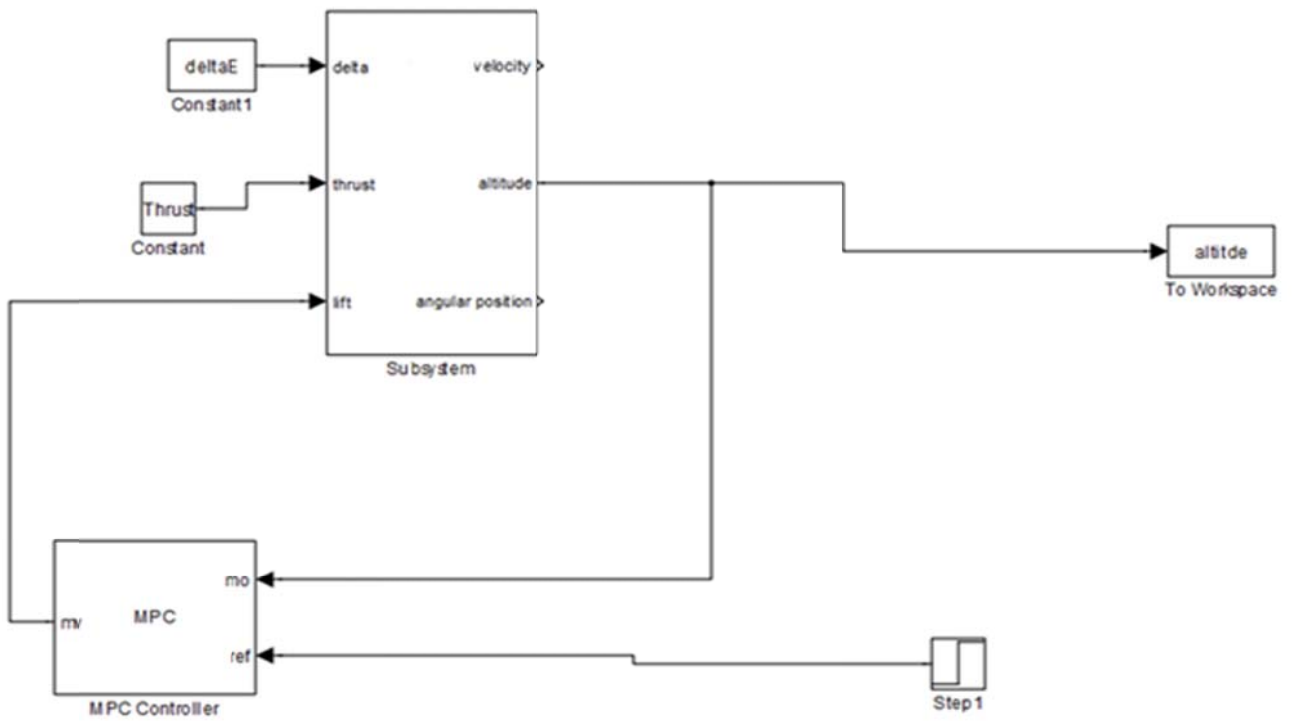


Figure 4.12. MPC controller with Manipulated Variable as the Lift



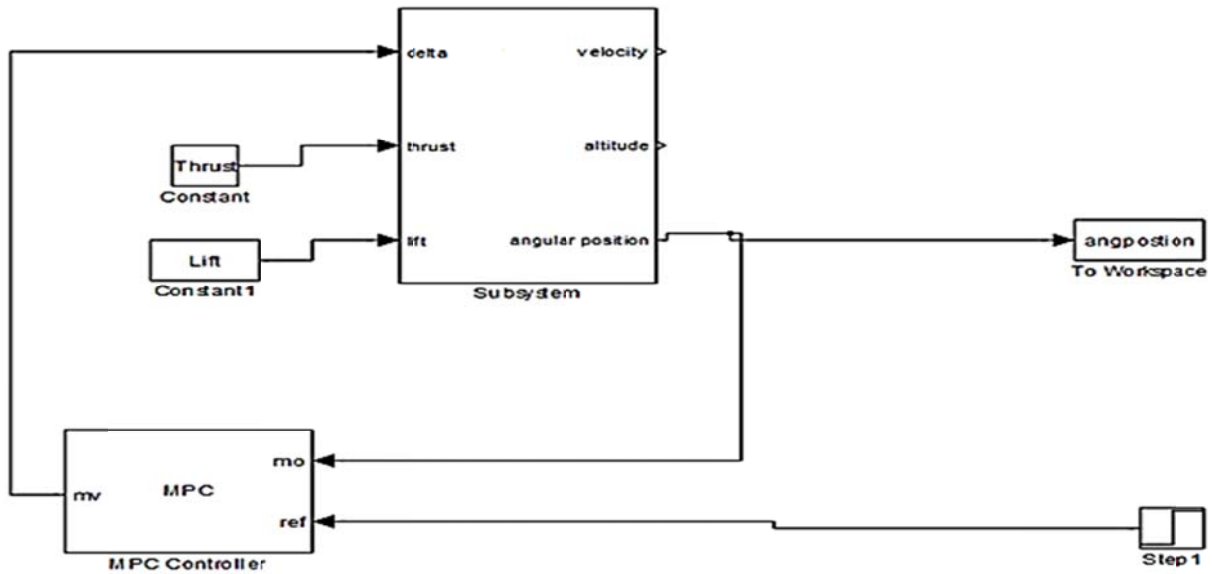


Figure 4.13 MPC controller with Manipulated Variable as the Tail Command angle

Finally a Multiple Input Single Output (MISO) Simulink Model was simulated using the MPC controller. PID controllers are generally quite difficult to control such MISO systems and require Neural Networks or Fuzzy Logic intelligent control adapted to the PID controllers [7][14][18].for carrying out such operations. Hence only MPC controllers were utilized for controlling the output variables.

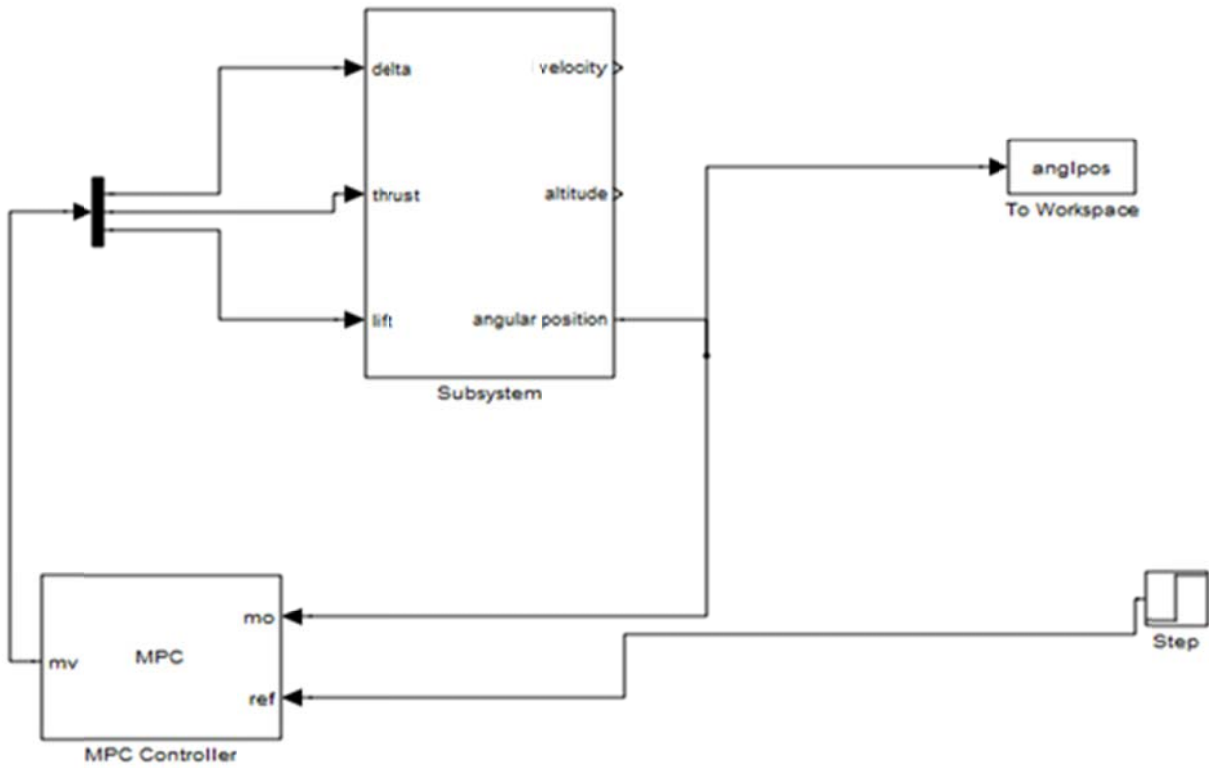


Figure 4.14 MPC Controller with three Manipulated Variables and Angular Position as Output

The Simulink models used for carrying out this process is shown below:

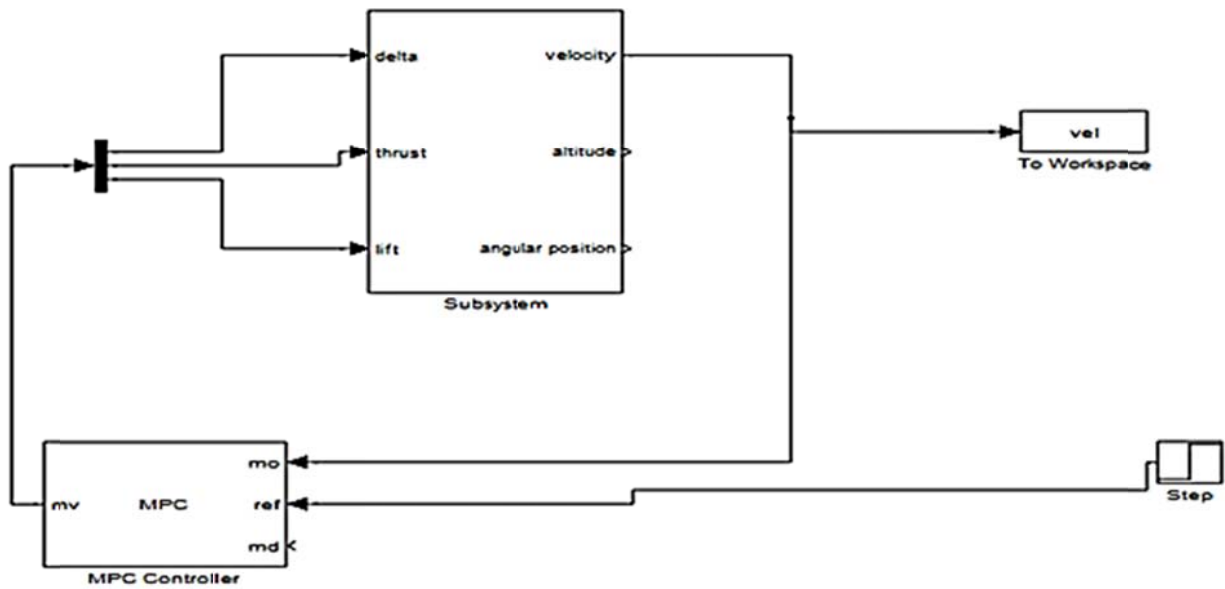


Figure 4.15 MPC Controller with three Manipulated Variables and Velocity as Output

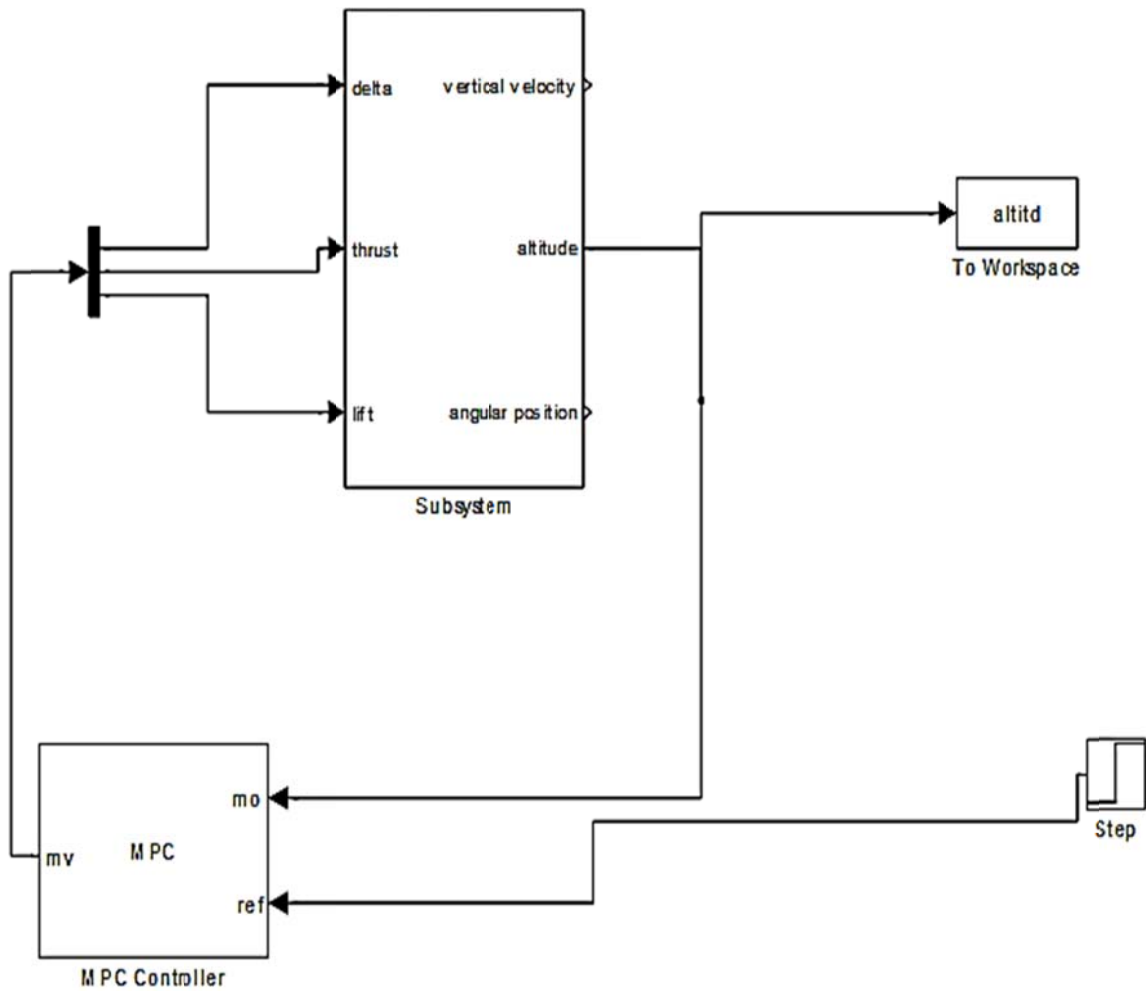


Figure 4.16 MPC Controller with three Manipulated Variables and altitude as Output

#### 4.4.2 MIMO Model Predictive Controller in the Flight Control of the Ornithopter

Finally a complete model was developed with Simulink which involved controlling all the outputs which are the velocity, altitude and angular position respectively. The Simulink model for such a scheme using MPC controller is shown below:

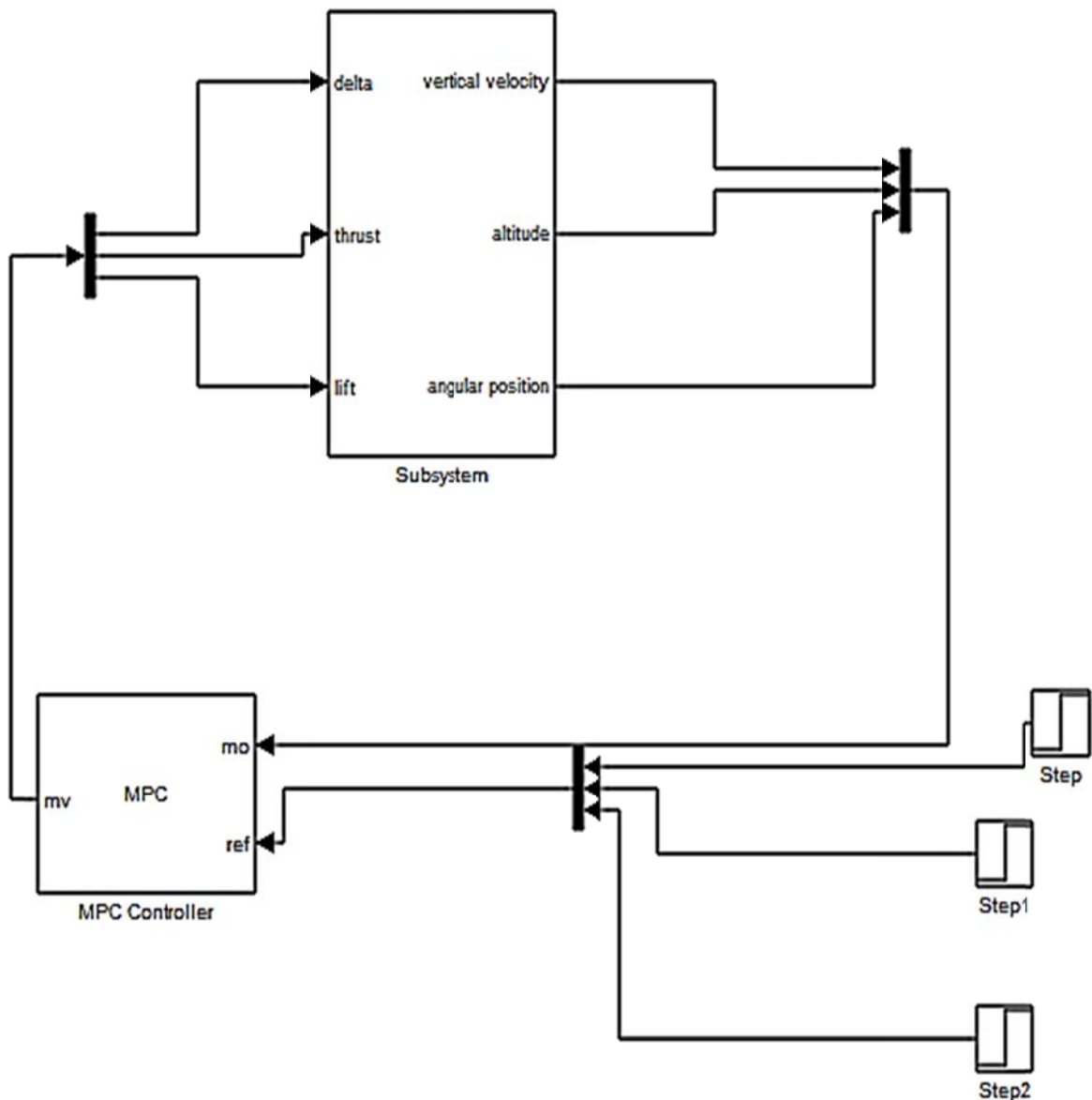


Figure 4.17 MPC Controller with three Manipulated Variables and Velocity, Altitude and Angular Position as the Output

The control of the initial acceleration of the ornithopter to the point of cruise operation at steady velocity was manifested with the MIMO model of the Model Predictive Controller.

The Representation of the Simulink Model that features the initial acceleration mode of the Ornithopter is shown below:

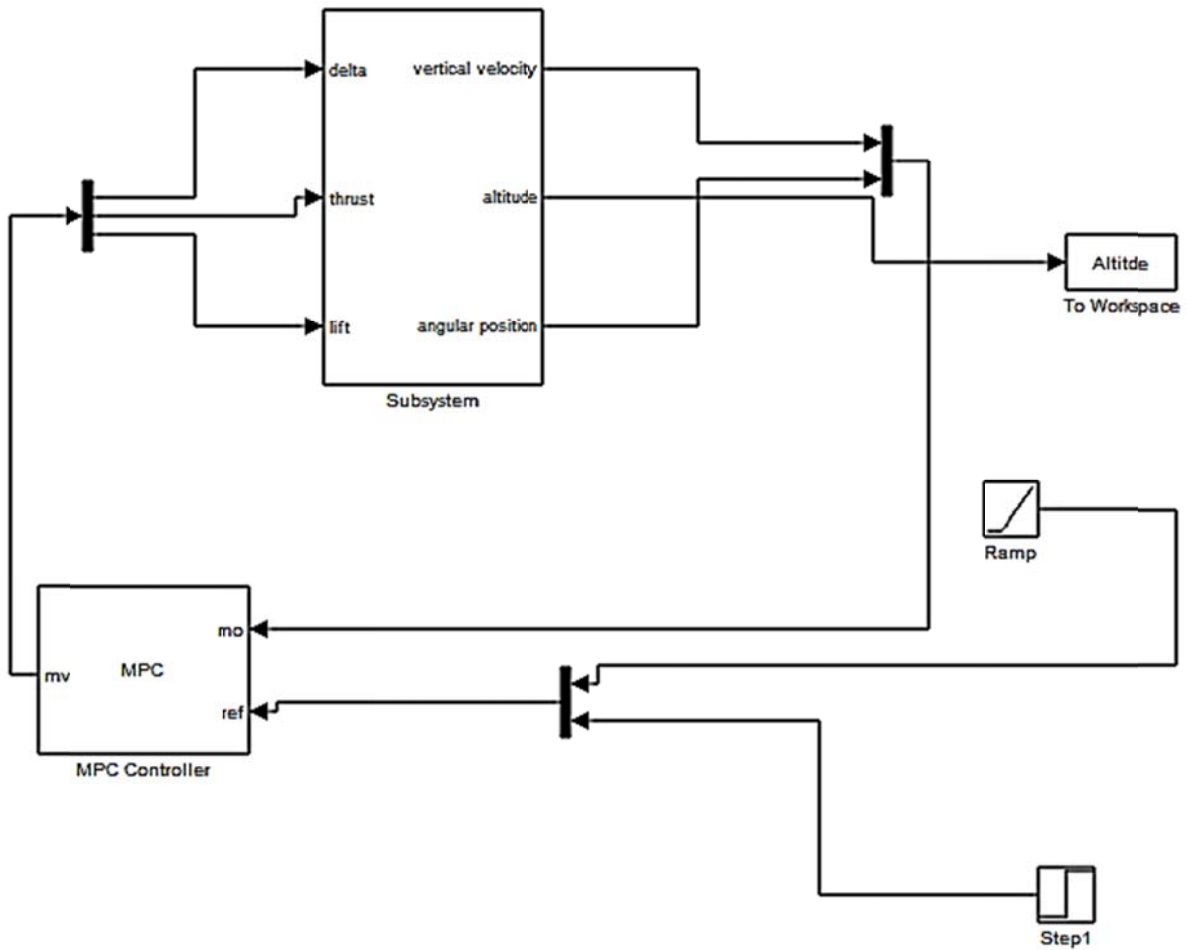


Figure 4.18 Model Predictive Controller featuring the Initial Acceleration Mode of Operation.

The control was carried out by using a ramp reference velocity signal of slope 1 and the reference angular position as 1 p.u. The expected altitude response is supposed to be a parabolic curve if at all it were to accelerate. So the main observation is really depends immly on the altitude response of the ornithopter.

## 4.5 Linearized Model of the Ornithopter

The linearization of the complex nonlinear model of the ornithopter was carried out by the Matlab command `linmod` with initial operating points set at the necessary values. The entire process was carried out by simulations involving linearization in Matlab.

The Linearization Results yielded from Matlab resulted in the State Space Model of the Entire Two Dimensional Ornithopter System as shown below:

$$\begin{bmatrix} \dot{x}_1 \\ \dot{x}_2 \\ \dot{x}_3 \\ \dot{x}_4 \\ \dot{x}_5 \end{bmatrix} = \begin{bmatrix} -10.42 & 0 & 0 & 0 & -4.828 \\ 0 & -10.42 & 0 & 0 & 3.89 \times 10^{-9} \\ 0 & 1 & 0 & 0 & 0 \\ 0 & 0 & 0 & 0 & 0 \\ 0 & 0 & 0 & 1 & 0 \end{bmatrix} \begin{bmatrix} x_1 \\ x_2 \\ x_3 \\ x_4 \\ x_5 \end{bmatrix} + \begin{bmatrix} 0 & 10.42 & 1.65 * 10^{-8} \\ 0 & 1.65 * 10^{-8} & 10.42 \\ 0 & 0 & 0 \\ -2.909 & 0 & 0 \\ 0 & 0 & 0 \end{bmatrix} \begin{bmatrix} u_1 \\ u_2 \\ u_3 \end{bmatrix}$$

$$y_1 = x_1$$

$$y_2 = x_3$$

$$y_3 = x_5$$

where  $y_1$ ,  $y_2$  and  $y_3$  represents the outputs of Velocity, Altitude and Angular Position respectively. The variables  $u_1$ ,  $u_2$  and  $u_3$  represent the input of tail command angle  $\delta_E$ , Thrust and Lift respectively.

The eigenvalues of the system matrix are -10.42, 0, -10.42, 0, 0 respectively and since they are negative the system is stable.

## CHAPTER 5

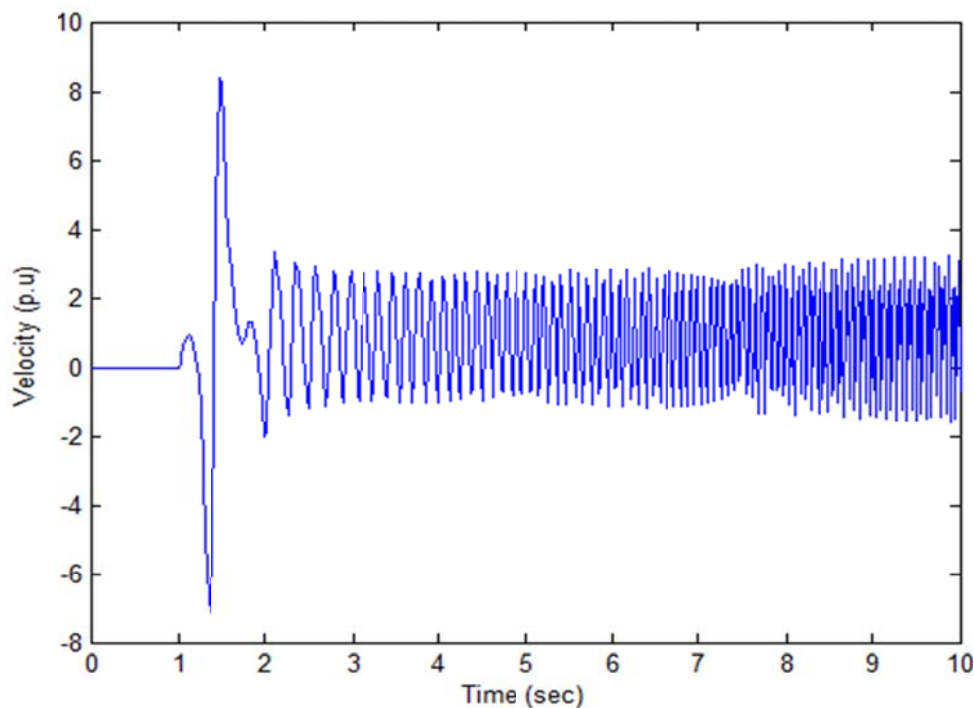
### PERFORMANCE ANALYSIS OF MPC AND PID CONTROLLER

#### ON THE FLIGHT CONTROL OF THE ORNITHOPTER

The performance analysis and comparative study of the flight control of the ornithopter was thoroughly undertaken by observing the simulation results obtained by running the various Simulink models designed.

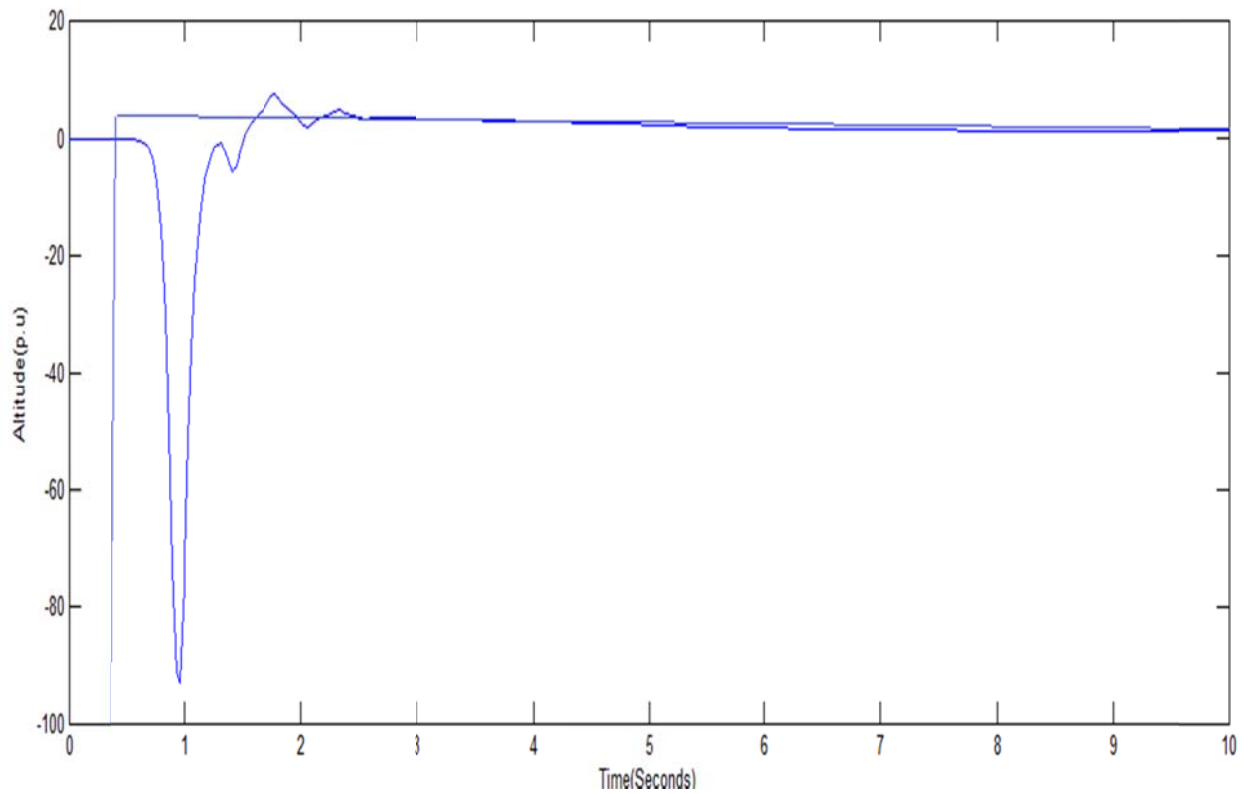
#### 5.1 Simulation results using the Adaptive PID Controller

##### Step Response of the Velocity of the Ornithopter using Thrust as the Manipulated Variable



From the result, we see that the control has been very poor with a high frequency oscillation taking place about the reference velocity of 1 p.u

### Step Response of the Altitude of the Ornithopter using Lift as the Manipulated Variable



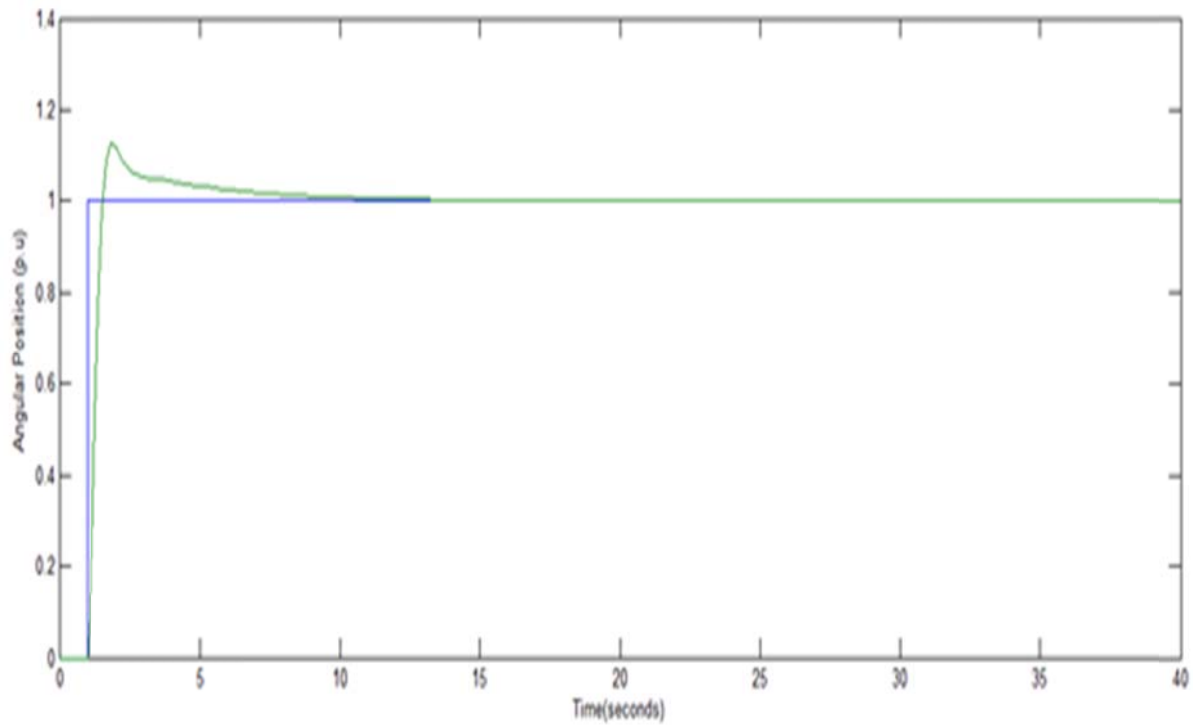
Settling time = 9 sec

Overshoot and damping response was severely affected.

From the result, we see that the adaptive PID controller was not very efficient for controlling the altitude of the ornithopter.



Step Response of the Angular Position of the Ornithopter using Tail command  $\delta_E$  as the Manipulated Variable



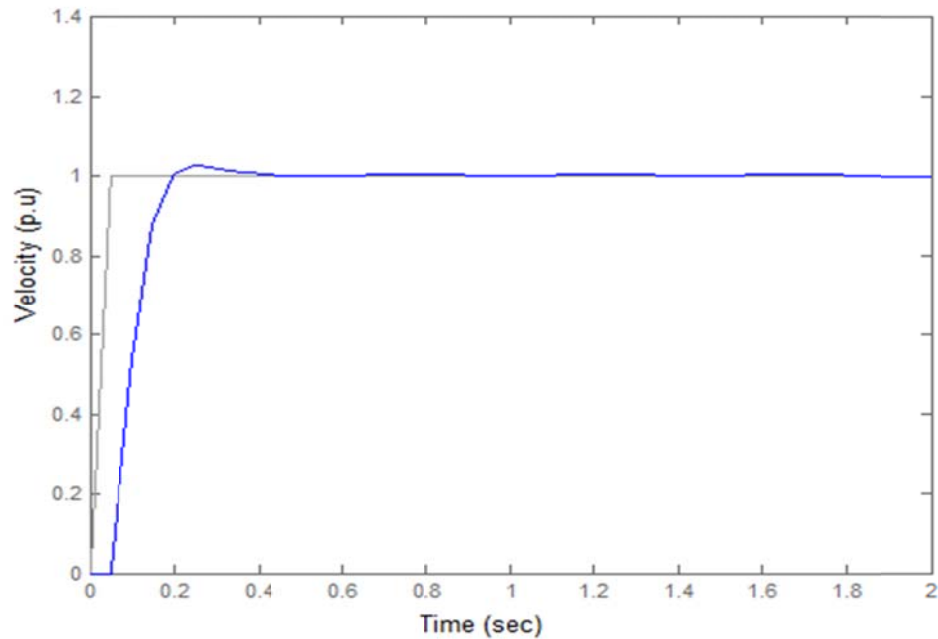
Settling time = 13 sec

Overshoot = 12%

From the result, we see that the response is slow and the overshoot percentage has not improved very well.

## 5.2 Simulation Results using the SISO (Single Input Single Output) MPC Controller.

### Step Response of the Velocity of the Ornithopter using Thrust as the Manipulated Variable



Settling time = 0.5 seconds

Overshoot Percentage = 6%.

From the result we can inevitably say that the performance has been dramatically improved by using the MPC controller.

## Step Response of the Altitude of the Ornithopter using Lift as the Manipulated Variable

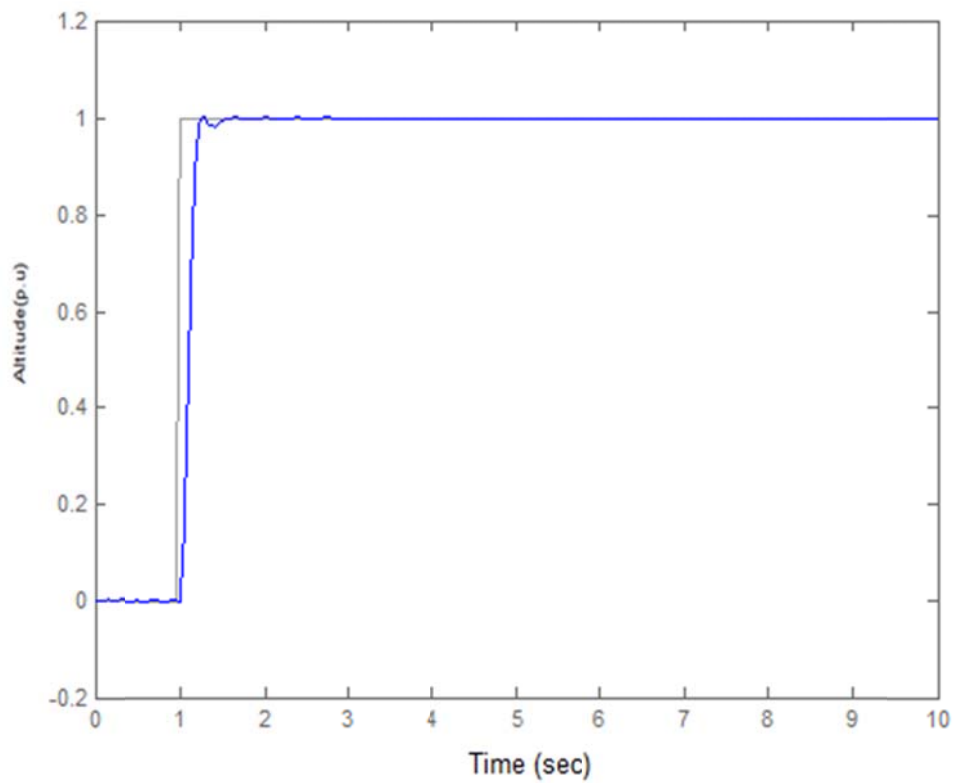


Figure 5.5 Step response for a reference altitude of 1 p.u

Settling time = 0.9 seconds.

Overshoot = negligible.

From the result we see that a remarkable improvement have taken place by using the MPC controller.

Step Response of the Angular Position of the Ornithopter using Tail command angle  $\delta_E$  as the Manipulated Variable

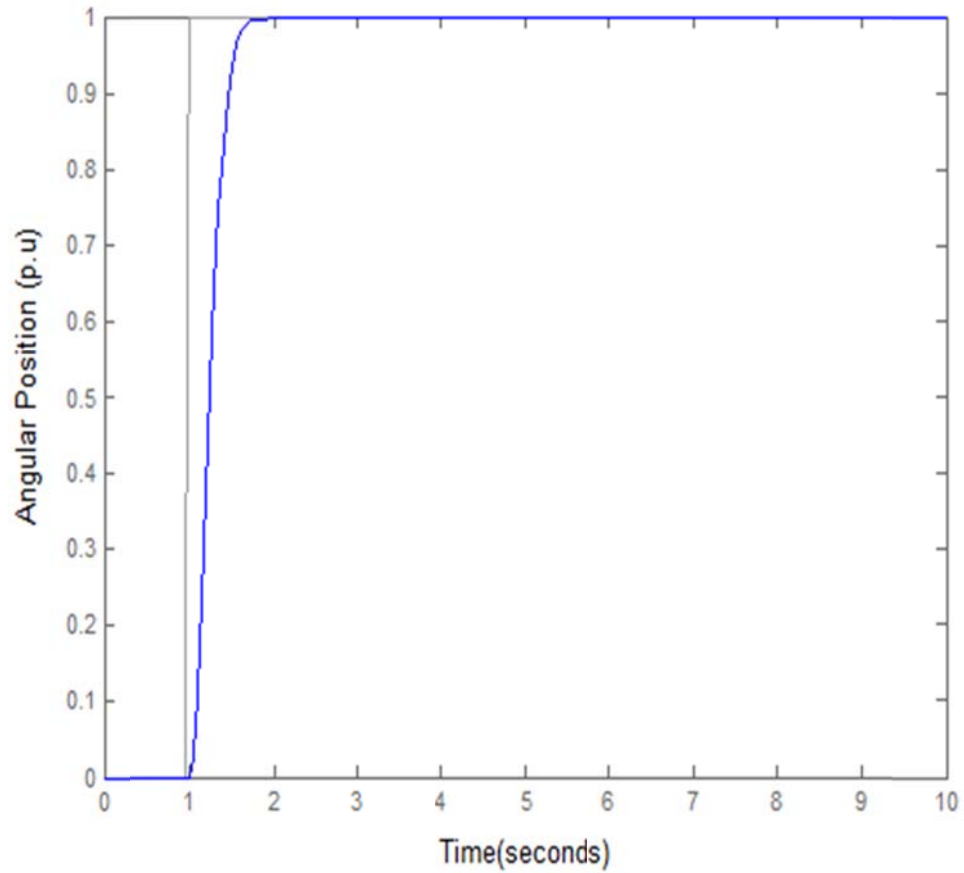


Figure 5.6 Step response for a reference angular position of 1. P.u

Settling time = 0.8 seconds

Overshoot = 0%.

From the result we see a improved performance using the MPC controller.

### 5.3 Simulation Results using the MISO (Multiple Input Single Output) MPC Controller.

Step Response of the Velocity of the Ornithopter using all the inputs (Thrust, Lift and Tail command angle  $\delta_E$ ) as the Manipulated Variables

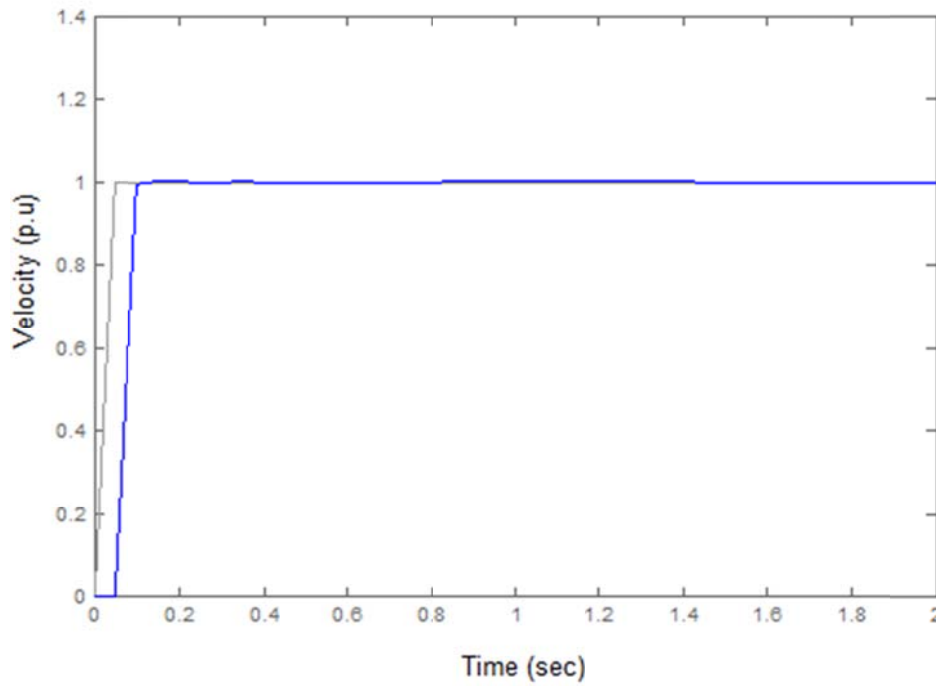


Figure 5.7 Step response for a reference velocity of 1 p.u

Settling time = 0.12 seconds.

Overshoot = 0%

From the result we see that there is a further improved using the MISO MPC controller. The settling time has reduced significantly and the overshoot has been totally eliminated.

Step Response of the Altitude of the Ornithopter using all the inputs (Thrust, Lift and Tail command angle  $\delta_E$ ) as the Manipulated Variables

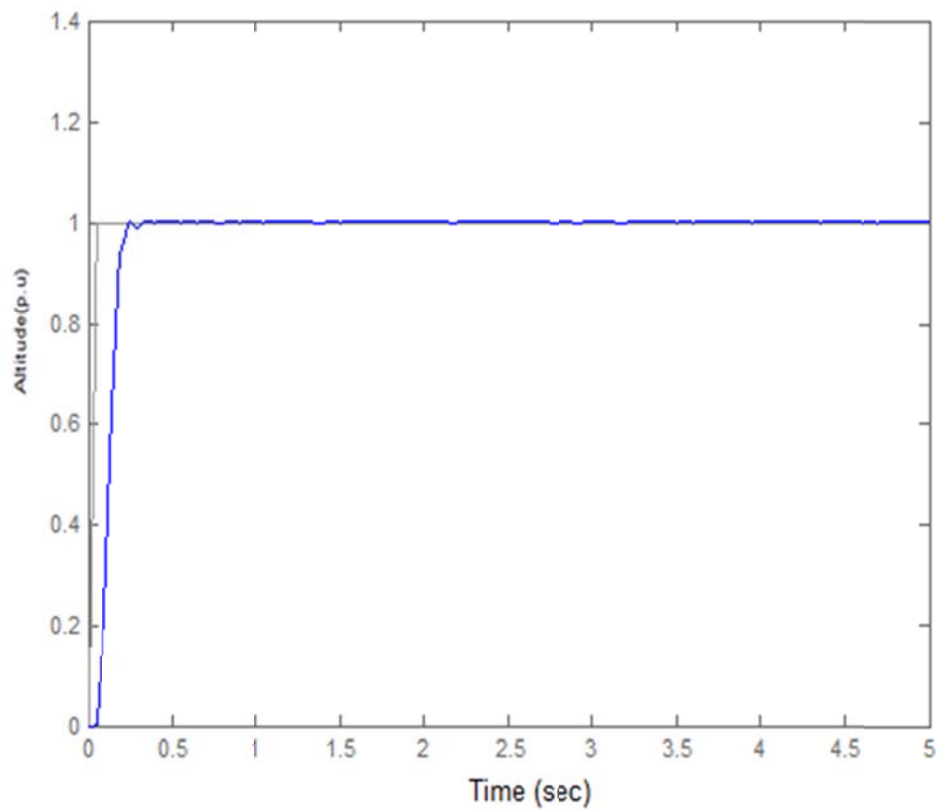


Figure 5.8 Step Response for a reference altitude of 1 p.u.

Settling time = 0.52 seconds

Overshoot almost totally eliminated

From the result we can see a further improvement in the response with a decrease in the settling time and a better overshoot performance.

Step Response of the Angular Position of the Ornithopter using all the inputs (Thrust, Lift and Tail command angle  $\delta_F$ ) as the Manipulated Variables

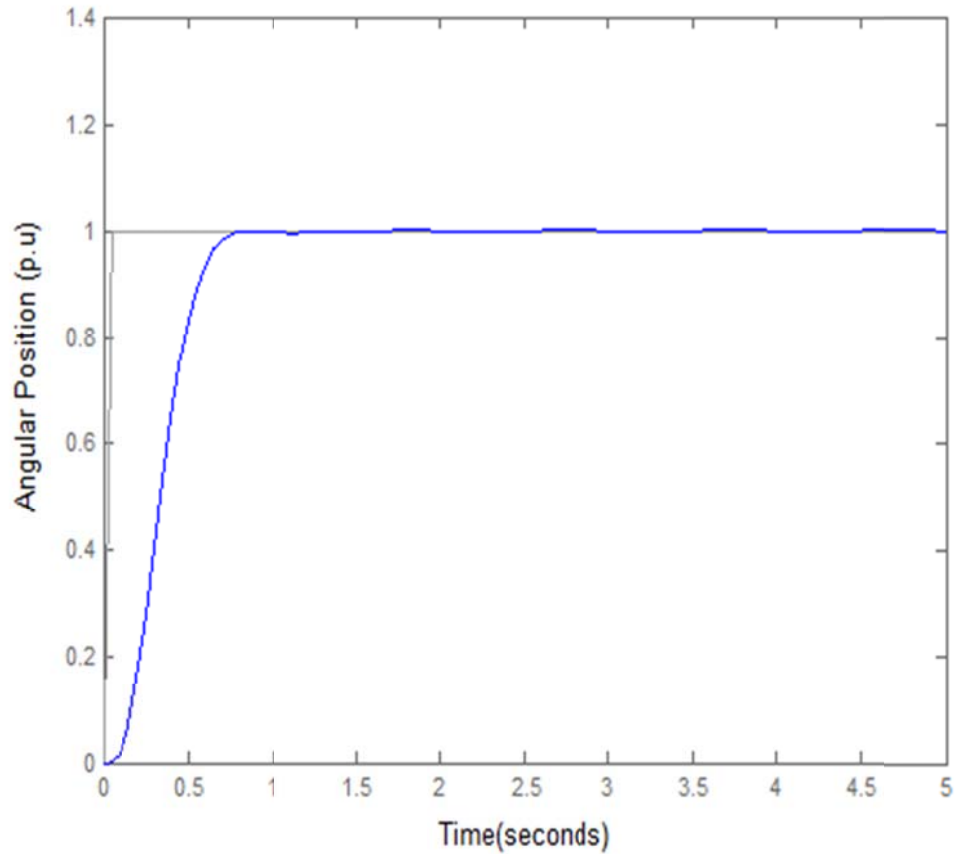


Figure 5.9 Step Response for a reference angular position of 1 p.u

Settling time = 0.8 seconds

Overshoot = 0 %

From the result we see a further improvement in the performance using the MISO MPC controller.

#### 5.4 Simulation Results using the MIMO (Multiple Input Multiple Output) MPC Controller.

Step Response of all the outputs (Velocity, Altitude and Angular Position) of the Ornithopter using all the inputs (Thrust, Lift and Tail command angle  $\delta_F$ ) as the Manipulated Variables

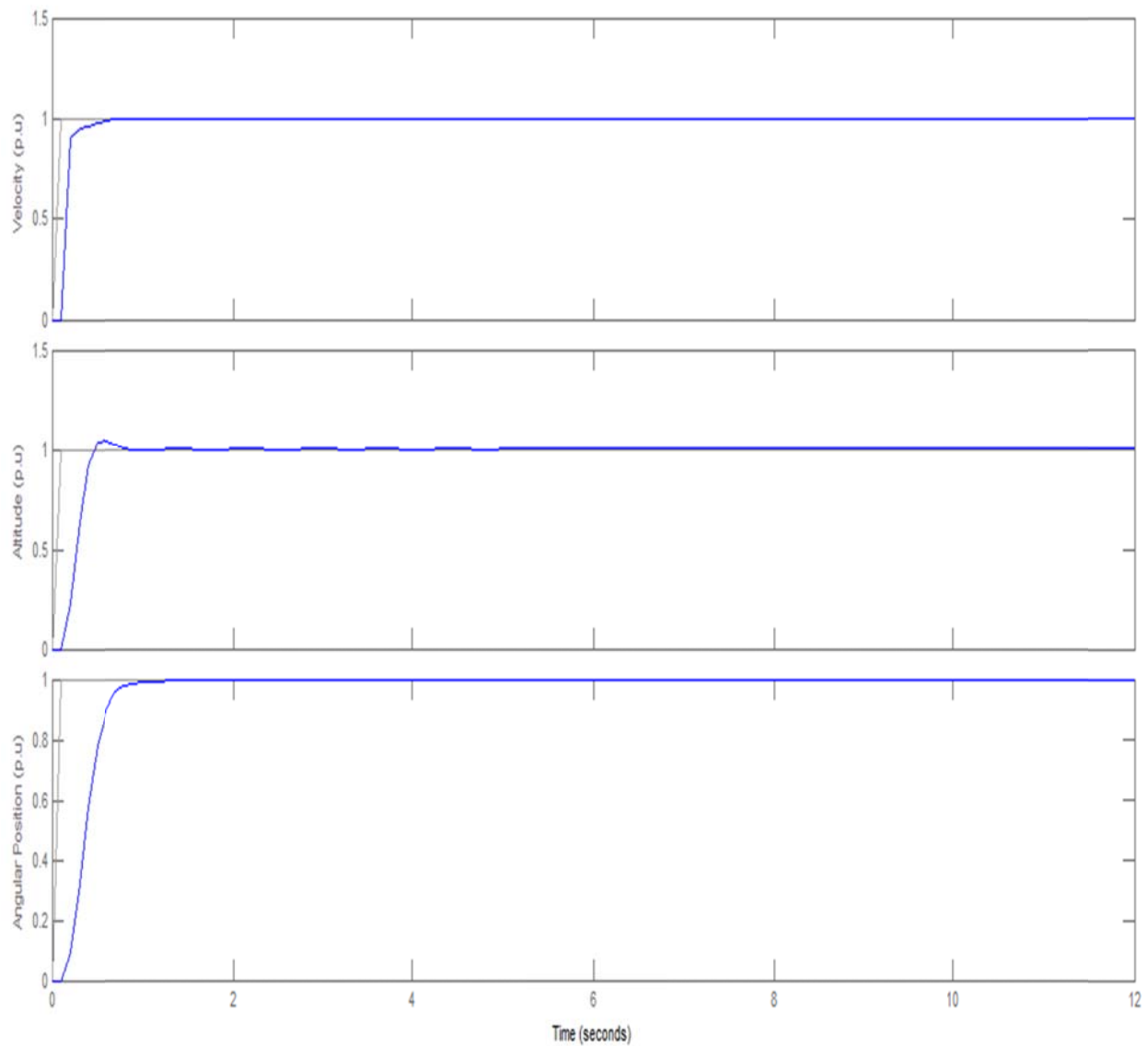


Figure 5.10 Step response for a reference velocity, altitude and angular position of 1 p.u

Settling time for the velocity = 0.7 seconds



Settling time for the altitude = 0.9 seconds

Settling time for the Angular Position = 0.98 seconds

Overshoot for the velocity = 0 %

Overshoot for the altitude = 8 %

Overshoot for the angular position = 0 %

From the result we observe that the performance has declined to some extent from the MISO MPC controller but nevertheless the main objective of incorporating the thrust and lift as one basic component for the control of ornithopter in terms of its output as the velocity, altitude and angular position was possible to be implemented in this design. The performance is not only satisfactory but also provided a somewhat complete picture of the control mechanism of the ornithopter using MPC controller.

### 5.5 Tuning Parameters for the MPC Controller

The parameters were tuned following the general principle of selecting the key parameters. All the simulations were carried out using the same control parameters of the MPC Controller. The parameter values are tabulated as shown below:

Table 5.1 Control parameters of the MPC for the Ornithopter system

Parameters	Values
Control Interval	0.05 seconds
Prediction Horizon	20
Control Horizon	5

The control interval was selected such that it was always less than the settling time of the system which if not selected properly would give erroneous results. The Prediction Horizon was selected on the basis of the complexity of the system. If the system dynamics is a third order transfer function, it is recommended to increase the prediction horizon. According to the general principle, it is also necessary not to make the prediction horizon very large. And the control horizon was selected such that it was less than the prediction horizon and not very large so that it does not hard track the reference signal. This otherwise would lead to a steady state error which is highly undesirable.

## **5.6 Tuning method employed for the PID controller**

In case of the PID controller, the tuning block of the Simulink model was used. It was tuned such that the system doesn't lose stability in the process and more importantly manages to obtain an optimum tracing of the reference signal with optimum settling time. The overshoot tuning parameter was also stipulated to stop the presence of overshoot. It was hard constraint.

## **5.7 Simulation Results for the initial acceleration stage of the ornithopter using the ramp actuating signal**

The initial stage involves rising from ground to the holding position with acceleration. This involves continuous change (increase) of velocity with time. This aspect was analyzed using a reference velocity ramp signal of slope 1 while taking the reference angular position be a step signal of angle 1 p.u. The angular position was allowed to stay at its rated 1 p.u for providing the tail spin necessary for an improved velocity response.

Ramp Response of the outputs (Velocity ) and zero angular position of the Ornithopter using all the inputs (Thrust, Lift and Tail command angle  $\delta_F$ ) as the Manipulated Variables

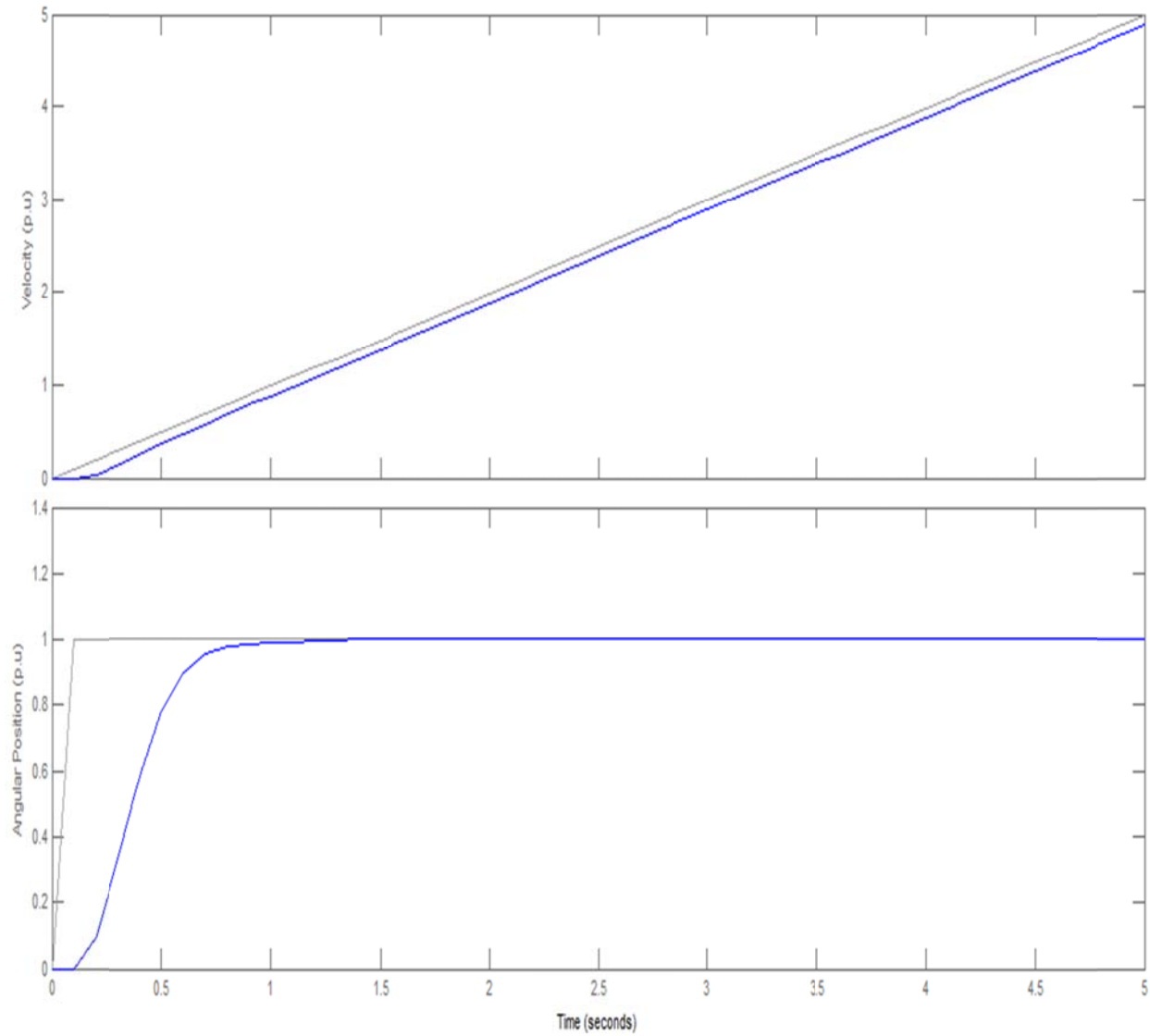


Figure 5.11 Ramp response for a reference ramp velocity of slope 1 and Step response reference angular position of 1 p.u.

The corresponding altitude response of the MIMO system is shown below.

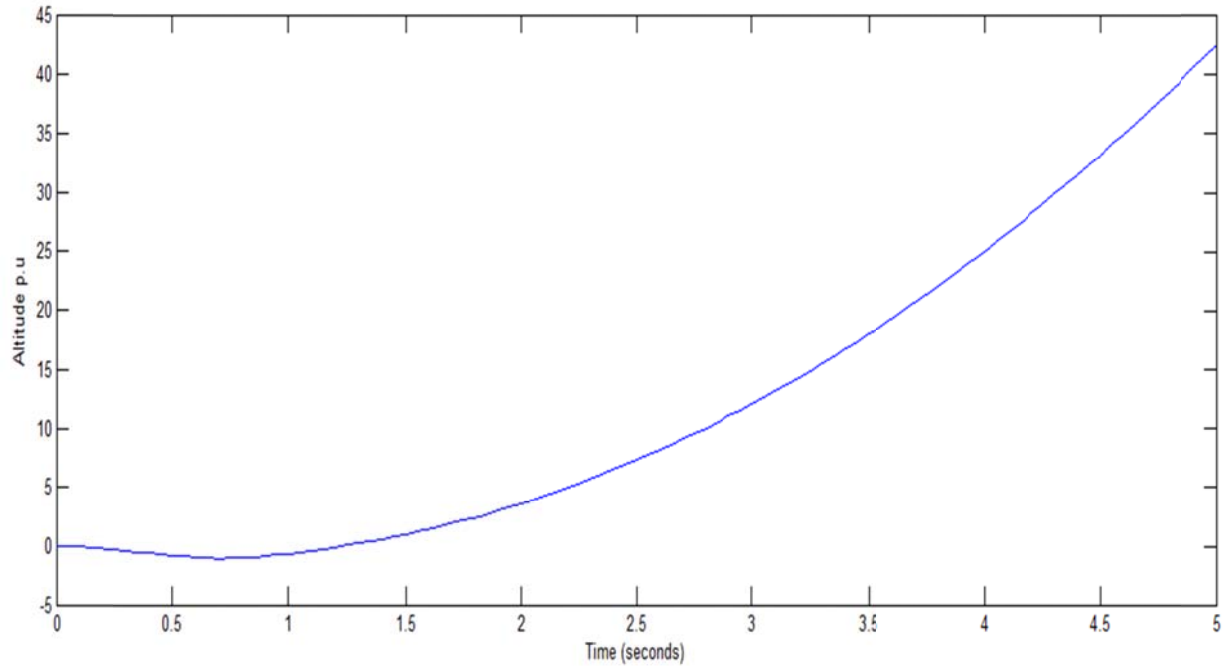


Figure 5.12 Altitude response for the reference ramp velocity of slope 1 and reference angular position of 1 p.u

From the result we see that the velocity was able to track the reference ramp velocity of slope 1 with a steady state error of 2 % which is quite within the tolerance level. Moreover the settling time of the angular position was only 0.9 seconds which is satisfactory. The altitude response displayed a parabolic pathway which completely agrees with the fact that the ornithopter was in acceleration mode.

### 5.8 Simulation Results shown in a tabulated format

The results are comparatively analyzed using the table as shown below:

Table 5.2 Simulated Results of the Ornithopter Tabulated

Control	Input Variables			Settling Time for different Outputs (seconds)			Overshoot for different Outputs (%)		
	$\delta_E$	Thrust	Lift	Velocity	Altitude	Angu Posit	Velocity	Altitude	Angu Posit
PID	4	Manipula Variable	0	Very Poor Oscillatio around the reference velocity	N/A	N/A	Very Poor	N/A	N/A
	4	50	Manipula Variable	N/A	9	N/A	N/A	Very Poor	N/A
	Manipula Variable	50	0	N/A	N/A	13	N/A	N/A	12
MPC	4	Manipula Variable	0	0.5	N/A	N/A	6	N/A	N/A
	4	50	Manipula Variable	N/A	0.9	N/A	N/A	Negligible	N/A
	Manipula Variable	50	0	N/A	N/A	0.8	N/A	N/A	0
	Manipula Variable	Manipula Variable	Manipula Variable	0.15	N/A	N/A	0	N/A	N/A
	Manipula Variable	Manipula Variable	Manipula Variable	N/A	0.52	N/A	N/A	0	N/A
	Manipula Variable	Manipula Variable	Manipula Variable	N/A	N/A	0.8	N/A	N/A	0
	Manipula Variable	Manipula Variable	Manipula Variable	0.7	0.9	0.98	0	8	0
	Manipula Variable (Ramp Reference)	Manipula Variable	Manipula Variable	Good Tracking	Expected Parabolic Response	0.9	No overshoot but presence some steady state error	N/A	0

Finally the overall responses with the MISO MPC controller proved to improve the flight control of the ornithopter quite remarkably. On the other hand the MIMO MPC controller provided a great breakthrough because of the fact that both thrust and lift along with tail command angle  $\delta_E$  was incorporated as whole in the system dynamics and proved to function with a very satisfactory performance. Moreover the initial acceleration phase from ground to the hold position where the ornithopter moves with a steady velocity (cruise), was also possible to be controlled by the MIMO MPC making the whole control operation very compact with all phases considered and made controllable. The response time of the system was also significantly less thus proving MPC to be very successful in the flight control of the ornithopter.

## Chapter 6

# Conclusions and Future Work

## 6.1 Summary

The purpose of this thesis was to investigate the performance of MPC in controlling systems encompassing various fields ranging from electrical to chemical and finally in the field of aerodynamics. The first phase of this thesis dealt with simple nonlinear models which included the temperature control of the STH invariably used in chemical process plants and the current & speed control of a SRM which in recent years have supplanted the induction motor in its use in electric motor drive applications. A very simple nonlinear model of a robotic leg was taken as the base to observe the ability of MPC to control simple systems as well.

Although many nonlinear systems were analyzed but the main emphasis of this thesis was the flight control of an ornithopter. To thorough analyze the superior performance of MPC a complex nonlinear system involving the ornithopter was considered. A 2D model of the ornithopter was investigated which is described by three second order differential equation. After linearization a  $5 \times 5$  system matrix was generated and the system also incorporated all the manipulating variables together. The thrust and the lift input was inseparably included into the dynamics of the system which thereby provided a comprehensive model of the ornithopter. (MAV) ornithopter was the basis of research and a MISO, SISO and finally a MIMO representation of the ornithopter was modeled using Matlab Simulink as the environment for simulation. Moreover not only was the control of the steady state motion of the ornithopter (cruise motion in which the ornithopter moves at a constant velocity) investigated but also the control of the initial accelerating phase from the ground to the point of hovering of the ornithopter was analyzed using the MPC. To evaluate the performance of the MPC the adaptive PID controller was used to control the nonlinear systems. Finally a comparison of the performance of the PID controller and the MPC controller was undertaken.

The simulation results showed remarkable and significant improvement of the control responses of the nonlinear systems considered in this thesis. Mainly in the flight control of the ornithopter where the adaptive PID controller performance was very poor, the MPC showed convincing and distinguished performance compared to the adaptive PID controller. The performance was very good and thus can prompt researchers to think of MPC as the future means of controlling a more complex 3D model of an ornithopter.

The research in itself was very comprehensive in depicting the control feature of MPC because it also showed how a plant which in this thesis was the STH bounded by input constraints can be quite effectively controlled by Model Predictive Controller where the adaptive PID controller was found incompatible.

Eigen values are also found to check the stability of the systems considered in this thesis which in other words are bound to give positive values because otherwise MPC by no means could be used to control the system.

## **6.2 Contribution**

A significant improvement in the response and controlled operation of the nonlinear systems considered in this thesis was observed compared to the results obtained from the PID controller. The results show that in almost all cases of various operating conditions, the MPC controller not only provided a faster response but also is able to eliminate the presence of overshoot that is quite evident in the responses while using the adaptive PID controller. Adaptive PID controllers are generally implemented in the control of single input single output (SISO) systems, but Model Predictive Controller has the versatility of controlling both MISO and MIMO systems. The performance analysis of the control of Model Predictive Controller of such systems is thoroughly analyzed under different operating conditions. The results obtained from the use of Model Predictive Controller for the flight control of the (MAVs) ornithopter shows comprehensively that MPC can be used as the future means for the control of these sophisticated and very complex ornithopters. This is because almost all possible scenarios involved in the flight control of the ornithopter were simulated using the Model Predictive Controller and showed remarkable



performance in the responses of the ornithopter. Moreover the accelerating phase is also considered and MPC was able to provide a very satisfactory result, which in the case of the PID Controller had little effect in controlling the flight modes of the ornithopter.

### **6.3 Conclusion**

Model predictive controller (MPC) was implemented as the controller in various systems. Performance of MPC was significantly better than the adaptive PID controller. The versatile and the smart feature of MPC to work with MIMO plants was observed in this thesis which in case of adaptive PID controller is very difficult to implement and also provides unsatisfactory results unless updated to a rather complex controller by incorporating intelligent algorithms such as Particle Swarm Optimization, Genetic Algorithm and Neural Network in the PID controller. The complexity of avoided in this thesis work. However Model Predictive Controller works very well without any combination of other controllers for operation. This feature of MPC was very vividly manifested in its superlative performance of the flight control of the ornithopter in its different flight modes including both the cruise and accelerating phase of motion of the ornithopter. Hence the ability of MPC to handle multiple manipulated input variables for the control of multiple outputs and also the superlative performance observed in the flight control of the Ornithopter has made it an effective choice for using it as the future controller for a more complex and comprehensive 3D model of an ornithopter.

### **6.4 Recommendations for Future Work**

In the following, some recommendations are given for future scopes of research in the area or research present in this thesis.

- Further research can be done in implementing Model Predictive Controller as the means for the flight control of a more complex 3D modeling of the ornithopter.

- Future research work can be done for the flight control that involves angular velocity, angular acceleration control of the ornithopter
- A more rigorous comparative study can be analyzed by implementing genetic algorithm and neural network based adaptive PID controller as a means for evaluating the performance of the responses of the systems with MPC controllers.
- Future Research work can be done by adding disturbances ranging from wind speed change and non-stationary air flow environments to better analyze the flight control of the ornithopter using MPC controller.
- Future Research can be done by assimilating the lift force as a function of the angle of attack and hence can more closely imitate the control mechanism of birds.

## **References**

- [1] Tahir Rashid “The Flight Dynamics of a Full Scale Ornithopter” Master’s Thesis, University of Toronto, 1995
- [2] DeLaurier, James “An Aerodynamic Model for Flapping-Wing Flight”, The Aeronautical Journal, April 1993
- [3] Fowler, Stuart “A Feasibility Study for the Design of a Human - Powered Flapping-Wing Aircraft”, B.A.Sc Thesis, University of Toronto, 1993
- [4] Katherine Sarah Shigoeka "Velocity and Altitude Control of an ornithopter Micro Aerial Vehicle” Master’s thesis, University of Utah, May 2007
- [5] Z. A. Khan and S. K. Agrawal, “Force and moment characterization of flapping wings for micro air vehicle application,” 2005, pp. 1515–1520 vol. 3.
- [6] L. Schenato, W. C.Wu, and S. Sastry, “Altitude control for a micromechanical flying insect via sensor output feedback,” Robotics and Automation, IEEE Transactions on, vol. 20, no. 1, pp. 93–106, 2004.
- [7] S. Baek, K. Ma, and R. Fearing, “Efficient resonant drive of flapping-wing robots,” in IEEE/RSJ International Conference on Intelligent Robots and Systems, St. Louis, MO, October 2009, pp. 2854–2860.

[8] Zach Votaw –Zach Gatson, "Design Analysis of a Bio-Inspired Warping Tail for MAV Applications" American Institute of Aeronautics and Astronautics AIAA, May 2012

[9] Dong, H. Koehler, C. Liang, Z. Wan, H., and Gaston, Z. "An Integrated Analysis of a Dragonfly in Free Flight," 40th AIAA Fluid Dynamics Conference and Exhibit, 2010-4390, 2010.

[10] Ifju, P., Stanford, B., Sytsma, M., "Analysis of a Flexible Wing Micro Air Vehicle," 25th AIAA Aerodynamic Measurement Technology and Ground Testing Conference, San Francisco, California, 2006.

[11] Kim, D. K., Han, J. H., "Optimal Design of a Flexible Flapping Wing Using Fluid-Structure Interaction Analysis," The 8<sup>th</sup> International Conference on Motion and Vibration Control, TUM, Munich, Germany, Sep. 15-18, 2008.

[12] The MATLAB help files, the Mathworks Company, 2012.

[13] Kaya, M., Tuncer, H. I., Jones, D. K., and Platzer, M., "Optimization of Flapping Motion Parameters for Two Airfoils in a Biplane," Journal of Aircraft, Vol. 46, No. 2, 2009, pp 583-592.

[14] Young, J., Walker, S. M., Bomphrey, R. J., Taylor, G. K., and Thomas, L. R., "Details of Insect Wing Design and Deformation Enhance Aerodynamic Function and Flight Efficiency," Science, Vol.325, No.5947, 2009, pp. 1549-1552.

[15] Stanley Seunghoon Baek "Autonomous Ornithopter Flight with Sensor-Based Behavior" PhD thesis, University of California at Berkley, May 2011.

- [16] J.-C. Zufferey, A. Beyeler, and D. Floreano, “Flying Insects and Robots”. Edited by Dario Floreano, Jean-Christophe Zuffery, Mandyam V. Srinivasan, and Charlie Ellington Springer, 2009, ch. 6: Optic Flow to Steer and Avoid Collision in 3D, pp. 73–86.
- [17] R. C. Michelson and S. Reece, “Update on flapping wing micro air vehicle research: Ongoing work to develop a flapping wing, crawling “Entomopter”,” in 13th Bristol International RPV Conference, April 1998, pp. 19 – 24..
- [18] Stanley S. Baek and Ronald S. Fearing “Flight Forces and Altitude Regulation of 12 gram I-Bird” manuscript, University of California at Berkley, May 2012
- [19] C. Roux, and M.M. Morcos, “On the Use of a Simplified Model for Switched Reluctance Motors”, IEEE Trans. on Energy Conversion 17, 2002
- [20] Dash, P K – Mishra, S – Panda, G “Damping multimodal power system oscillation using hybrid fuzzy controller for series connected FACTS devices” IEEE Transaction on Power Systems 15 No. 4 (2000), 1360-1366.
- [21] A.V. Radun, “Design Considerations for the Switched Reluctance Motor”, IEEE Trans. on Industry Applications 31, 1995.
- [22] R. Krishnan “Switched Reluctance Motor Drives: Modeling, Simulation, Analysis, Design, and Applications”, CRC Press, 2001
- [23] I. Husain and M. Ehsani,” Torque Ripple Minimization in Switched Reluctance Motor Drives by PWM Current Control”, Proc. APEC’94, 1994.

[24] Moritz Diehl, " Real-time optimization and nonlinear model predictive control of processes governed by differential-algebraic equations", Journal of Process Control (Elsevier) 2002

[25] M. Fawzy, M.A.S. Aboeela, "Design of Missile Control System using Model Predictive Control", Online Journal on Computer Science and Information Technology (OJCSIT), vol. 1, no. 3, 2001

[26] J.H. Blakelock, "Automatic Control of Aircraft and Missiles", John Wiley & Sons, Inc., USA, 2<sup>nd</sup> edition, 1996

[27] P. E. Orukpe, "Basics of Model Predictive Control", Master degree of Science in Control Engineering, Imperial College, London, April 2005.

[28] Martin Bogseth Hanger, "Model Predictive Control Allocation", Master of Science in Cybernetics, NTNU, June 2011

[29] Qin S.J. and Badgwell, "An overview of nonlinear model predictive control applications," in Nonlinear Predictive Control, Eds F. Allgoewer and A. Zheng, Birkhauser, 2000

[30] Montarnal Philippe, "Nonlinear Aircraft dynamics and PIO", Master of Science in Mechanical Engineering, Hamburg University of Applied Science, July 2009

[31] Ashish, "Modern Control Design with Matlab and Simulink" Indian Institute of Technology, Kanpur, India, John Wiley & Sons, 2002

[32] G. D. Buckner, "Simulink, A graphical tool for Dynamic System Simulation", ASME, North Carolina State University, Fall 2011.

[33] Bret K. Stanford and Philip S. Beran, U.S. Air Force Research Laboratory, "Analytical Sensitivity Analysis of an Unsteady Vortex-Lattice Method for Flapping-Wing Optimization", Journal of Aircraft, DOI: 10.2514/1.46259, (2010)

[34] Yang, T. H., & Polak, E. (1993). "Moving horizon control of nonlinear systems with input saturation, disturbances and plant uncertainty.International", Journal of Control, 58, 875}903.

[35] Dr. Kevin Craig "Stirred Water Tank Heater A Case study", Rennsselaer Polytechnique University, 2005

[36] Chun Htoo Aung, Khin Thandar Lwin, and Yin Mon Myint," Modeling Motion Control System for Motorized Robot Arm using MATLAB", World Academy of Science, Engineering and Technology 42 2008.

[37] S. Skogestad, "MATLAB Distillation column model" (ColumnA),Online:[http://www.nt.ntnu.no/users/skoge/book/matlab\\_m/cola/cola.html](http://www.nt.ntnu.no/users/skoge/book/matlab_m/cola/cola.html). Accessed 29th July 2012.

[38] F. Loquasto, D.E. Seborg, "Monitoring model predictive controlsystems using pattern classification and neural networks", Industrial and Engineering Chemistry Research 42 (2003) 4689–4701.

[39] B.A. Ogunnaike, W.H. Ray, Process Dynamics, Modeling, and Control (Topics in Chemical Engineering), Oxford University Press, 1994.

[40] D.E. Seborg, T.E. Edgar, D.A. Mellichamp, "Process Dynamics and Control", second ed., John Wiley, Hoboken, NJ, 2004.

[41] Lars Imslanda, Rolf Findeisen, Eric Bullinger, Frank Allgower, Bjarne A. Foss "A note on stability, robustness and performance of output feedback nonlinear model predictive control", Journal of Process Control, 2001.

[42] D. Q. Mayne, J. B. Rawlings, C. V. Rao, P. O. M. Scokaert, "Constrained model predictive control: Stability and optimality", Automatica, 2000.

[43] Rawlings, J. B., Meadows, E. S., & Muske, K. R., "Nonlinear model predictive control: A tutorial and survey". ADCHEM'94 Proceedings, Kyoto, Japan (pp. 185-197), 1994

[44] Qin S.J. and Badgwell T.A. "An overview of industrial model predictive control technology", In F. Allgower and A. Zheng, editors, Fifth International Conference on Chemical Process Control – CPC V, pages 232–256. American Institute of Chemical Engineers, 1996.

[45] Qin S.J. and Badgwell T.A. : "An overview of nonlinear model predictive control applications", In F. Allgower and A. Zheng, editors, "Nonlinear Predictive Control", pages 369–393. Birkhäuser, 2000.

[46] Eduardo F. Camacho and Carlos Bordons: "Model Predictive Control Advanced Textbooks in Control and Signal Processing", Springer Publication, 1998.



- [47] Allgower, F., Badgwell, T. A., Qin, S. J., Rawlings, J. B., & Wright, S. J. (1999). Nonlinear predictive control and moving horizon estimation—an introductory overview. In P. M. Frank (Ed.), *Advances in control: highlights of ECC '99*. Berlin: Springer.
- [48] Mayne, D. Q., Rawlings, J. B., Rao, C. V., & Sokaert, P. O. M. (2000). Constrained model predictive control: Stability and optimality. *Automatica*, 36, 789–814.
- [49] Qin, S. J., & Badgwell, T. A. (1997). An overview of industrial model predictive control technology. In J. C. Kantor, C. E. Garcia, & B. Carnahan (Eds.), *Chemical process control—V, Fifth international conference on chemical process control CACHE and AICHE*, (pp.232–256).
- [50] Young, R. E., Bartusiak, R. B., & Fontaine, R. B. (2001). Evolution of an industrial nonlinear model predictive controller. In *Preprints: Chemical process control—CPC VI, Tucson, Arizona* (pp. 399– 410). CACHE.
- [51] Downs, J. J. (2001). Linking control strategy design and model predictive control. In *Preprints: Chemical process control-6, assessment and new directions for research (CPC VI), Tuscon, AZ, January 2001* (pp. 411–422)
- [52] Hillestad, M., & Andersen, K. S. (1994). Model predictive control for grade transitions of a polypropylene reactor. In *Proceedings of the 4th European symposium on computer aided process engineering (ESCAPE 4), Dublin, March 1994*.
- [53] Ohshima, M., Ohno, H., & Hashimoto, I. (1995). Model predictive control: Experiences in the university-industry joint projects and statistics on MPC applications in Japan. *International workshop on predictive and receding horizon control, Korea, October 1995*.

[54] Richalet, J., Rault, A., Testud, J. L., & Papon, J. (1976). Algorithmic control of industrial processes. In Proceedings of the 4th IFAC symposium on identification and system parameter estimation. (pp. 1119–1167).

[55] Richalet, J., Rault, A., Testud, J. L., & Papon, J. (1978). Model predictive heuristic control: Applications to industrial processes. *Automatica*, 14, 413–428

[56] Norman Nise, “Control Systems Engineering”, Book Wiley 4<sup>th</sup> Edit

## Appendices

### Appendix A

The system parameters used for simulation of the robotic leg are  $J = 0.4177 \text{ kg m}^2/\text{s}^2$ ,  $D = 0.11 \text{ N-m/s/rad}$ ,  $K_b = 1 \text{ V-s/rad}$ ,  $K_t = 1 \text{ N-m/rad}$ ,  $L_a = 2 \text{ H}$ ,  $M = 0.5 \text{ kg}$ ,  $g = 9.8 \text{ m/s}^2$  and  $R_a = 1 \Omega$  respectively [36]

### Appendix B

The parameters used for modeling and simulation of the STH is tabulated and shown below:

Table 6.1 System Parameters of the STH system

Parameters	Values
$V_j$	$1 \text{ ft}^3$
$V_t$	$10 \text{ ft}^3$
$\rho_j C_{pj}$	$61.3 \frac{\text{Btu}}{^\circ\text{F-ft}^3}$
$\rho_t C_{pt}$	$61.3 \frac{\text{Btu}}{^\circ\text{F-ft}^3}$
$hA$	$183.9 \frac{\text{Btu}}{^\circ\text{F-min}}$

## Appendix C

The specifications for the 5-hp SRM drive are listed below [43]:

Table 6.2 Motor and system parameters

Motor and system parameters	
Command signal levels	+10
Dc link voltage	400 V
Max. current	15 A
PWM chopping frequency	8 kHz
Phase resistance	0.931 $\Omega$
Power	5 hp
Rated current	10 A (1 p.u.)
Rated speed	2500 rpm
Rotor friction constant	0.001 N · m/rad/sec
Rotor inertia	0.006 kg/m <sup>2</sup>
Speed feedback gain	0.0383 V/rad/sec
Speed feedback time constant	0.1 sec

## Appendix D

The parameters used for modeling and simulation of the ornithopter system is tabulated and shown below:

Table 6.3 System Parameters of the ornithopter system

Parameters	Values
$b_x$	1
$b_y$	1
$b_\theta$	$8 \times 10^{-4}$
$K_t$	0.0032
$I$	$3 \times 10^{-4}$
$m$	0.096
$l$	0.1524
$g$	9.8
$h$	0.1016